Asian Journal of Tropical Biotechnology

| Asian J Trop Biotechnol | vol. 18 | no. 1 | June 2021 |
| ISSN 2775-300X | E-ISSN 2775-4715 |

Salmonella typhimurium (red) photo by Rocky Mountain Lab., NIAID, NIH, USA

Asian Journal of Tropical Biotechnology

| Asian J Trop Biotechnol | vol. 18 | no. 1 | June 2021 |

Characterization, fractionation and functional properties of *Acacia oerfota* gum **1-12**
MUSTAFA ELOBIED AHMED, MOHAMMED ELMUBARK OSMAN, ELFATIH AHMED HASSAN

The carotenoid biosynthesis pathway in the asexual intraerythrocytic stages of *Plasmodium falciparum* **13-27**
RICHARD NORTEY-MENSAH, MARIAN A. TEYE, MICHAEL F. OFORI

Short Communication: Analysis of purity and concentration of DNA extracted from intron patho gene-spin extraction on crab processed food product samples **28-31**
ALFI SOPHIAN, RATNA PURWANINGSIH, MUINDAR, EKA PUTRI JUNIARTI IGIRISA, MUHAMMAD LUTHFI AMIRULLAH

The density of coliform bacteria in well water filtered using a filter coated with silver nanoparticles **32-36**
LILIS NURVIANTI MUFIDAH, PRABANG SETYONO, ARI SUSILOWATI

Screening of phosphate solubilizing bacteria from sugarcane plant rhizosphere as biofertilizer agent for sorghum growth (*Sorghum bicolor*) **37-45**
RISKI MARETA AYU PRISILLIA, ARI SUSILOWATI, SOLICHATUN

Published semiannually **PRINTED IN INDONESIA**

ISSN: 2775-300X E-ISSN: 2775-4715

Asian Journal of Tropical Biotechnology

| Asian J Trop Biotechnol | vol. 18 | no. 1 | June 2021|

ONLINE
http://smujo.id/bbs

p-ISSN
2775-300X

e-ISSN
2775-4715

PUBLISHER
Society for Indonesian Biodiversity

CO-PUBLISHER
Universitas Sebelas Maret, Surakarta, Indonesia

OFFICE ADDRESS
Jl. Ir. Sutami 36A Surakarta 57126, Central Java, Indonesia. Tel./Fax.: +62-271-663375, email: editors@smujo.id

PERIOD OF ISSUANCE
June, December

Society for Indonesian Biodiversity

Universitas Sebelas Maret Surakarta, Indonesia

Published by Smujo International for The Society for Indonesian Biodiversity and Sebelas Maret University, Surakarta, Indonesia

GUIDANCE FOR AUTHORS

Aims and Scope ***Asian Journal of Tropical Biotechnology*** (**Asian J Trop Biotechnol**)(*formerly Bioteknologi, Biotechnological Studies*) encourages submission of manuscripts dealing with all aspects of biotechnology, especially from tropical regions, that emphasize issues germane to improve human life, includes cell biochemistry, enzymes and proteins, applied genetics and molecular biotechnology, genomics and proteomics, applied microbiology and cell physiology, environmental biotechnology, improvement of crop productivity, public health and waste management, as as well as product formation and manipulation of biological processes for use in the agricultural, pharmaceutical biotechnology and allied industries.

Article types The journal seeks original full-length: (i) **Research papers**, (ii) **Reviews**, and (iii) **Short communications**. Original research manuscripts are limited to 8,000 words (including tables and figures) or proportional to articles in this publication number. Review articles are also limited to 8,000 words, while Short communications should be less than 2,500 words, except for pre-study.

Submission: The journal only accepts online submissions through the open journal system **(https://smujo.id/bbs/about/submissions)** or, for login problems, email the editors at unsjournals@gmail.com (or editors@smujo.id). Submitted manuscripts should be the original works of the author(s). Please ensure that the manuscript is submitted using the template, which can be found at (https://biodiversitas.mipa.uns.ac.id/D/template.doc). The manuscript must be accompanied by a cover letter containing the article title, the first name and last name of all the authors, and a paragraph describing the claimed novelty of the findings versus current knowledge. Please also provide a list of five potential reviewers in your cover letter. They should come from outside your institution and better from three different countries. Submission of a manuscript implies the submitted work has not been published (except as part of a thesis or report, or abstract) and is not being considered for publication elsewhere. When a group writes a manuscript, all authors should read and approve the final version of the submitted manuscript and its revision; and agree on the submission of manuscripts for this journal. All authors should have made substantial contributions to the concept and design of the research, acquisition of the data and its analysis, drafting the manuscript, and correcting the revision. All authors must be responsible for the work's quality, accuracy, and ethics.

Ethics Author(s) must be obedient to the law and/or ethics in treating the object of research and pay attention to the legality of material sources and intellectual property rights.

Copyright If the manuscript is accepted for publication, the author(s) still hold the copyright and retain publishing rights without restrictions. For the new invention, authors must manage its patent before publication.

Open Access The journal is committed to free-open access that does not charge readers or their institutions for access. Readers are entitled to read, download, copy, distribute, print, search, or link to the full texts of articles, as long as not for commercial purposes. The license type is CC-BY-NC-SA.

Acceptance Only articles written in US English are accepted for publication. Manuscripts will be reviewed by editors and invited reviewers (double-blind review) according to their disciplines. Authors will generally be notified of acceptance, rejection, or need for revision within 1 to 2 months of receipt. Manuscripts will be rejected if the content does not align with the journal scope, does not meet the standard quality, is in an inappropriate format, or contains complicated grammar, dishonesty (i.e., plagiarism, duplicate publications, fabrication of data, citations manipulation, etc.), or ignoring correspondence in three months. The primary criteria for publication are scientific quality and significance. **Uncorrected proofs** will be sent to the corresponding author by system or email as .doc or .docx files for checking and correcting typographical errors. The corrected proofs should be returned in 7 days to avoid publication delays. The accepted papers will be published online in chronological order at any time but printed at the end of each month.

Free of charge This publication is dedicated entirely to the advancement of science and technology, therefore author(s), or author institution(s) are not subject to publication fees. **Reprints** The sample journal reprint is only available by special request. Additional copies may be purchased when ordering by email and sending back the uncorrected proofs.

Manuscript preparation Manuscript is typed on A4 (210x297 mm^2) paper size, in a single column, single space, 10-point (10 pt) Times New Roman font. The margin text is 3 cm from the top, 2 cm from the bottom, and 1.8 cm from the left and right. Smaller lettering sizes can be applied in presenting tables and figures (9 pt). Word processing program or additional software can be used; however, it must be PC compatible, use the template, and be Microsoft Word based (.doc or .rtf; not .docx). **Scientific names** of species (incl. subspecies, variety, etc.) should be written in italics, except in italicized sentences. Scientific names (genus, species, author) and cultivar or strain should be mentioned completely for the first time mentioning it in the body text, especially for taxonomic manuscripts. The genus name can be shortened after the first mention, except in early sentences, or where this may generate confusion; name of the author can be eliminated after the first mention. For example, *Rhizopus oryzae* L. UICC 524 can be written hereinafter as *R. oryzae* UICC 524. Using trivial names should be avoided. **Biochemical and chemical nomenclature** should follow the order of the IUPAC-IUB. For DNA sequences, it is better to use Courier New font. Standard chemical abbreviations can be applied for common and clear used, for example, completely written butilic hydroxyl toluene (BHT) to be BHT hereinafter. **Metric measurements** should use IS denominations, and other systems should use equivalent values with the denomination of IS mentioned first. A dot should not follow abbreviations like g, mg, mL, etc. Minus index (m^{-2}, L^{-1}, h^{-1}) suggested being used, except in things like "per-plant" or "per-plot." **Mathematical equations** can be written down in one column with text; in that case, they can be written separately. **Numbers** one to ten are written in words, except if it relates to measurement, while values above them are written in number, except in early sentences. The fraction should be expressed in decimal. In the text, it should be used "%" rather than "percent." Avoid expressing ideas with complicated sentences and verbiage/phrasing, and use efficient and effective sentences.

The title of the article should be written in compact, clear, and informative sentence, preferably not more than 20 words. Name of author(s) should be completely written, especially for the first and the last name. **Name and institution** address should also be completely written with street name and number (location), postal code, telephone number, facsimile number, and email address. We choose local names in Bahasa Indonesia for universities in Indonesia. The mention of "strata" program, should be avoided. Manuscript written by a group, author for correspondence along with address is required (marked with "♥"). **The title page** (first page) should include title of the article, full name(s), institution(s) and address(es) of the author(s); the corresponding authors detailed postage and e-mail addresses (P), and phone (O) and fax numbers (O).

Abstract A concise abstract is required (about 200 words). The abstract should be informative and state briefly the aim of the research, the principal results and major conclusions. An abstract is often presented separately from the article, thus it must be able to stand alone (completely self-explanatory). References should not be cited, but if essential, then cite the author(s) and year(s). Abbreviations should be avoided, but if essential, they must be defined at their first mention. **Keywords** are about five words, covering scientific and local name (if any), research themes, and special methods used; and sorted from A to Z. **Abbreviations** (if any): All important abbreviations must be defined at their first mention there. **Running title** is about five words.

Introduction is about 600 words, covering the aims of the research and provide an adequate background, avoiding a detailed literature survey or a summary of the results. **Materials and Methods** should emphasize on the procedures and data analysis. **Results and Discussion** should be written as a series of connecting sentences, however, for a manuscript with long discussion should be divided into subtitles. Thorough discussion represents the causal effect mainly explains why and how the results of the research were taken place, and do not only re-express the mentioned results in the form of sentences. **Concluding** sentence should be given at the end of the discussion. **Acknowledgements** are expressed in a brief; all sources of institutional, private and corporate financial support for the work must be fully acknowledged, and any potential conflicts of interest are noted.

Figures and Tables of a maximum of three pages should be clearly presented. The title of a picture is written down below the picture, while the title of a table is written above the table. Colored figures can only be accepted if the information in the manuscript can lose without those images; the chart is preferred to use black and white images. The author could consign any picture or photo for the front cover, although it does not print in the manuscript. All images property of others should be mentioned the source. Author is suggested referring to Wikipedia for international boundaries and Google Earth for satellite imagery. If not specifically mentioned, it is assumed to refer to these sources. **There is no appendix**, all data or data analysis is incorporated into Results and Discussions. For broad data, it can be displayed on the website as a supplement.

References Preferably 80% of it comes from scientific journals published in the last 10 years. In the text, give the author names followed by the year of publication and arrange from oldest to newest and from A to Z; in citing an article written by two authors, both of them should be mentioned; however, for three and more authors only the first author is mentioned followed by et al. For example, Saharjo and Nurhayati (2006) or (Boonkerd 2003a, b, c; Sugiyarto 2004; El-Bana and Nijs 2005; Balagadde et al. 2008; Webb et al. 2008). Extent citation should be avoided, as shown with the word "cit." Reference to unpublished data and personal communication should not appear in the list but should be cited in the text only (e.g., Rifai MA 2007, pers. com. (personal communication); Setyawan AD 2007, unpublished data). In the reference list, the references should be listed in alphabetical order. Names of journals should be abbreviated. Always use the standard abbreviation of a journal's name according to the **ISSN List of Title Word Abbreviations** (www.issn.org/2-22661-LTWA-online.php). Please include DOI links for journal papers. The following examples are for guidance.

Journal:

Saharjo BH, Nurhayati AD. 2006. Domination and composition structure change at hemic peat natural regeneration following burning; a case study in Pelalawan, Riau Province. Biodiversitas 7: 154-158. DOI: 10.13057/biodiv/d070213.

The usage of "et al." in long author lists will also be accepted:

Smith J, Jones M Jr, Houghton L et al. 1999. Future of health insurance. N Engl J Med 965: 325-329. DOI: 10.10007/s002149800025.

Book:

Rai MK, Carpinella C. 2006. Naturally Occurring Bioactive Compounds. Elsevier, Amsterdam.

Chapter in the book:

Webb CO, Cannon CH, Davies SJ. 2008. Ecological organization, biogeography, and the phylogenetic structure of rainforest tree communities. In: Carson W, Schnitzer S (eds.). Tropical Forest Community Ecology. Wiley-Blackwell, New York.

Abstract:

Assaeed AM. 2007. Seed production and dispersal of *Rhazya stricta*. 50th annual symposium of the International Association for Vegetation Science, Swansea, UK, 23-27 July 2007.

Proceeding:

Alikodra HS. 2000. Biodiversity for development of local autonomous government. In: Setyawan AD, Sutarno (eds.). Toward Mount Lawu National Park; Proceeding of National Seminary and Workshop on Biodiversity Conservation to Protect and Save Germplasm in Java Island. Universitas Sebelas Maret, Surakarta, 17-20 July 2000. [Indonesian]

Thesis, Dissertation:

Sugiyarto. 2004. Soil Macro-invertebrates Diversity and Inter-Cropping Plants Productivity in Agroforestry System based on Sengon. [Dissertation]. Universitas Brawijaya, Malang. [Indonesian]

Information from the internet:

Balagadde FK, Song H, Ozaki J, Collins CH, Barnet M, Arnold FH, Quake SR, You L. 2008. A synthetic *Escherichia coli* predator-prey ecosystem. Mol Syst Biol 4: 187. DOI: 10.1038/msb.2008.24. www.molecularsystembiology.com.

THIS PAGE INTENTIONALLY LEFT BLANK

ASIAN J TROP BIOTECHNOL
Volume 18, Number 1, June 2021
Pages: 1-12

ISSN: 2775-300X
E-ISSN: 2775-4715
DOI: 10.13057/biotek/c180101

Characterization, fractionation, and functional properties of *Acacia oerfota* gum

MUSTAFA ELOBIED AHMED, MOHAMMED ELMUBARK OSMAN♥, ELFATIH AHMED HASSAN
College of Science, Sudan University of Science and Technology. P.O. Box 407, Khartoum, Sudan

Manuscript received: 24 December 2020. Revision accepted: 13 March 2021.

Abstract. *Ahmed ME, Osman ME, Hassan EA. 2021. Characterization, fractionation, and functional properties of Acacia oerfota* gum. *Asian J Trop Biotechnol 18: 1-12.* Thirty gum samples were collected at two locations around Senga and Wadel Hadad, Sudan during 2015. Fifteen samples of *Acacia oerfota* were taken from each location. For the fifteen samples, four composite samples were made for each position by mixing. Chemical, physicochemical, rheological behavior, distribution of molecular weight and molecular weight, and emulsification properties of *A. oerfota* gum were all performed. The results show the range for moisture content (11.8-13.1%), protein percentage (2.19-3.93%), tannin (268-292 ppm), acid equivalent weight (2941-5357), total uronic acid percentage (3.62-6.60%). The percentage of Senga's cationic composition was calcium 0.287, potassium 0.131, strontium 0.004, and iron 0.010. While the percentage of Wadel Hadad had a caionic composition of calcium 0.242, potassium 0.145, strontium 0.005, sulphur 0.002, and iron 0.001. The rheological actions of *A. oerfota* gum demonstrates Newtonian conduct (when applied stress is removed, the molecular form is restored). For the two composite sites of Senga and Wadel Hadad, oerfota gum varied between 1.68x105 and 1.80x105 g/mol respectively. The molecular weight was determined by gel permeation chromatography (GPC-MALLS). This was 6.23x105 g/mole and 9.59x105 g/mole for the two sites. Samples of *A. oerfota* gum obtained from the Senga location indicate three fractions; Arabinogalactan protein (AGP) with a molecular weight of 1.11% by 4.77x105 mass and Rg 50%. The second and third fractions (Arabinogalactan AG + Glycoprotein GP) were 5.76x105 g/mole molecular weight, 98.89 percent mass. For A, GPC-MALLS. An AGP with a molecular weight of 4.19x105, percent mass 0.84, and Rg 187 is shown by *A. oerfota* gum samples obtained from Wadel Hadad. The second and third fractions had a molecular weight of 8.24x105 g/mole, 99.16 percent mass (AG + GP). Both emulsions exhibit broad droplet size, displaying a standard distribution of bimodal droplet size with a pronounced shoulder representing weak uniformity and unstable emulsions.

Keywords: *Acacia oerfota*, characterization, fractionation

INTRODUCTION

The species *Acacia*, commonly known as acacia, thorn tree, whistling thorn, or wattle, is a genus of shrubs and trees. There are approximately 1300 species in the genus *Acacia*, of which about 960 are native to Australia, with the remainder spread across the tropical to warm-temperate regions of both hemispheres, including Africa, Asia, and the Americas (Smith and Figueiredo 2011).

Sudan is endowed with the largest ranging species, such as *Acacia senegal* (Hasab) *Acacia seyal* (Talha), *Acacia polyacantha* (Kakamut); *Acacia laeta* (Shubahi); *Acacia mellifere* (Kitir), *Acacia oerfota* (Lao't), *Acacia sieberiana* (Kuk). There are more than 30 *Acacia* species, the vast majority of which are gum species (Elamin 1990; Abdel Nour 1999).

Gums have a high molecular weight hydrophilic polysaccharides, typically with colloidal properties that can dissolve or swell in a suitable solvent to create gels or highly viscous suspension. Therefore, the term gum is applied to a wide range of *gum* characteristic substances and cannot be precisely described. Hydrophobic compounds sometimes referred to as gums, are hydrocarbons and other petroleum products with high molecular weight, rubbers, some synthetic polymers, trendy for chewing gum, and resinous saps that sometimes exude from evergreens, often commercially tapped, such as gum balsam and gum resin (Anderson and Cree 1968).

The objectives of this research were (i) to classify *Acacia oerfota* gum by investigating the general properties of the gum physiochemically; (ii) to perform the comparison and contrast of *A. oerfota* gum's physicochemical characteristics with *Acacia senegal* gum and *Acacia seyal*, as well as (iii) to examine: *A. oerfota* gum's rheological behavior, molecular weight and distribution of molecular weight, and *A. oerfota* gum's emulsifying properties.

MATERIALS AND METHODS

Sample collection

In February 2015, gum of *A. oerfota* samples were collected from two locations, namely Senga City Blue Nile State and Wadel Hadad Aljazeera State (15 samples from each location) (Table 1 and Figure 1). 10 samples were collected from each position (sample/tree) and 5 samples were collected (3 trees/sample). By making incisions of about 15vcm long and 3 cm wide using an axe, many *A. oerfota* trees were tapped. There were 10 to 20 blazes on the branches of the trees.

Figure 1. Gum *oerfota* samples.

Table 1. Samples code and location of *A. oerfota* gum (Collection date February 2015).

Wadel Hadad location		Senga location	
No.	**Code**	**No.**	**Code**
1	Sample.1	20	Sample.16
2	Sample.2	21	Sample.17
3	Sample.3	22	Sample.18
4	Sample.4	23	Sample.19
5	Sample.5	24	Sample.20
6	Sample.6	25	Sample.21
7	Sample.7	26	Sample.22
8	Sample.8	27	Sample.23
9	Sample.9	28	Sample.24
10	Sample.10	29	Sample.25
11	Sample.11	30	Sample.26
12	Sample.12	31	Sample.27
13	Sample.13	32	Sample.28
14	Sample.14	33	Sample.29
15	Sample.15	34	Sample.30
16	Comp.1	35	Comp.5
17	Comp.2	36	Comp.6
18	Comp.3	37	Comp.7
19	Comp.4	38	Comp.8

Note: Comp.1 prepared by mixing equal amount of (sample 1-4) Wadel Hadad. Comp.2 prepared by mixing equal amount of (sample 5-10) Wadel Hadad. Comp.3 prepared by mixing equal amount of (sample11-15) Wadel Hadad. Comp.4 prepared by mixing equal amount of (sample 1-15) Wadel Hadad. Comp.5 prepared by mixing equal amount of (sample 1-5) Senga. Comp.6 prepared by mixing equal amount of (sample 6-10) Senga. Comp.7 prepared by mixing equal amount of (sample 11-15) Senga. Comp.8 prepared by mixing equal amount of (sample 1-15) Senga.

Purification of gum samples

All of the gum samples were dried and washed by hand at room temperature to remove foreign particles. Using a mortar and pestle, the samples were then ground and kept for further examination in containers.

Determination of physicochemical properties

Moisture content

The humidity content was calculated by FAO (1990). At 105°C, one gram of ground gum was oven-dried to a steady weight. The sum of humidity was measured as the proportion of the weight loss to the original weight.

$$\text{Moisture content\%} = \frac{\text{Initial weight-final weight}) \times 100}{\text{Initial weight}}$$

Total ash content

The total ash content was calculated by FAO (1990). Placed in a crucible, one gram of gum sample ignited in a muffle furnace at 550 ° C for 5 hours. The estimation of total ash was as follows:

$$\text{Total ash (\%)} = \frac{w_2 x 100}{w_1}$$

Where:
W_1: Original weight of the sample,
W_2: weight of the sample after ignition

pH

Using the Berkman Zeromatic IV pH meter at room temperature, the pH of 1% aqueous solution of gum was determined.

Specific optical rotation

For the 1% aqueous gum solution, the observed optical rotation was determined using a Bellingham and Stanley polarimeter equipped with a sodium lamp and a cell with a path length of 20 cm at measurements, and the precise optical rotation was measured using the following equation:

$$\text{Specific rotation } [\alpha]_D^T = [\ (\alpha \times 100)/(C \times L)\ ].$$

Where:
α : observed optical rotation
C : concentration of gum solution
D : sodium imitation line = 532 nm
T : temperature
L : length of polarimeter tube in decimeters

Viscosity measurements

The viscosity of gum solution was measured using a U-tube viscometer immersed in a water bath with a constant temperature set at 25 C °. In 0.2 M NaCl, gum solutions (0.5%, 1%, 2%, 3%, and 4%) were prepared, then filtered and transferred to the viscometer. Intrinsic viscosity has been defined by:

$$\text{Relative viscosity } [\eta_{rel}] = \eta/\eta_\circ = t/t_\circ$$
$$\text{Specific viscosity } [\eta_{sp}] = \eta_{rel}\text{-}1$$
$$\text{Reduced viscosity } [\eta_{red}] = \eta_{sp}/C$$
$$\text{Intrinsic viscosity } [\eta] = \lim_{c\to 0}\ \eta_{sp}/C]$$

The intrinsic viscosity [η] is determined from the intercept in the plot of $\eta_{reduced}$ as a function of a sample concentration at zero concentration (infinite dilution). The inherent viscosity is determined from the intercept in the plot of η_{rel}/c as a function of a sample concentration at zero concentration (infinite dilution).

Calorific value

The IKA C1 calorimeter system was calibrated by 1g (2 Tabs) regular IKA C723 Benzoic acid tabs, with cal.val cross-section, 26461J/g, RSD 0.03%, and LOT SZBD2180V. The temperature was 19 C, 30 bar gas pressure (oxygen) and had 2700 rpm pump flow. The bag was then covered by rolling and placed in a decomposition vessel enclosed by a water jacket, weighing around 0.5g of *A. oerfota* gum and placed in a small plastic bag that has a cross value of 46463j/g. In an oxygen atmosphere, the sample was combusted, and the calorific value of the sample was measured.

Nitrogen and protein content

The total nitrogen in gum samples was calculated according to AOACAC by the Kjeldahl method (1990). The process consists of three basic steps: step one, digestion of the samples with a catalyst in sulfuric acid resulting in the conversion of nitrogen to ammonia, step two, distillation of ammonia into a trapping solution, and step three, quantification of ammonia with a regular solution by titration. The reactions to these steps can be seen as follows:

$$\text{Sample} + H_2SO_4\ (\text{conc.}) + \text{Heat} \rightarrow (NH_4)_2SO_4$$
$$(NH_4)_2SO_4 + 2\ NaOH \rightarrow 2NH_3 + Na_2SO_4 + 2H_2O$$
$$NH_3 + H_3BO_3 \rightarrow NH_4^+ + H_2BO_3^-$$
$$H_2BO_3\text{-} + HCl \rightarrow H_3BO_3 + Cl^-$$

The method

0.5 grams of each sample was weighed and transferred to Kjeldahl digestion flasks and a Kjeldahl tablet (copper sulfate-potassium sulfate catalyst) was applied to each. 10 cm3 concentrated, nitrogen-free, sulphuric acid was also added. The tube was then installed in the digestion heating system, which had previously been set to 240°C and capped with an aerated manifold. The solution was then heated at the above temperature until a strong pale yellowish-green color was observed. This signaled the completion of the digestion. The tubes were then allowed to reach room temperature. Their contents were moved quantitatively to the Kjeldahl distillation apparatus, followed by the addition of distilled water and 30% (w/v) sodium hydroxide. Steam distillation began and the release of ammonia was absorbed by 25 cm3 of 2% boric acid. Back titration of the produced borate was then performed versus 0.02M of hydrochloric acid, using methyl red as an indicator. This was the same way with the blank titration.

$$\%N = \frac{14.01 \times M \times (\text{volume of titrant-volume of blank}) \times 100}{\text{Weight of sample (grams)}}$$

Where: M is the molarity of hydrochloric acid. Protein content was calculated using nitrogen conversion factor resulting from amino acid analysis as follows:% protein =% N x 6.51.

Acid equivalent weight

An Amberlite Resin IR (180H+) was packed with a column of glass. Once the resin was thoroughly washed with the acid, HCl 0.2M was transferred through the column. This was then accompanied by distilled water until the chloride-free column was 20 cm3 eluent equalize to one drop 0.1N NaOH. The column was then passed through 50 cm3 of 3.0% gum solution, followed by purified water until 250 mL of the eluent and washing volume were obtained. This 250 cm3 of eluent is titrated against NaOH of 0.1N. The apparent equivalent acid weight was determined by means of:

$$\text{Equivalent weight} = \frac{\text{Weight of the sample x 1000}}{\text{Volume of liter x Molarity of alkali}}$$

Total uronic acid

Uronic acid was determined by multiplying the molecular weight of uronic acid (194) by 100 and dividing by the apparent equivalent weight of gum sample as follows:

$$\text{Uronic acid\%} = \frac{194 \times 100}{\text{Eq. wt.}}$$

Determination of total polyphenol (tannin%)

The tannin content was calculated based on the Prussian blue assay originally conceived by Price and Butler and subsequently adjusted (Graham 1992). The tannin content is taken to reflect the "total phenols" and more specifically, the "Gallic acid equivalents" as Gallic acid-99% in purity purchased from Sigma Aldrich was used as an analytical criterion for the determination of hydrolyzable tannins. 500 µg/g Gallic acid has been prepared in distilled water. This was then diluted in series to achieve a concentration of 400, 300, 200, 100 and 50 µg/g as normal. 0.10 mL of each sample or norm was dispensed in a universal 30 mL. 3 mL of distilled water was applied by vortex mixing for 30sec. Next 1.00 mL of 0.016M (0.526g/100 mL,w/v) potassium hexacyano ferrate(III) [$K_3[Fe(CN)_6]$, followed by 1.00 mL of 0.02(0.324g$FeCl_3$/100 mL d.w+ 0.83 mLHCl) ferric chloride ($FeCl_3$) were added and immediately mixed by vortex mixer for 30sec. The stabilizer was prepared by a combination of 10.00 metric mL (85%) of 85% phosphoric acid (H_3PO_3), 1.00 mL (1%) of arabic, 30 mL of distilled water, exactly after 15 min (Perkin Elmer Lambda XLS+, UV/ Vis's), in three versions, using an absorptive content, exactly 15 minutes after applying the reagent to the sample 5.00 mL, and the vortex 30 mL of the distilling water. Instead of *A. oerfota* gum or gallic acid standards, solvents are prepared blank by using all reagents and solvent 0.1 mL instead. For all users of Perkin Elmer Lambda 40 UV/Vis spectroscopy, the absorbance was estimated at 700 nm. The measurement error for both samples was less than 10% and the average.

Determination of number average molecular weight by Osmotic pressure

One hundred fifty micrometer of different concentrations (0.25%, 0.5%, 1%, 1.5%, 2%, 2.5%, and 3%) of *A. oerfota* gum samples were ejected into Osmometere 150 and the osmotic pressure was digital determined at 25°C. The number average molecular weight determined using equation:

$$\text{The Intercept} = \lim_{C \to 0} \pi = \frac{RT}{M_n}$$

Where:
π : osmotic pressure,
R : Gas constant,
T : Temperature,
C : Concentration,
Mn : Number average molecular weight.

Rheological measurement

50% w/w of the *A. oerfota* gum solution (based on dry weight) was prepared in distilled water, then the solution was agitated overnight on a tube roller mixer (SRT9. Stuart Scientific, UK) to ensure that the sample dissolves and hydrates completely. The solutions were then centrifuged at a speed of 3000 rpm for 10 minutes using a centrifuge (Megafuge 1.0R, Heraeus SEPATECH, Germany). One dilution was prepared from the stock solution (25% w/w) and re-refused to examine the rheological activity as a prior practice. Rheological measurements were carried out using the Malvern Series KINEXUS pro+ rheometer (Malvern Instruments Ltd., Malvern, Worcester, UK), equipped with a 40 mm cone diameter and a 20 mm angle cone and plate geometry. For gum solutions ranging from 10 to 50% w/v, steady shear viscosity curves were determined both by shear rate ramp-up (from 0.01 to 10000 s-1) and corresponding shear rate ramp-down (from 10000 back to 0.01 s-1). In the 0.1-10 Hz frequency range, dynamic rheological measurements were performed to determine the elastic module (G'), viscous module (G'') and dynamic viscosity. The linear viscoelastic area, at 1 Hz, was evaluated. Using a Peltier element, the temperature of the samples were regulated at 0.1 C. The control and data processing of the rheometer was performed using computer software.

Molecular weight and molecular weight distribution

Sample preparation

Gum samples were prepared (based on dry weight) in 1 mM phosphate buffer at pH 7 containing 0.2 M NaCl, 2.0 mg/mL followed by one dilution (1.0 mg/mL). Then they were hydrated by roller (SRT9. Stuart Scientific, UK) mixing the solution overnight to ensure that the sample was fully dissolved and hydrated. Using Megafuge 1.0R (Heraeus SEPATECH, Germany), the solutions were then centrifuged for 10 minutes at a speed of 3000 rpm. The gum solutions were then filtered prior to injection into the GPC-MALLS system using a 0.45-µm nylon filter (Whatman, 13 mm).

GPC-MALLS

Average molecule weight (Mw) and molecular weight distribution analysis were done using various techniques such as Osmometere, gel permeation chromatography, were subjected to gum exudates from *A. oerfota* tree (GPC-MALLS). The machine used was the Model 6000A Solvent Delivery System Waters (Division of Millipore, USA) connected to a column containing the Superose 6 (Amersham Biosciences) (10 x 300mm), Rheodyne Model 7125 manual syringe. Three detectors, the refractive index (RI) Wyatt Optilab DSP interferometric refractometer operated at 633 nm (Wyatt Technology Corporation, USA), the multi-angle laser light dispersion photometer DAWN EOS operated at 690 nm with He-Ne laser (Wyatt Technology Corporation, USA) and the Agilent 1100 series G1314A UV detector were monitored (214 nm, Agilent Technologies). MALLS makes absolute molecular mass and gyration radius (Rg), and UV detects the protein components of the gum. RI provides a precise concentration profile (Katayama et al. 2006). Data was processed by the program Astra for Windows (version 4.90.07, Wyatt Technology Corporation).

Emulsification properties of the gum

Emulsion preparation

In a glass container, distilled water was applied to 8 g of the gum sample (based on dry weight) to give 40 g in total with a 20% (w/w) gum solution concentration. The specimen was mixed overnight on a roller mixer until the specimen was fully dissolved. For each sample (ranging from approximately 19.97 to approximately 20 g), the exact measured grams of the prepared gum solution was filtered using 100 µm mesh, then combined with 0.52 mL of 10% (w/v) sodium benzoate solution as a preservative. Next, 0.48 mL of 10% (w/v) citric acid solution was added to change the pH to 4, 15.71 mL. Follwed by 15.73 mL of distilled water being added, before 4.2 g of ODO oil was applied. Using a POLYTRON homogenizer (PT 2100, KINEMA TICA AC) at 22000 rpm, the mixed solution was homogenized for 3 minutes. As a dispersing instrument, the Impeller (PTDA21 9 mm tip diameter) was used. The pre-emulsified mixture was homogenized using a high-pressure NanoVater to achieve a small particle size < 1 micron (NV30-FA, MITSUBISHI GOT1000.). It was passed twice at 75 MPa to achieve effective disaggregation of the gum. The final emulsion was held in closed universal glass, and the particle size of the emulsion was measured. Then it was put it in the Vacuum Oven at 60oC (GALLENKAMP. OVA031.XX1.5). After 3 and 7 days, the droplet size was measured again.

Droplet size analysis

Using Mastersizer 3000, a laser diffraction particle size analyzer, the droplet size distribution of the emulsions was measured (Malvern Instruments). As a dispersant, distilled water was used and a value of 1.45 was used for the oil phase refractive index (ODO). After an accelerated stability test for 3 and 7 days, the emulsification stability of samples was maintained at 60C and was evaluated by particle size change. The particle size of the emulsions was determined by the median diameter of the volume (VMD).

Emulsion stability index of *A. oerfota*.

The change in emulsion particle size measured emulsification stability after acceleration check. The emulsion stability index (ESI) was determined using an equation according to the PHRC grading system:

ESI= d0.5as prepared + (d0.53 days@60C-d0.5as prepared) + (d0.57days@60C-d0.5as prepared)

RESULTS AND DISCUSSION

Moisture content

Table 2 shows that with an average value of 12.45%, the moisture content of *A. oerfota* gum obtained from the location of Senga varied between 11.8-13.1%. These findings are the same as those of the samples obtained from the area of Wadel Hadad (11.8-13.4%) with an average value of 12.60%, as shown in Table 3. These findings indicate higher levels of moisture compared to 4.60%, which is supported by Karamalla (1999). These findings comply with the moisture content of The Sudanese Standards (not more than 15%).

Ash content

Tables 2 and 3 reveal that the ash percentage of *A. oerfota* gum is within the range of (1.12-1.40%). The average is 1.26%, which is almost the ash content of the *A. oerfota* gum reported by Anderson (1976) and Karamalla (1999), which was found to be 1.54% and 1.03% respectively. These results are lower than the results reported by Osman (1993) in the *A. senegal* gum study collected from different locations in Sudan, with an average ash content of 3.6%. Results were also lower than those reported for *A. senegal* by Karamalla (1998), Omer (2006), Abdelrahman (2008) and Younes (2009), 3.77%, 3.27%, 3.32% and 4.89% respectively.

pH value

The average Senga value in Tables 2 and 3 show no significant variation between the two locations (4.88-5.26) and Wadel Hadad (4.55-5.28). The *A. oerfota* gum is therefore of low acidity nature. These results are lower than the results recorded by Karamalla (1999), namely 3.5. Compared to *A. senegal* gum, the findings are close to 4.66 as reported by Karamalla et al. (1998) and 4.78 reported by Younes (2009).

Specific optical rotation

Tables 2 and 3 indicate that *A. oerfota* gum's basic optical rotation is +65 to +80, with an average value of 72.5%. These findings align with the outcome stated by Karamalla (1999), which was +64.16. Compared to *A. senegal*, Anderson (1977), Osman (1993), Vavdevelde and Fenyo (1985) reported laboratory values of -30°, -29° to -31° and -29° to -34.4°, respectively. But research by Hassan (2000), Siddig et al. (2005), Omer (2006), Younes (2009), which were +40° to +62°, +45°, +49.4°, and +52° respectively, show a little increase compared to the results calculated, corresponding to *A. seyal*.

Cations composition

Using the electronic scanning microscope process, cationic composition was studied. Tables 4 and 5 show that calcium had the highest value among the cations studied at the location of Wadel Hadad, followed by silicon, potassium, iron, titanium, and strontium. Tables 6 and 7 show that calcium, potassium, silicon, sulfur, and iron are the cation composition of the Senga location.

Viscosity

Acacia oerfota gum viscosity was measured using the U-tube Ostwald viscometer. The results were found to be in the 3.94-10 cm^3g^{-1} range, as shown in Figure 2. Their similarity to the Gummiferae series illustrates these findings. They are distinguished by their low viscosity (Anderson and Herbich 1963, 1966). These findings are lower than the *A. senegal* (9.7-26.5 cm^3g^{-1}) which was obtained by Al-Assaf et al. (2005). For *A. seyal*, Hassan et al. (2005) reported 11.9-17.6 cm^3g^{-1}.

Calculations of the Huggin coefficient (k) and (α) using the Mark-Houwink equation were made based on the relationship of viscometer-determined intrinsic viscosity to GPC-MALLS-determining molecular mass and resulted in 0.86 and 0.0136 respectively.

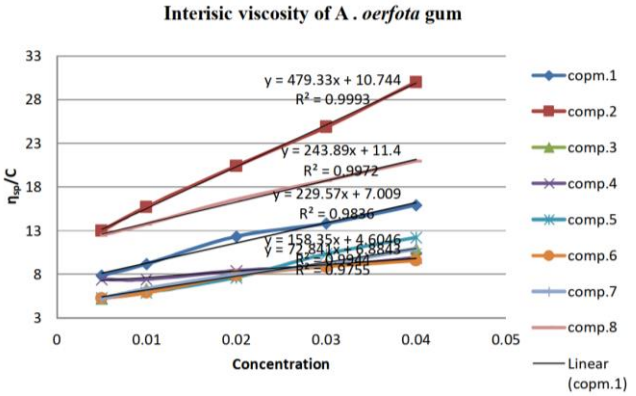

Figure 2. The intrinsic viscosity of six composite sample of *Acacia oerfota* gum.

Table 2. Physicochemical properties of *Acacia oerfota* gum of Senga location.

No.	S. name	Moisture %	Ash %	pH	S.O. Rotation
1	Sample.1	12.37	1.10	4.88	+80
2	Sample.2	13.65	1.12	5.09	+70
3	Sample.3	11.23	1.16	4.97	+65
4	Sample.4	11.67	1.24	5.15	+60
5	Sample.5	13.46	1.22	4.90	+80
6	Sample.6	12.90	1.34	5.22	+60
7	Sample.7	11.13	1.26	5.09	+80
8	Sample.8	12.5	1.28	5.03	+80
9	Sample.9	12.67	1.22	5.13	+65
10	Sample.10	11.98	1.40	5.26	+65
11	Sample.11	12.79	1.30	5.20	+75
12	Sample.12	11.21	1.30	5.08	+65
13	Sample.13	12.02	1.49	5.26	+80
14	Sample.14	12.25	1.29	5.21	+80
15	Sample.15	11.98	1.26	5.18	+80
16	Comp.1	12.35	1.26	4.90	+70
17	Comp.2	12.47	1.27	5.15	+65
18	Comp.3	12.33	1.24	5.16	+75
19	Comp.4	12.16	1.30	5.05	+70
Ranges		11.8-13.1	1.12-1.40	4.88-5.26	+65-+80

Table 3. Physicochemical properties of *Acacia oerfota* gum of Wadel Hadad location.

No.	S. name	Moisture %	Ash %	pH	S.O. Rotation
1	sample.16	12.8	1.60	4.55	+75
2	sample.17	12.2	1.86	4.94	+65
3	sample.18	12.5	1.56	4.96	+65
4	sample.19	12.7	1.58	4.65	+70
5	sample.20	13.1	1.83	5.02	+70
6	sample.21	12.2	1.43	4.88	+80
7	sample.22	12.6	1.62	4.88	+65
8	sample.23	12.9	1.61	4.94	+80
9	sample.24	13.4	1.27	4.97	+75
10	sample.25	11.9	1.83	4.60	+75
11	sample.26	12.6	1.40	4.90	+75
12	sample.27	11.8	1.53	4.90	+70
13	sample.28	12.4	1.16	5.28	+75
14	sample.29	12.6	1.20	4.87	+70
15	sample.30	13.0	1.65	4.90	+75
16	Comp.5	12.2	1.60	4.83	+80
17	Comp.6	12.6	1.63	4.90	+75
18	Comp.7	12.9	1.31	4.88	+65
19	Comp.8	12.5	1.65	4.86	+70
Ranges		11.8-13.4	1.18-1.31	4.55-5.28	+65-+80

Table 4. The cationic composition of *A. oerfota gum*-Wadel Hadad location.

Element	Result	Unit
Ca	0.287	%
K	0.131	%
Fe	0.010	%
Sr	0.004	%

Table 5. The cations composition% to the total amount of cations included in *A. oerfota* gum of Wadel Hadad location

Element	Ca	Si	K	Fe	Ti	Sr
Percentage %	58.783	18.670	16.248	3.955	1.285	1.099

Table 6. The cationic composition of *A. oerfota* of Senga location

Element	Result	Unit
Ca	0.242	%
K	0.145	%
Sr	0.005	%
S	0.002	%
Fe	0.001	%

Table 7. The cationic composition% to the total amount of cations included in *Acacia oerfota* gum of Senga location.

Element	Ca	K	Sr	S	Fe
Result	62.633	19.628	12.729	3.549	1.461

Calorific value

Table 8 shows that the calorific values of the *A. oerfota* gum are like the calorific values of the gums and were approximately 4 Kcal/g. This calorific value is very low, so after evaluating the toxicity value, the *A. oerfota* gum is very suitable for use as a food additive.

Nitrogen and protein content

The average nitrogen and protein content of *A. oerfota* gum samples was higher than the nitrogen and protein content of *A. senegal* and *A. seyal* gum. The average nitrogen and protein content of *A. oerfota* gum was found to be 0.53 and 3.28% respectively in Table 9. Anderson (1977) estimated that *A. senegal* gum's nitrogen content was 0.29% and 0.14% for *A. seyal*. Osman (1993) reported a nitrogen content of 0.31% and a protein content of 2.4% for *A. senegal* gum. Hassan et al. (2005) reported that *A. seyal*'s protein content had a mean value of 0.96%. Younes (2009) estimated a nitrogen content of 0.35% and a protein content of 2.3% for *A. senegal*. *A. senegal*'s nitrogen content was analyzed by Idris et al. (1998), from various age groups and locations. The range between 0.22-0.39% and the protein content was therefore found to vary, 1.5-2.6%.

Equivalent weight and total uronic acid

Table 10 revealed that *A. oerfota* has an acid equivalent weight and total uronic acid percentages of gum (2941-5357) and (3.62-6.60) of *A. oerfota*, and *A. oerfota*'s rule acidity (1993), while Osman (1993) estimated that the acid equals 1040, while the uronic acid is 17%.

Table 9. Nitrogen and protein content of *Acacia oerfota* gum

location	Sample code	Nitrogen content	Protein%
Wadel Hadad	Comp.1	0.49	3.06
	Comp.2	0.63	3.94
	Comp.3	0.51	3.11
	Comp.4	0.49	3.06
Senga	Comp.5	0.35	2.19
	Comp.6	0.77	4.81
	Comp.7	0.43	2.71
	Comp.8	0.42	2.63

Table 8. The calorific values of gum *Acacia oerfota* gum.

Sample name	Sample location	Sample weight	bag Cal. value J/g	Cross cal. Value	Net Cal. value J/g	net.Cal.value. cal/g	Cal Value Kcal/g
A.*Oerfota* gum	Senga	0.5189	46463	15805	17024	4067	4.067
A.*Oerfota* gum	Wadel Hadad	0.5066	46463	15596	16829	4020	4.020

Color Gardner and Tannin content

The color Gardner of gum *Acacia oerfota* is 0.1 for Senga composite sample and 0.2 for Wadel Hadad composite sample. Table 11 shows that the values increase with time (24 hours and 48 hours) due to oxidation of polyphenol. Tannin content was calculated according to Kjeldahl method. The two composite samples have tannin content of about 268.0 and 292.1 mg/g, respectively.

Determination of number average molecular weight by Osmotic pressure

The results obtained for gum *Acacia oerfota* are consistent with the observation that *Gummiferae* series typically possess a high molecular weight. Figure 3 shows the values of number average molecular weight (Mn) of gum *Acacia oerfota* obtained by osmotic pressure are 1.68×10^5 and 1.80×10^5g/ Nol for the two total composites of two locations. These values were lower than the values obtained by gel permeation chromatography $6.23x10^5$ and $9.59x10^5$. The difference in the results is probably due to the differences between the two techniques. The values of number average molecule weight (Mn) of A. *oerfota* gum is not more variable than that of A. *senegal* 2-3 x 10^5 (Osman, et.al.1993).

Table 10. Equivalent weight and uronic acid of *Acacia oerfota* gum.

Location	Sample	Acid eq. weight	Uronic acid%
Wadel Hadad	comp.1	3409	5.69
	comp.2	3571	5.43
	comp.3	3333	5.82
	comp.4	2941	6.60
Senga	comp.1	5357	3.62
	comp.2	3846	5.04
	comp.3	3192	6.08
	comp.4	3409	5.69

Table 11. Color and tannin value of *Acacia oerfota* gum.

Location	off Hue	L*	a*	b*	Gardner	Tannin (ppm)
After 3 hours						
Senga	0	99.3	-0.02	0.84	0.1	268.0
Wadel hadad	0	98.71	-0.05	1.37	0.2	292.1
After 24 hours						
Senga	0	99.6	-0.11	0.86	0.1	268.0
Wadel hadad	0	99.14	-0.08	1.46	0.3	292.1
After 48 hours						
Senga	0	98.04	-0.07	2.09	0.3	268.0
Wadel hadad	0	97.83	-0.17	2.63	0.3	292.1

Infrared spectroscopy (FTIR)

Acacia oerfota defined different functional classes in the entire spectrum (FTIR) (Figure 4). Glucurónic acid covers a wide range of 3600-3000 cm-1 in an O-H stretch, which is the most prominent and strongest band. Simultaneously, the belt displays a vibration of C=O stretching in the center of the spectrum in 1730 cm-1. The deep stretching vibration occurs with 1031 cm-1 hydroxyl grouping of composite sugars with phenol like C-O band. Aliphatic C-H strain and still vibration are respectively the cause of the bending weakness of the beak at 2929 cm-1 with approximately 1,500 cm-1.

Rheology of the gum

In two different concentrations, 25% and 50%, the Rheological activity of *A. oerfota* gum was researched. *A. oerfota* gum displays Newtonian behavior according to Figures 5, 6 and 7 (viscosity is constant with increasing applied shear rate), and the molecules maintain initial viscosity to remove the applied stress (Braun and Rosen 2000).

The dynamic rheology

Figure 8 indicates that *A. oerfota* gum's loss modulus (G") was higher than the storage modulus (G') and they do not cross, so *A. oerfota* gum is not viscous, elastic, or viscoelastic.

The frequency sweep offers gel strength information, where a high G curve slope indicates low strength, and a small slope indicates high strength (Mezger 2002). Both gums exhibited similar gel strength. As the G' modulus is frequency-dependent, but the G' modulus depends on the frequency square (Barnes et al. 2001). G' at higher frequencies becomes more important. G" is greater than G' compared to *Acacia tortilis*, and then *Acacia tortilis* has viscose properties at a lower frequency. Systematically, with increasing frequency over a wide spectrum, the *Acacia tortilis* solution transitions from viscose to elastic properties (Mezger 2002). Above critical frequency, *Acacia tortilis* forms solid gels (0.5 HZ).

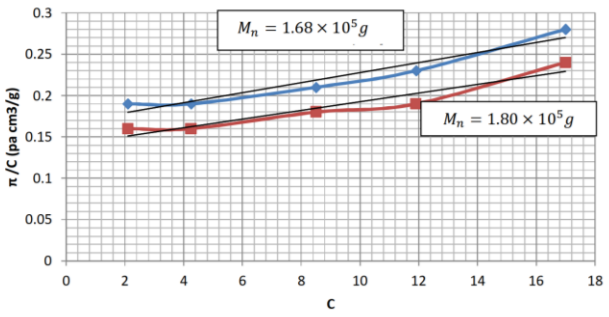

Figure 3. A plot of G versus C for *Acacia oerfota* gum at 25 C.

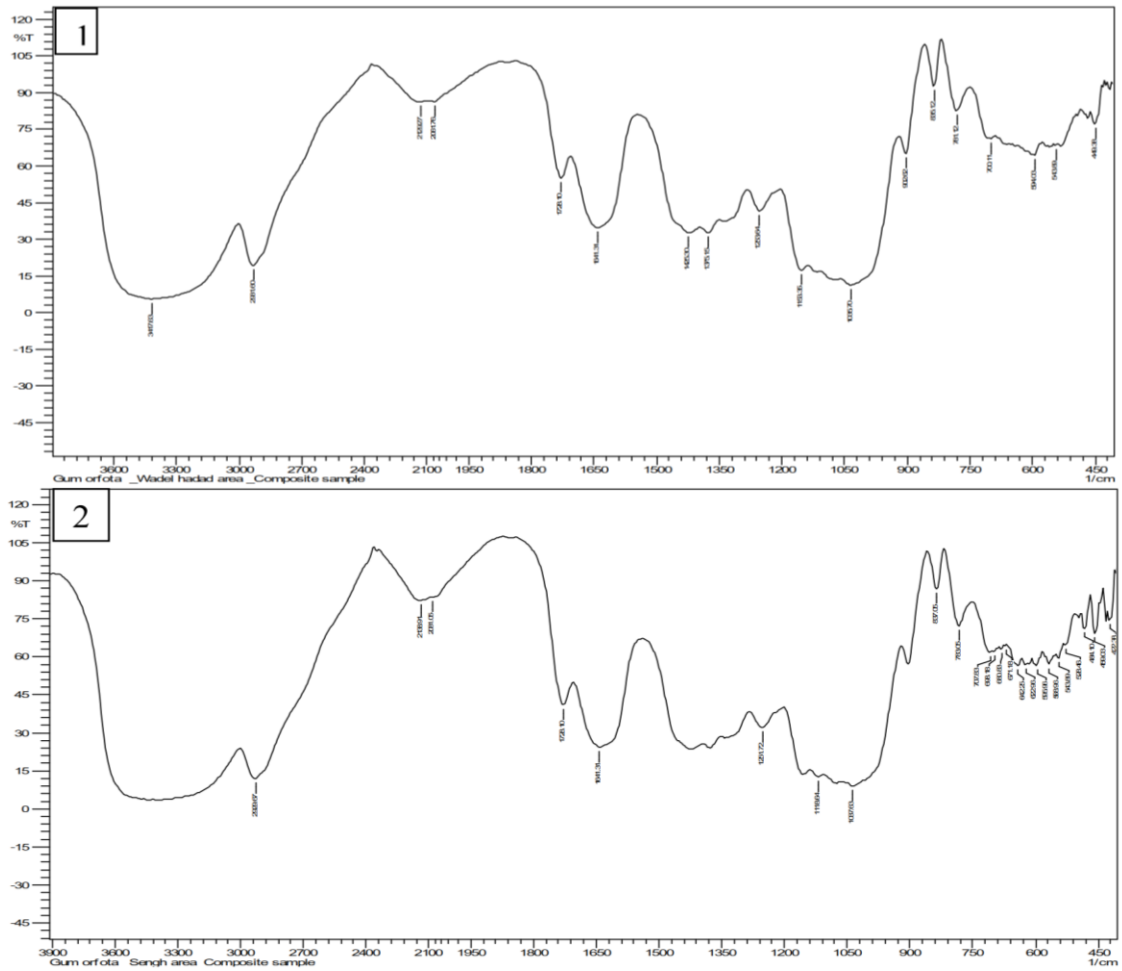

Figure 4. FTIR of composite sample of *Acacia oerfota* from (1) Senga location, (2) Wadel Hadad location.

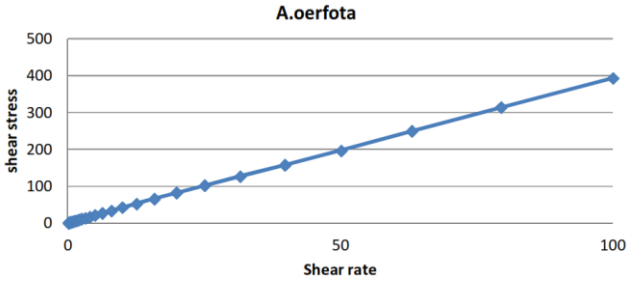

Figure 5. Shear rate versus shear stress of *Acacia oerfota* gum.

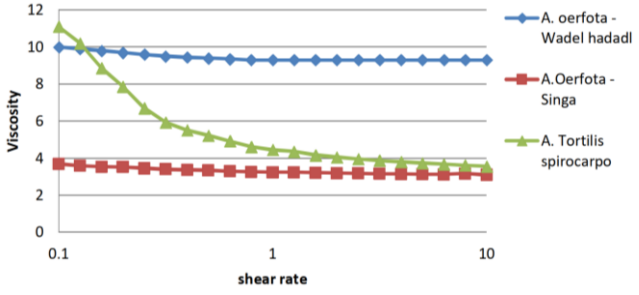

Figure 6. Viscosity profile of *Acacia* gum emulsions with shear rate-conc. 25%.

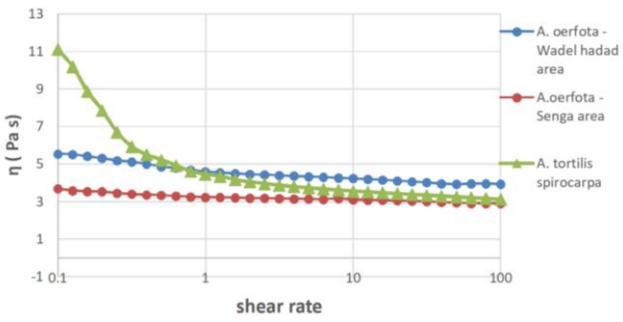

Figure 7. Viscosity profile of *Acacia* gums emulsions with shear rate-conc. 50%.

Gel permeation chromatography (GPC MALLS)

GPC-MALLS with on-line monitoring used RI, LS, and UV absorbance detectors. The GPC-MALLS result for *A. oerfota* and *A. senegal* gum are shown in Table 12.

GPC MALLS-RI

RI profiles of *A. oerfota* and *A. senegal* gums are shown in Figure 9. The profile consists of three AGP, AG and GP highlights. In the first AGP peak, the situation is very different. In contrast to *A. senegal* gum AGP, the mass percent of the AGP of the two *A. oerfota* gums are very poor.

Table 12. The GPC-MALLS result for *Acacia oerfota* and *A. senegal* gum.

Function/sample	*A. oerfota*.1	*A. oerfota*.2	*A. senegal*
Mw whole gum (x10^5)	6.23	9.59	5.95
% Mass recovery	108.685	105.78	113.97
Rg (whole gum)/nm	178	178	50.6 (6%)
Mw AGP	4.77	14.19	1.68
% mass (AGP)	1.11	0.84	17.73
Rg-AGP	50	187	38. (3%)
Mw (AG+GP) (x10^5)	5.76	8.24	3.59
% mass (AG+GP)	98.89	99.16	82.27

GPC MALLS-LS

Light scattering profiles for AGP and AG of the two *A. oerfota* and *A. senegal* gums are shown in Figure 10. The first peak illustrates the substantial difference between the molecular weights of the protein components of Arabinogalactan in the gums of *A. oerfota* and *A. senegal*. In contrast, the molecular weight of the Arabinogalactan protein in *A. oerfota* is very low. However, *A. oerfota*'s AG+GP molecular weight is higher than that of *A. senegal* gum.

GPC MALLS-UV

The UV and GPC profiles for *A. oerfota* and *A. senegal* gums are shown in Figure 11. Clearly, they demonstrate a large difference in protein content. In contrast to that of *A. senegal* gum, the AGP signal of *A. oerfota* gum is very weak. However, the AG and GP signals are nearly identical, suggesting a similar composition of proteins.

The emulsification properties of *A. oerfota* gum

Good emulsions are characterized by a narrow band and a wide particle diameter of between 0.1 and 1 micron. The emulsification properties of *A. oerfota* gum have been analyzed by assessing the emulsion particle size at zero and after 3 and 7 days of incubation at 60°C.

The position had no major impact on the emulsification properties of *A. oerfota* gum, as seen in Table 13. The mean weighted surface D(3,2) and the mean weighted volume D(4,3) increased, and the percentage of the duration decreased with time.

Compared to D, D(4,3) is more susceptible to the presence of large particles in an emulsion (3,2). Thus, D(4,3) is more susceptible to the flocculation phenomenon. As all emulsions display large droplets, this could explain the higher value of D(4,3) relative to D(3,2). According to the emulsion stability index value used as a criterion to determine the grade of the gum sample, the gum is built to be grade 3.

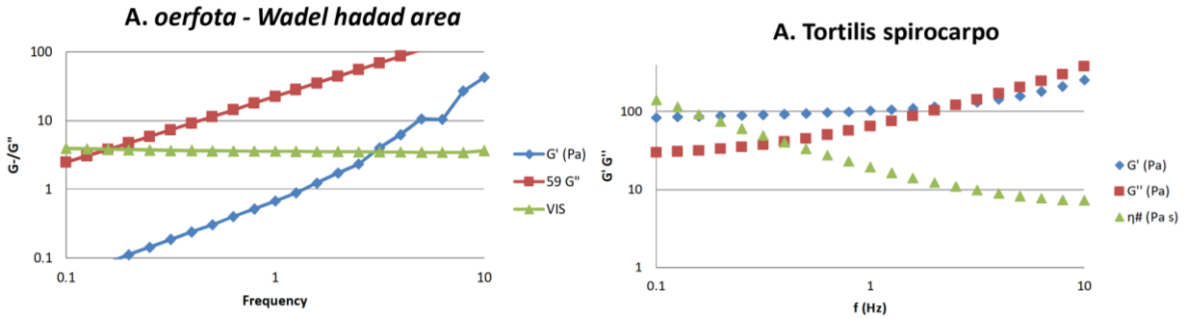

Figure 8. The effects of frequency on G' and G".

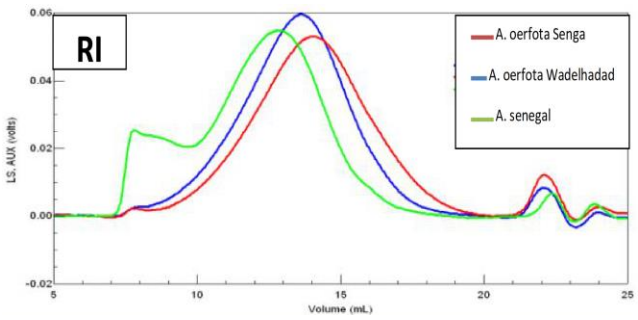

Figure 9. The RI of two Composite samples of *Acacia oerfota* and *A. senegal.*

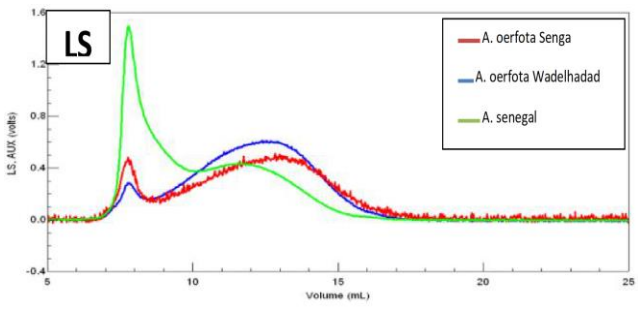

Figure 10. The LS of two composite samples of *Acacia oerfota* and *A. senegal.*

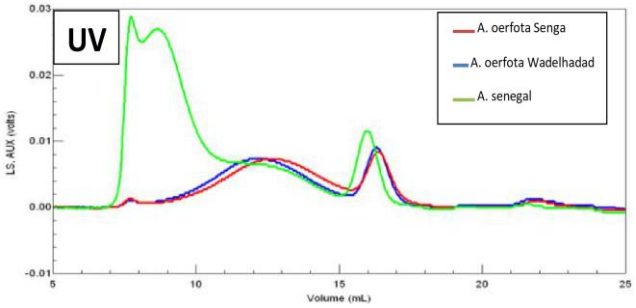

Figure 11. The UV of two Composite samples of *Acacia oerfota* and *A. senegal.*

Figure 12 shows more variable particle sizes spread over a wide range of microns (0.1-10) and most particle diameter sizes are high, suggesting *A. oerfota* gum emulsion instability (Billmeyer 1971). A standard bimodal droplet size distribution with a pronounced shoulder representing two droplet groups with the small and largest diameter was seen in the emulsions. In the range of good emulsion particle size, it decreased with time according to the phase of flocculation and coalescence. The instability of the emulsions was confirmed by the pig droplet size and low viscosity (3.4 11.4 cm^3g^{-1}) and pig rate of gyration of *Acacia oerfota* gum.

Figure 13 shows a high polydispersity index value (percent span) for fresh emulsions and after incubation at 60oC for 3 and 7 days, respectively. Two positions suggest low droplet size uniformity. These values indicate emulsion instability by reducing the amount of protein that is associated with the emulsion droplet surface.

Relevant surface area (m^2/g) of cumulative droplet distributions of (D.5, D.9, >1 micron and >2 micron) are shown in Figure 14. The results clearly showed that drastic changes in emulsions were observed during incubation at 60oC for 3 and 7 days. Emulsion instability has also increased by reducing the region of D(0.5) to less than 6% and increasing the size of droplet particles with a diameter of more than one micron to more than 80%.

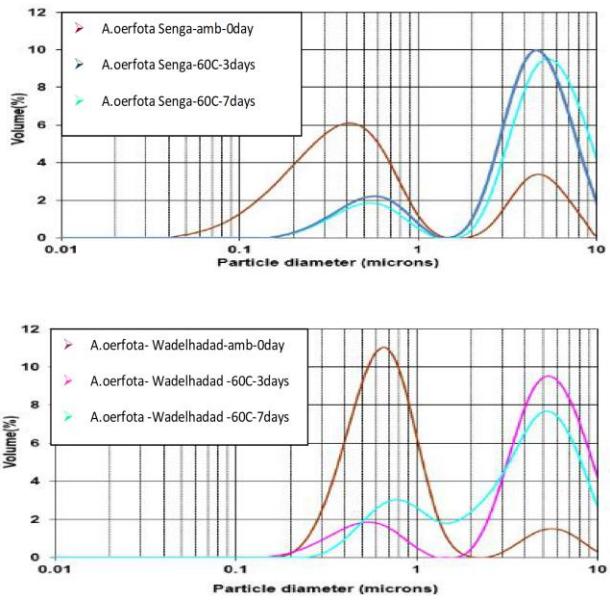

Figure 12. The emulation particle size profile of *Acacia oerfota* from two locations.

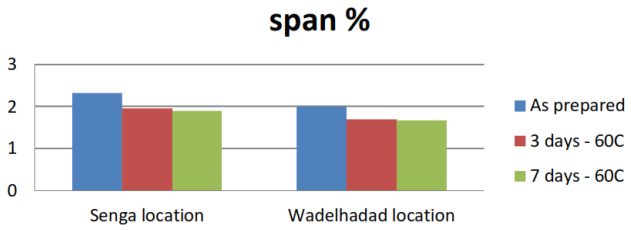

Figure 13. The span% of *Acacia oerfota* gum from two locations

Table 13. The emulsification properties of *Acacia oerfota* gum.

	Senga location			Wadel Hadad location		
Character	**As prepared**	**After 3 days**	**After 7 days**	**As prepared**	**After 3 days**	**After 7 days**
D(3,2)	0.674	1.81	1.99	0.364	2.08	1.79
D(4,3)	1.26	4.43	4.34	1.56	5.42	4.46
span%	2.32	1.95	1.9	1.98	1.74	1.68
Dx(10)	0.40	0.69	0.74	0.166	0.63	0.58
Dx(20)	0.49	0.96	1.16	0.238	2.95	2.17
Dx(50)	0.72	4.26	4.08	0.477	3.23	4.42
Dx(80)	1.1	7.3	6.91	3.51	8.1	6.63
Dx(90)	2.1	8.98	8.49	5.4	9.71	7.98
Grade	3	3	3	3	3	3

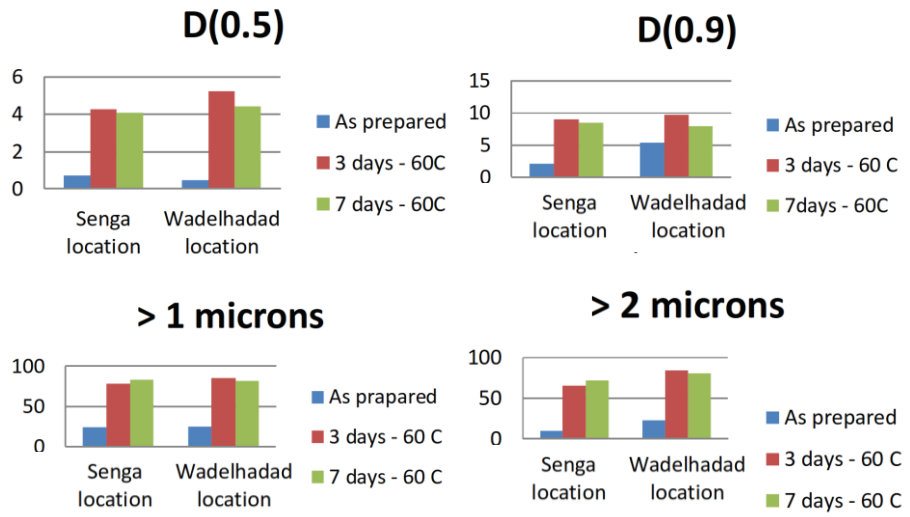

Figure 14. The volume-weighted mean diameter of *Acacia oerfota* gum emulsion from two locations

In conclusion, *Acacia oerfota* gum displays physicochemical properties that indicate its similarity to the sequence of Gummiferae. The rheology of *A. oerfota* solution gum indicates that Newtonian fluid is formed by the gum. The modulus of loss of *A. oerfota* gum is larger than the module for storage. *A. oerfota* gum's molecular weight varies between (6.23x105 and 9.59x105 g/mole) with the same gyration radius. In contrast to *A. senegal*, the Arabinogalactan protein of *A. oerfota* gum has just 1% mass and low molecular weight. *A. oerfota* gum forms an unstable emulsion that is weak.

REFERENCES

Abdel Nour HO. 1999. Gum Arabic in Sudan: Production and socio-economic aspect. International Expert Meeting on Medicinal, Culinary and Aromatic Plants in the Near East, Cairo (Egypt), 19-21 May 1997.

Abdelrahman MA. 2008. Characterization, thermodynamic, denaturation and molecular expansion properties of *A. seyal*, *A. senegal* and *A. Polyacantha*. [Doctoral dissertation, Ph. D Thesis]. Chemistry Department, Faculty of Science, Sudan University of Science and Technology, Sudan.

Al-Assaf S, Phillips GO, Williams PA. 2005. Studies on *Acacia* exudate gums: part II. Molecular weight comparison of the Vulgares and Gummiferae series of *Acacia* gums. Food Hydrocoll 19 (4): 661-667.

Anderson DMW, Cree GM. 1968. Studies on uronic acid materials: Part XXVII. The structure of the gum from *Acacia* nubica Benth. Carbohydr Res 6 (4): 385-403.

Anderson DMW, Herbich MA. 1963. Studies on uronic acid materials. Part VI. The variation in composition and properties of gum nodules from *Acacia seyal* del. J Chem Soc: 1-6.

Anderson DMW, Stoddart JF. 1966. Studies on Uronic Acid Materials. Part XV. The use of molecular-sieve chromatography in studies on *Acacia senegal* gum (Gum Arabic). Carbohydr Res 2: 104-114.

Anderson DMW. 1976. Analytical method for identification of gum exudates from *Acacia* species fourth international symposium. Gum and Hydro-Soluble Natural Vegetal Colloids, 5th-8th November, France.

Anderson DM. 1977. Water-soluble plant gum exudates. Gum Arabic. Porc Biochem 12: 24.25.

AOAC. 1984. Official Methods of Analysis. Association of Official Analytical Chemists, fourth Edition. Washington D.C.

Australian National Herbarium. Retrieved October 24, 2013.

Barnes HA, Hutton JF, Walters K. 2001. An Introduction to Rheology. Elsevier Science Pub Co.

Billmeyer FW. 1971. Textbook of Polymer Science. Interscience Publisher, New York.

Braun DB, Rosen MR. 2000. Rheology Modifiers Handbook-Practical Use and Application. William Andrew Publishing, Norwich, New York, USA.

Clemens J, Jones PG, Gilbert NH. 1977. Effect of seed treatments on germination in *Acacia*. Australian Journal of Botany, 25(3), 269-276.

Elamin HM. 1973. Sudan *Acacias*. Publishing Section Information Department, Sudan.

Elamin HM. 1990. Trees and shrubs of Sudan. [Dissertation]. University of Khartoum, Sudan.

Elmer P. 1994. Analytical Methods for Atomic Absorption Spectrometry. The Perkin Elmer Corporation, USA.

El-Gazali GE. 1985. The Pollen Flora in Sudan, with Special Reference to Pollen Identification. John Willy & Son Inc., London.

FAO. 1990. Specification for identity and purity of certain food additives. Food Nutrition Paper, FAO, Rome.

Gibreel HH. 2008. A taxonomic study on trees and shrubs of Alnour natural forest reserve, Blue Nile State. [Thesis] University of Khartoum, Sudan.

Graham HD. 1992. Stabilization of the Prussian blue color in the determination of polyphenols. J Agric Food Chem 40 (5): 801-805.

Hassan EA. 2000. Characterization and Fractionation of *Acacia seyal* Gum. [Dissertation]. University of Khartoum, Sudan.

Hassan EA, Al-Assaf S, Phillips GO, Williams PA. 2005. Studies on *Acacia* gums: Part III molecular weight characteristics of *Acacia seyal* var. *seyal* and *Acacia seyal* var fistula. Food Hydrocoll 19 (4): 669-677.

Idris OHM, Williams PA, Phillips GO. 1998. Characterisation of gum from *Acacia senegal* trees of different ages and locations using multidetection gel permeation chromatography. Food Hydrocoll 12 (4): 379-388.

Karamalla KA, Siddig NE, Osman ME. 1998. Analytical data for *Acacia senegal* var. senegal gum samples collected between 1993 and 1995 from Sudan. Food Hydrocoll 12 (4): 373-378.

Karamalla KA. 1999. Gum arabic production, chemistry and applications. University of Khartoum, Sudan.

Katayama T, Nakauma M, Todoriki S, Phillips GO, Tada M. 2006. Radiation-induced polymerization of gum arabic (*Acacia senegal*) in aqueous solution. Food Hydrocoll 20 (7): 983-989.

Mezger TG. 2002. The Rheology Handbook for Users of Rotational and Oscillatory Rheometers. Coating Compendia, Hannover.

Omer IE, Bakheit TN. 2006. Determination of tracer 240 SC (spinosad) and sumigold (esfenvalerate) residues in *Acacia* plant and soil. In Proceedings: The 75th meeting of the national pests and diseases

committee. Agricultural Research Corporation Conference Hall, Wad Medani (Sudan), September 2006.

Osman ME. 1993. Industrial uses of Gum Arabic (*Acacia senegal*). [Dissertation]. Salford University, UK.

Siddig NE, Osman ME, Al-Assaf S, Phillips GO, Williams PA. 2005. Studies on *Acacia* exudate gums, part IV. Distribution of molecular components in *Acacia seyal* in relation to *Acacia senegal*. Food Hydrocoll 19 (4): 679-686.

Singh G. 2004. Plant Systematics: An Integrated Approach. Science Publishers, New Delhi.

Smith GF, van Wyk AE, Luckow M, Schrire B. 2006. Conserving *Acacia* Mill. with a conserved type. What happened in Vienna?. Taxon 55 (1): 223-225.

Thanukos. 2009. A name by any other tree. Evolution: Education and Outreach 2 (2): 303-309. DOI:10.1007/s12052-009-0122-7.

USDA. 2008. ARS, National Genetic Resources program. Germplasm Resources Information Network, National Germplasm Resources Laboratory, Beltsville, MD.

Younes AAO. 2009. Physicochemical Studies on some *Acacia* Gum sand their Fractions. [Dissertation]. Sudan University of Science and Technology, Khartoum, Sudan.

ASIAN J TROP BIOTECHNOL
Volume 18, Number 1, June 2021
Pages: 13-27

ISSN: 0216-6887
E-ISSN: 2301-8658
DOI: 10.13057/biotek/c180102

The carotenoid biosynthesis pathway in the asexual intraerythrocytic stages of *Plasmodium falciparum*

RICHARD NORTEY-MENSAH[1], MARIAN A. TEYE[1], MICHAEL F. OFORI[2,♥]

[1]Department of Biochemistry, Cell and Molecular Biology, University of Ghana. Legon, Accra, Ghana
[2]Noguchi Memorial Institute for Medical Research (NMIMR), University of Ghana. Legon, Accra, Ghana. ♥email: mofori@noguchi.ug.edu.gh, moforiori@noguchi.mimcom.org

Manuscript received: 30 November 2020. Revision accepted: 26 March 2021.

Abstract. *Nortey-Mensah R, Teye MA, Ofori MF. 2021. The carotenoid biosynthesis pathway in the asexual intraerythrocytic stages of Plasmodium falciparum. Asian J Trop Biotechnol 18: 13-27. Plasmodium falciparum*, like other Apicomplexans, possesses a dormant plastid called the apicoplast. Because it houses metabolic pathways peculiar to the parasite, such as isoprenoid production, this organelle promises a new target for the chemotherapeutic control of malaria. Although the phytoene synthase (PSY) gene has been shown to be critical for carotenogenesis; nothing is known about its evolutionary relationship with *P. falciparum* and other Apicomplexans. The goal of this work was to identify the evolutionary history and relatedness of the PSY gene in Apicomplexans and other animals, as well as to profile the carotenoids generated in the asexual intraerythrocytic stages of *P. falciparum.* Fluridone's IC50 and effect on parasite population were determined utilizing in vitro inhibition experiments on the asexual intraerythrocytic stages of *P. falciparum.* To examine the evolutionary history and relatedness of the PSY gene in Apicomplexans and other taxa, HPLC was used to profile carotenoids created at the asexual phases, and an unrooted phylogenetic tree was built using MEGA 6. Dose-dependent inhibition of parasite population was observed with fluridone treatment on all the asexual stages, with the ring stages being the most vulnerable. The carotenoid profiles revealed that carotenoids are generated cumulatively in *P. falciparum* throughout the asexual intraerythrocytic phases, with carotenoids such as lycopene, α-, β-carotene among those synthesized. The discovery of relatively high quantities of abscisic acid (ABA) in the schizont stages, but not in the other stages was an interesting novel finding of this study. This is the first time ABA has been shown to be synthesized by *P. falciparum*, and additional research into the specific role of ABA in *P. falciparum* schizont phases would be groundbreaking. The phylogenetic study revealed that the *P. falciparum* PSY was most closely related to *P. reichenowi*, a chimpanzee strain of the malaria-causing parasites, supporting the hypothesis that malaria species in humans originated in chimps.

Keywords: Bioinformatics analysis, carotenoids, HPLC, in vitro, inhibition assays, *Plasmodium falciparum*

INTRODUCTION

Malaria is still one of the most serious parasite infections that affect humans, producing significant morbidity and mortality in tropical areas. According to the World Malaria Report, 198 million cases of malaria were reported worldwide, resulting in 580,000 fatalities (WHO 2014). Malaria is still endemic across five continents, despite ongoing and extensive attempts to suppress the illness. As a result, more than half of the world's population is at risk. *Plasmodium* parasites, of which there are five species, namely *P. falciparum*, *P. vivax*, *P. ovale*, *P. malariae* and *P. knowlesi* (Jiang et al. 2010; Sermwittayawong et al. 2012), cause human malaria, with the great majority of malaria-related deaths are caused by *P. falciparum* (Bousema and Drakeley 2011; Hay et al. 2009). The failure of vector control initiatives, the lack of a vaccine, and an increase in parasite resistance to routinely used therapeutic medicines have all contributed to the global spread of the disease (Sharma and Dutta 2011; Shiff 2002). The development of new chemotherapeutic techniques and medicines to attack *Plasmodium* necessitates a thorough understanding of the parasite's metabolic pathways. These new chemotherapeutic strategies and agents can be developed in one of three ways: (i) by developing new drug candidates based on previously validated parasite targets, (ii) by identifying new potential parasite targets for malaria chemotherapy, or (iii) by performing high-throughput drug library testing (Choi et al. 2008).

As in other apicomplexans (e. g. *Toxoplasma* spp.), *Plasmodium* parasites have retained a relic plastid organelle known as apicoplast which comes from plastid-bearing red algae of secondary endosymbiosis millions of years ago (Foth and McFadden 2003). As a result, the apicoplast is prokaryotic in origin, containing pathways that do not exist in the human host. It possesses a genome that is like that of plants and algae, and according to proteome research, its metabolic processes include type II fatty acid and isoprenoid production (Sato 2011). A range of new plant-like enzymes has recently been found in malaria parasites, particularly the most virulent species, *P. falciparum*, with some of these being linked to the apicoplast (Kalanon and McFadden 2010). These enzymes are known to be part of many important biochemical pathways in plants and algae (Foth and McFadden 2003; Gornicki 2003; Seeber 2003). The carotenoid biosynthesis pathway is one of these metabolic pathways. It is an intriguing topic for research because it is required in algae,

higher plants, bacteria, and fungi but not in mammals. The pathway's products are engaged in a variety of vital metabolic functions (Paniagua-Michel et al. 2012).

Plasmodium also retains biosynthesis of isoprenoids (resident in apicaloplast) resulting in the synthesis, by the pathway mevalonate-independency, of isopentenyl pyrophosphates (IPP) and dimethylallyl phosphates (DMAPP) (Jordão et al. 2011; Rodríguez-Concepción and Boronat 2013). These isoprene units serve as building blocks for the synthesis of isoprenoids, rather than being an end in themselves (for example, carotenoids). Fosmidomycin, an inhibitor of non-mevalonate isoprenoid precursor production in the apicoplast, has previously been shown to impede the proliferation of asexual blood-stage *P. falciparum* (van der Meer and Hirsch 2012; Wiesner et al. 2003). Supplementation with IPP, the pathway product, chemically reversed fosmidomycin inhibition in *P. falciparum*, according to Yeh and DeRisi (2011). In addition, abscisic acid (a product of the isoprenoid pathway) has been linked to the control of calcium-dependent parasite egress in *T. gondii*, a similar apicomplexan, with suppression of its synthesis resulting in dose-dependent delays in parasite egress from the host cell (Nagamune et al. 2008). The isoprenoid biosynthetic pathway is required for the survival of apicomplexan parasites during their infective phases, according to these findings. Most of the downstream products of this pathway, as well as their roles in the asexual intraerythrocytic stages of *P. falciparum* parasites, are unclear currently.

In *Plasmodium*, various genes have been proposed to play a role in the carotenoid biosynthesis pathway, but only the phytoene synthase (*PSY*) gene (PfB0130w) has been definitively identified through functional experiments (Rodrguez-Villalón et al. 2009; Toledo-Ortiz et al. 2010). The phytoene synthase (*PSY*) gene encodes the enzyme phytoene synthase (PSY), which is a crucial protein because it catalyzes the first committed and rate-limiting step in the carotenoid biosynthesis pathway (Welsch et al. 2000) and acts as a key regulator of carbon inflow into the process. Rodrguez-Villalón et al. (2009) and Welsch et al. (2000) found that it catalyzes the condensation of two molecules of geranylgeranyl diphosphate (GGPP) to create phytoene, the basic C-40 carotenoid skeleton of all carotenoids. The *PSY* protein's structure (secondary and tertiary), function, and phylogenetic history in apicomplexans, plants, bacteria, and algae have all been studied (Tonhosolo et al. 2005; Agarwal et al. 2015). The evolutionary history and relatedness of PSY gene have been studied in other species. However, there are no studies on the gene's evolutionary history and relatedness in apicomplexans.

The specific goals of this study were to: (i) investigate the effect of fluridone on the asexual intraerythrocytic stages of *P. falciparum* using in vitro inhibition assays, (ii) to profile the carotenoids synthesized by the asexual intraerythrocytic stages of *P. falciparum* using High-Performance Liquid Chromatography (HPLC), and (iii) to figure out the evolutionary history and relatedness of the phytoene synthase gene in *P. falciparum* and other organisms through bioinformatics analysis.

MATERIALS AND METHODS

All work relating to parasite culture was performed in a biological safety cabinet (BSC) using aseptic techniques.

Media preparation and parasite culture

Preparation of media for culturing

RPMI 1640 [with L-glutamine and HEPES (N-2-hydroxyethyl piperazine-N'-2-ethane sulfonic acid)] (Gibco, UK) which was supplemented with 7.5 % NaHCO3 (Sigma-Aldrich, USA) (working concentration, 32 mM), 20 % glucose (Sigma-Aldrich, USA) solution (working concentration, 20 mM), and gentamycin (Gibco, UK) (working concentration, 10g/ml) was used to generate 500mL parasite washing media (PWM). PWM supplemented with 5mg/ml Albumax II (Invitrogen, USA) and 0.2g/mL hypoxanthine (Sigma- Aldrich, USA) was used to produce complete parasite medium (CPM). All of the culture mediums were kept between 4 - 8°C of temperature.

Thawing of cryopreserved parasite

Plasmodium falciparum 3D7 strain [which was cryopreserved and obtained from the Immunology Department of the Noguchi Memorial Institute for Medical Research (NMIMR), Ghana] was removed from liquid nitrogen storage and thawed in a 37ºC water bath for 1 minute. After that, for every 100L of parasite suspension, 12 % NaCl (Sigma-Aldrich, USA) was added. After a 5-minute incubation period at room temperature, one-tenth of a parasite suspension in 1.6 % NaCl was introduced drop by drop to the tube while gently rotating it. At room temperature, the suspension was centrifuged for 5 minutes at 1500 revolutions per minute (rpm) (RT). The erythrocytes were resuspended in complete parasite medium (RPMI 1640 containing 5mg/mL Albumax II, 10g/mL gentamycin, 0.2g/mL hypoxanthine, 2 mM L-glutamine, 25 mM HEPES, 23.8 mM NaHCO3) after the supernatant was removed. After that, the suspension was centrifuged at 1500 rpm for 5 minutes at room temperature. The parasitized RBCs were added to 200l of freshly generated sickling negative, O+ human erythrocytes in a 25ml tissue culture flask (Corning, USA) containing 5ml CPM after the supernatant was removed.

Parasite culture and maintenance

Plasmodium falciparum 3D7 strain (NMIMR, Ghana) was cultured as described by Trager and Jensen (1976), with a few changes (Maier and Rug 2013). In either 25ml or 75ml tissue culture flasks, site cultures were maintained in CPM with human O+, sickling negative erythrocytes at 4% hematocrit (Corning, USA). In 25ml and 75ml tissue culture flasks, five milliliters (5ml) or twenty-five milliliters (25ml) of CPM were employed to keep the cultures alive. The flasks were then gently flushed with the gas combination, firmly closed, and incubated at 37°C. The RBCs utilized to sustain the cultures were obtained from a donor and placed in CPD vacutainers (BD biosciences, UK). Before processing, the blood was kept at 4-8°C for 48 hours. The blood was then placed into 15ml centrifuge

tubes and washed three times with PWM by centrifuging at 1500 rpm for five minutes and discarding the supernatant. After centrifuging for 5 minutes at room temperature in a swinging bucket rotor at 2,000 rpm, the hematocrit was calculated from the packed RBC volume. This was then refrigerated at 4-8°C for two weeks before being utilized for culture. Unless otherwise noted, spent CPMs were replaced with new ones, and the population and health of the cultures were monitored daily. By forming thin smears of the culture on a microscope slide, fixing them with methanol and staining them with 10% Giemsa (Fluka chemicals, UK) for 15 minutes, the parasite population was calculated. Parasitemia was determined by counting at least 1,000 erythrocytes with a 100-fold oil-immersion objective to determine the percentage of infected erythrocytes. This technique was carried out daily.

Synchronization of parasites

D-Sorbitol synchronization for rings

With few changes, *P. falciparum* cultures were synchronized as described by Lambros and Vanderberg (1979). For synchronization, cultures with high ring stage parasite populations (8%) were chosen. The selected cultures were placed into 15ml centrifuge tubes and spun at 2000 rpm for five minutes to establish synchrony, with the supernatant discarded and the pellet resuspended in 5ml of aqueous 5% D-sorbitol solution pre-warmed to 37 °C in a water bath. The cell suspension was then cultured in a 37°C incubator for 10 minutes. The suspension was centrifuged at 2000 rpm for 5 minutes after the incubation period, the D-sorbitol solution was removed, and the pellet was washed twice with PWM and once with CPM. All the washing stages took 5 minutes at 2000 rpm. A small smear from the cleaned cultures was put on a microscope slide, fixed with methanol, and stained with 10% Giemsa for 15 minutes. It was viewed with the 100X magnification objective lens assured successful synchronization. When the majority (90 % or more) of the parasites spotted under the microscope were in the ring stages, synchronization was declared effective. The cleansed pellet was then transferred into a new 25ml tissue culture flask containing 5ml CPM and uninfected O+, sickling negative human RBCs at 4% hematocrit to start a new culture. The content of the flask was then gassed for 30 seconds with the specific gas mixture, sealed promptly and snugly, and put into an incubator at 37°C of temperature.

Percoll® synchronization *for schizonts*

Nine parts of 100 % Percoll® (Sigma-Aldrich, USA) were gently mixed with one part of 10X phosphate-buffered saline [(PBS), Gibco, USA] to make 90% Percoll® solution. By combining the 90 % Percoll® solution with PWM, 65 percent (65%) and 35 percent (35%) Percoll® solutions were produced. To make the 65 % Percoll® solution, mix 6.5ml of 90 % Percoll® with 2.5ml of parasite wash medium (PWM), and mix 3.5ml of 90 % Percoll® with 5.5ml of PWM to generate 35 % Percoll® solution. After that, a 0.22 µm filter (Millipore, France) was used to filter sterilize them. The purpose of these solutions was to establish a gradient. Meanwhile, the parasite cultures were placed into 15ml Fisherbrand centrifuge tubes, centrifuged at 2000 rpm for 5 minutes at room temperature. The supernatant was then discarded and the pellet resuspended in PWM to a 10% hematocrit (total of about 2.5ml). The Percoll® gradient (35 % /65 %) was created by gently transferring 3 ml of 65 % Percoll® into a 15 ml centrifuge tube and then gently transferring 3 ml of 35 percent Percoll® onto it along the tube's wall with a Pasteur pipette. The freshly generated Percoll® gradient was then carefully overlaid with the resuspended parasite culture (2.5 ml). This was then centrifuged for 15 minutes at 2500 rpm at room temperature without a break in a swing-out rotor. Parasites were retrieved from the 35-65 % interface after centrifugation, transferred to a new 15ml centrifuge tube, washed twice with PWM and once with CPM, and cultured at 6% hematocrit.

Preparation and sensitivity assays of test compounds

Preparation of test compounds

Fluridone [test compound (Sigma-Aldrich, Germany)] dissolved in dimethyl sulfoxide [DMSO (Sigma-Aldrich, Germany)] and artemisinin [control drug (Sigma-Aldrich, USA)] were uniformly coated in flat-bottom 96-well microtitre plates (Thermo Scientific NuncTM, USA). Two-fold serial dilutions of the test compounds were prepared in triplicates in the respective wells. For the sensitivity assays, the working concentrations for fluridone were 500 mM, 250 mM, 125 mM, 62.5 mM, 31.25 mM, and 15.625 mM, while for artemisinin, they were 152 nM, 76 nM, 38 nM, 19 nM, 9.5 nM, and 4.75 nM. Until they were ready to use, the drug-coated plates were kept at - 20°C.

Inhibition assays of test compounds against P. falciparum *asexual stages*

At 1% parasitemia and 2% hematocrit, *in vitro* inhibitory assays were performed for the asexual (rings, trophozoites, and schizonts) stages of *P. falciparum* 3D7 strain. The plates were put in an incubation chamber, gassed with a specific gas combination for 6 minutes, then incubated for 48 hours at 37°C. Following the incubation period, 100L of a 1:10,000 SYGR Green I (Sigma-Aldrich, USA) solution in lysis buffer (20 nM Tris base, 5 mM EDTA, 0.008% saponin, 0.08 percent Triton X-100, pH 7.5) was added to the cultures in the wells and carefully mixed. After that, the plates were incubated for an hour at room temperature in the dark. After incubation at excitation and emission wavelengths of 485 nm and 535 nm, the fluorescence intensity of the cells in each well was measured using a fluorescent plate reader (Tecan endless 200pro, Japan).

Extraction of carotenoids from *P. falciparum* asexual stages

Plasmodium falciparum 3D7 parasites were cultivated in three 75ml tissue culture flasks for each asexual stage to generate a high ring stage population. To synchronize for the ring stage parasites, these cultures were treated with 5% D-sorbitol. At a parasitemia of 8-10%, the synchronized cultures were allowed to proliferate to obtain rings, trophozoites, and schizonts. To obtain the cell pellet, the cultures at each stage were pooled and collected by

centrifuging at 2000 rpm for 5 minutes. The pellet was resuspended in 20ml of PBS, and the number of RBCs in the solution was determined using a hemocytometer. The parasitemia and RBC count were also used to estimate the number of infected RBCs. The number of parasites necessary for the extraction was set at 500 million. The cell pellets were obtained by centrifuging the pooled cultures at 3500 rpm for 10 minutes at room temperature. The pellets were then resuspended in 10ml PBS with 0.1 % saponin (0.007M Na2HPO4, 0.01M Na2HPO4, pH 7.4 and 0.15M NaCl). The resuspended pellet was rinsed three times with PBS before being centrifuged for 10 minutes at 6000 rpm. When extraction could not be done right away, the pellets were kept at -80°C until needed. The carotenoids were extracted by adding 1 mL of methanol to the parasite pellet, followed by 2 mL of hexane. After then, the suspension was vortexed for 2 minutes. After that, 1ml of water was added to the mixture, which was vortexed for another minute. This was then centrifuged for 20 minutes at 4,000 rpm. A 0.2m nylon filter was used to capture and filter the supernatant phase. Following that, the filtrate was used straight for HPLC analysis.

HPLC analysis of carotenoids extracted from *P. falciparum* asexual stages

The HPLC analysis was carried out on a Shimadzu Prominence (Shimadzu Corp.) separation module outfitted with a Shimadzu Prominence (CTO-10ASV, Shimadzu Corp.) column oven, SIL-20AC HT auto sampler (Shimadzu Corp.), Shimadzu Prominence DGU-20A3 online degasser (Shimadzu Corp.), Shimadzu Prominence LC-20AB solvent delivery system (Shim (Shimadzu Corp.). The analytical scale AcclaimTM C30 reversed-phase column employed (250 mm x 4.6 mm internal diameter, 5 m particle size) was set at 25°C. At a flow rate of 1 ml/min, the mobile phase was a non-linear gradient of acetone/water with a starting composition of 50:50 (v/v). The overall run time was 45 minutes, and the filtrate injection volume was 20µl. The eluents were detected using a UV-VIS detector with a wavelength of 475 nm. To determine the identity of the resulted peaks, the retention durations of six carotenoid standards (lycopene, -carotene, -carotene, abscisic acid, lutein, and apo-carotenal) were calculated separately under the circumstances described above and compared to those obtained from the filtrate.

Bioinformatics analysis of PSY PPS/O

Nucleotide sequences of phytoene synthase (*PSY*) or octaprenyl pyrophosphate synthase (OPPS) from *P. falciparum* (PF3D7_0202700, PFB0130w) and other organisms were obtained from the gene databases of National Center for Biotechnology Information (NCBI, www.ncbi.nlm.nih.gov/gene/), PlasmoDB (www.plasmodb.org/) and ToxoDB (www.toxodb.org/). Table S1 lists the primary accession numbers or gene IDs received for the PSY gene for the analysis. The *P. falciparum* OPPS/PSY gene sequence was utilized as a query for Basic Local Alignment Search Tool, nucleotide (BLASTn) (blast.ncbi.nlm.nih.gov) analysis to find homologs in other organisms. The best blast hits included *T. gondii* and T. thermophilus octaprenyl pyrophosphate synthase. The nucleotide sequences were chosen from the BLAST result because the carotenoid production pathway has been extensively explored in these organisms.

RESULTS AND DISCUSSION

In vitro inhibition assays

Artemisinin and fluridone were used as control and test drugs in in vitro inhibitory experiments on the *P. falciparum* 3D7 strain, respectively. The inhibition assays were performed on the parasite's intraerythrocytic asexual stages (rings, trophozoites, and schizonts) to assess the effect of the compounds on the parasites as well as the half-maximum inhibitory doses (IC50) against each stage. After 48 hours of incubation with the chemicals, the parasites were treated for an hour with a SYBR Green I in lysis buffer solution. The absorbance from the respective wells in the microtitre plates was measured with a fluorometer immediately after this incubation period. The fluorometer absorbance and chemical concentrations were put into Excel® spreadsheets and converted to % parasitemia and log concentrations, respectively. These were then entered into the GraphPad Prism® program (version 5) and a non-linear regression was run to obtain dose-response curves and IC50 values for the drugs tested.

As percentage parasitemia is plotted on the y-axis against the log of concentration of the test chemicals on the x-axis, a sigmoidal curve and a dose-dependent response are apparent in all the results from the inhibition assays performed. This was expected because high concentrations of the inhibitors, if effective against the parasite, will result in a higher level of inhibition of the targeted cellular process; resulting in a decrease in parasite population (lower parasitemia), if that biological process is essential for parasite survival, and vice versa. Figure 1 shows that fluridone therapy resulted in a gradual decline in the ring stage parasite population, with an IC_{50} of 17.00mM. Treatment of the parasites with artemisinin (Figure 1) revealed a minimal response of the parasites to the first two lower concentrations of the compound, followed by a gradual decline in parasite population as the concentration of artemisinin increased. This resulted in an IC_{50} of 11.53 nM against the ring stages. When the concentrations at which fluridone and artemisinin attained their half-maximal inhibition were compared, artemisinin (IC_{50} in nanomolar) demonstrated to be a far more effective inhibitor than fluridone, because its IC_{50} is substantially lower (IC_{50} in millimolar). This was observed in all the inhibition trials for the other asexual stages, where half-maximal inhibition values of artemisinin were obtained at considerably lower doses than fluridone against the same stages. Fluridone inhibited growth at rates ranging from 43% to 62%, while artemisinin inhibited growth at rates ranging from 55% to 75% (Figure 1).

The inhibition experiments for both compounds on the parasite's trophozoite stages (Figure 2) were comparable, with essentially little response to the effects of both fluridone and artemisinin at lower dosages. Both

compounds had a very flat line at the beginning of the graph (Figure 2). The slope of the graph for fluridone (Figure 2) increased sharply as the concentration of fluridone increased, resulting from a drop in percentage parasitemia. After treatment with the fourth-highest concentration of fluridone, the graph leveled off. After therapy with the sixth-highest concentration of artemisinin, the percentage of parasitemia begins to level off again.

As a result, additional increases in fluridone and artemisinin concentrations had no discernible effect on the parasite's trophozoite population. Fluridone treatment yielded a half maximum inhibitory concentration of 50.31mM, while artemisinin therapy yielded a value of 9.67 nM. Fluridone inhibited growth by 40 % to 60 %, while artemisinin inhibited growth by 50 % to 70 %. Figure 3 depicts the results of the inhibition experiments against the parasite's schizont stages. At this stage of the parasite life cycle, both drugs tested had a dose-dependent effect. The graph for fluridone treatment reveals a dose-dependent influence on the population of the parasite's schizont stages. From the beginning of the graph, there was a high slope. Fluridone's half-maximum inhibitory concentration was 25.10mM, while fluridone's growth inhibition on the schizont stage ranged from 15% to 60%.

In the instance of artemisinin (Figure 3), the compound's action can be seen even at the lowest concentration, when the parasite population begins to fall immediately, and this continues until the fourth-highest concentration, when the curve begins to level out. At 5.362 nm, artemisinin reached its half maximal inhibitory concentration against the schizont stage. With regards to both drugs in this investigation, this was the lowest IC50 for the asexual phases. The percentage of growth inhibition ranged from 45 to 70%. The ring stages were the most responsive to fluridone treatment, with an IC50 of 17.00mM, almost three times and one-and-a-half times higher than the trophozoite (50.31 mM) and schizont (25.10 mM) stages, respectively.

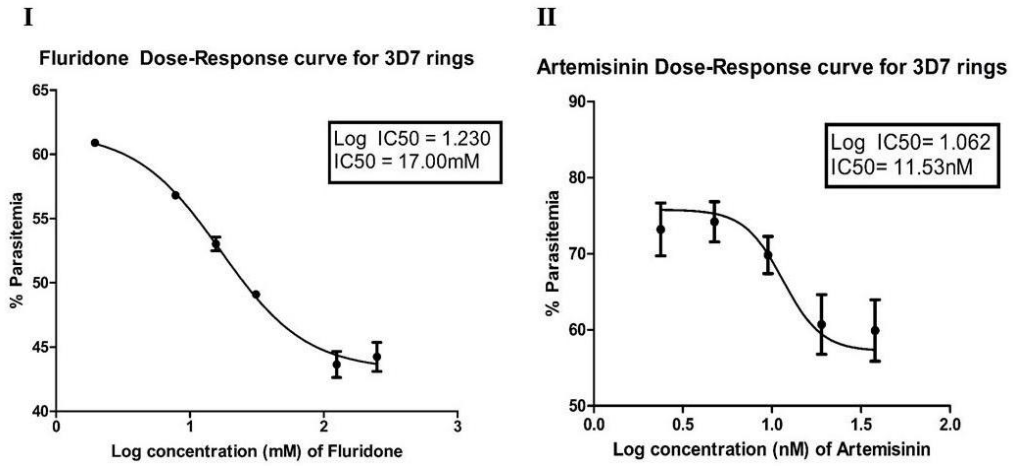

Figure 1. Dose-response curves for *Plasmodium falciparum* 3D7 ring stage parasites. Growth inhibitions by (I) fluridone and (II) artemisinin after incubating the parasites with different concentrations of these compounds for 48hrs. Error bars represent the standard error of mean (SEM) from triplicate readings of each concentration used.

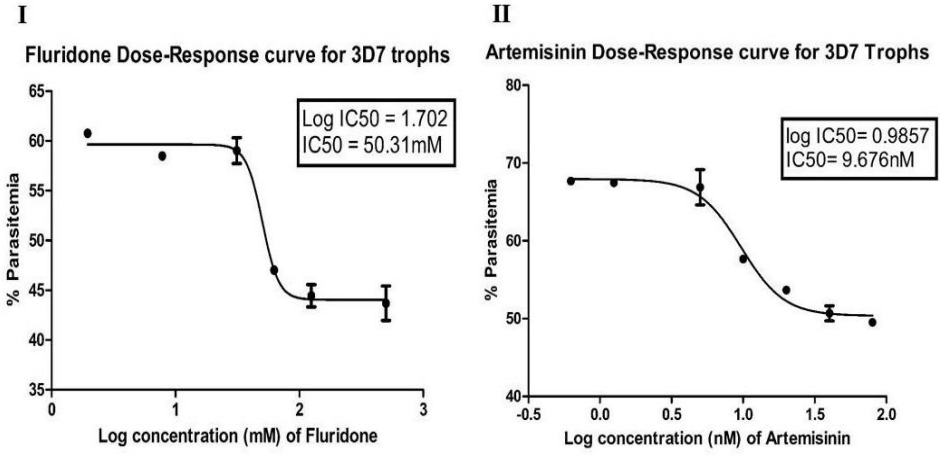

Figure 2. Dose-response curves for *Plasmodium falciparum* 3D7 trophozoite stage parasites. Growth inhibitions by **(I)** fluridone and **(II)** artemisinin after incubating the parasites with different concentrations of these compounds for 48hrs. Error bars represent the standard error of mean (SEM) from triplicate readings of each concentration used.

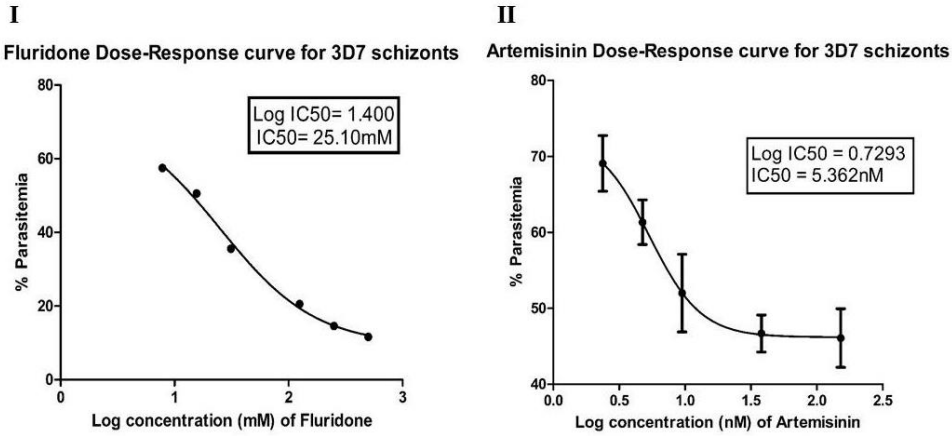

Figure 3. Dose-responses curve for *Plasmodium falciparum* 3D7 schizont stage parasites. Growth inhibitions by **(I)** fluridone and **(II)** artemisinin after incubating the parasites with different concentrations of these compounds. Error bars represent the standard error of mean (SEM) from triplicate readings of each concentration used.

Carotenoid extraction and HPLC analyses

Retention time is plotted on the x-axis and milli Absorbance Unit (mAU) is plotted on the y-axis in the chromatograms (Figures 4, 5, and 6) shown below. There were few detected or observed peaks on the chromatogram of the extract from the ring stage parasites (Figure 4). The organic solvents (methanol and hexane) utilized for the extraction have peaks at the beginning of the chromatogram with retention durations between 2-4 minutes. At the outset of the run, they elute rather quickly. These peaks can also be seen in the trophozoite (Figure 5) and schizont (Figure 6) stage extraction chromatograms. The lone peak with a retention time of 22.754 minutes that can be seen farther down the chromatogram from the ring stage extract (Figure 4) is lutein. The peak was identified by comparing its retention time to the retention time of the standards employed in the investigation. The lutein concentration in the ring stage was determined to be 0.0032 mg/ml. This was calculated using the HPLC machine's area under curve for each peak and the specific equation of line derived from the standard curves of the different carotenoid standards. Experiments that were duplicated yielded similar findings.

In comparison to the ring stages, the chromatogram for the trophozoite stage extraction (Figure 5) had a few more peaks. Aside from the initial peaks with retention periods of 2-4 minutes, three more peaks in the range of carotenoid retention durations were discovered. The peak's identification with a retention time of 17. The duration of 763 minutes is unclear because it does not relate to any of the standards' retention times. With a retention duration of 19.573 minutes, the next peak was recognized as -carotene. The amount of -carotene generated by the trophozoite stage parasites was calculated to be 0.0031 mg/ml. The last detectable peak (Figure 5) was recognized as carotene, with a retention period of 30.303 minutes and an estimated amount of 0.0019 mg/ml. The carotenoids produced by trophozoite stage parasites were not the same as those produced by ring stage parasites. Duplicate experiments yielded similar results yet again.

There were multiple peaks on the chromatogram for the schizont stage extract (Figure 6). Some of these peaks had retention periods that matched the criteria, while others did not and so were not detected. The peaks detected at retention times of 3-5 minutes are, once again, those of the extraction solvents. 19.550 minutes (α-carotene), 23.567 minutes (apo-carotenal), 24.114 minutes (abscisic acid), 30.086 minutes (lycopene), and 30.348 minutes (β-carotene) were the peaks having retention periods that corresponded to those of a standard utilized. The identity of the remaining peaks could not be validated because they did not have retention periods that corresponded to any of the criteria. In the schizont stage, the estimated levels of the detected carotenoids were 0.0824mg/ml (α-carotene), 0.0032mg/ml (apo-carotenal), 0.664mg/ml (abscisic acid), 0.8321mg/ml (lycopene), and 0.0022mg/ml (β-carotene). Experiments that were duplicated yielded similar findings. The largest peak in Figure 6 was recognized as abscisic acid. This indicates that high levels or quantities of this phytohormone are being generated, and it was only found during the parasite's schizont stage of life. As the parasites progressed from the young to the mature stages, the kind and quantity of the produced carotenoid clearly changed.

Evolutionary history and phylogenetic analysis

The phylogenetic link between the PSY gene of *P. falciparum* and homologs in other species is investigated (Figure 7). The PSY/OPPS gene sequence from *P. falciparum* was utilized as a query in a BLASTn search for homologs in other organisms. The PSY/OPPS sequences were chosen for the phylogenetic analysis using the BLAST results since the carotenoid production pathway has been extensively explored in these taxa. *P. falciparum PSY* was one of thirty PSY/OPPS gene sequences chosen from various taxonomic groups. Apicomplexans, fungi, plants, and bacteria were among the creatures chosen for the analysis. CLUSTAL W2 was used to align all the selected gene sequences, and MEGA6 was used to create an unrooted phylogenetic tree from the alignment using the Neighbor-Joining method. The numbers, along the branches, represent the evolutionary distance. These were calculated using the Maximum Composite Likelihood technique and was measured in number of base substitutions per site.

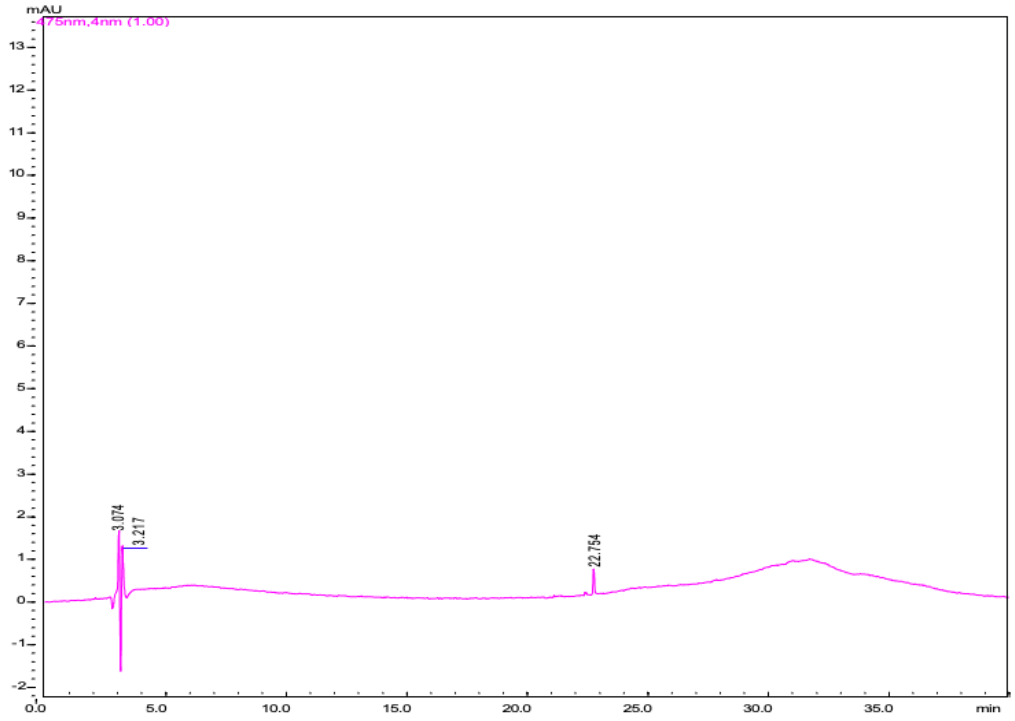

Figure 4. Chromatogram of carotenoids extracted from *Plasmodium falciparum* ring stage.

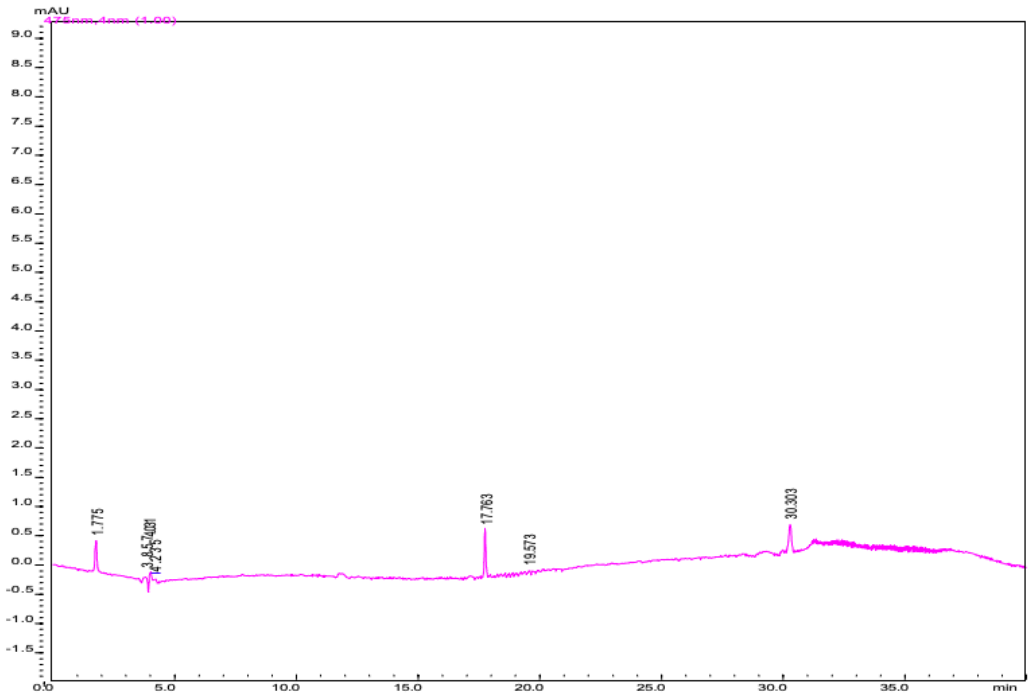

Figure 5. Chromatogram of carotenoid extracted from *Plasmodium falciparum* trophozoite stage.

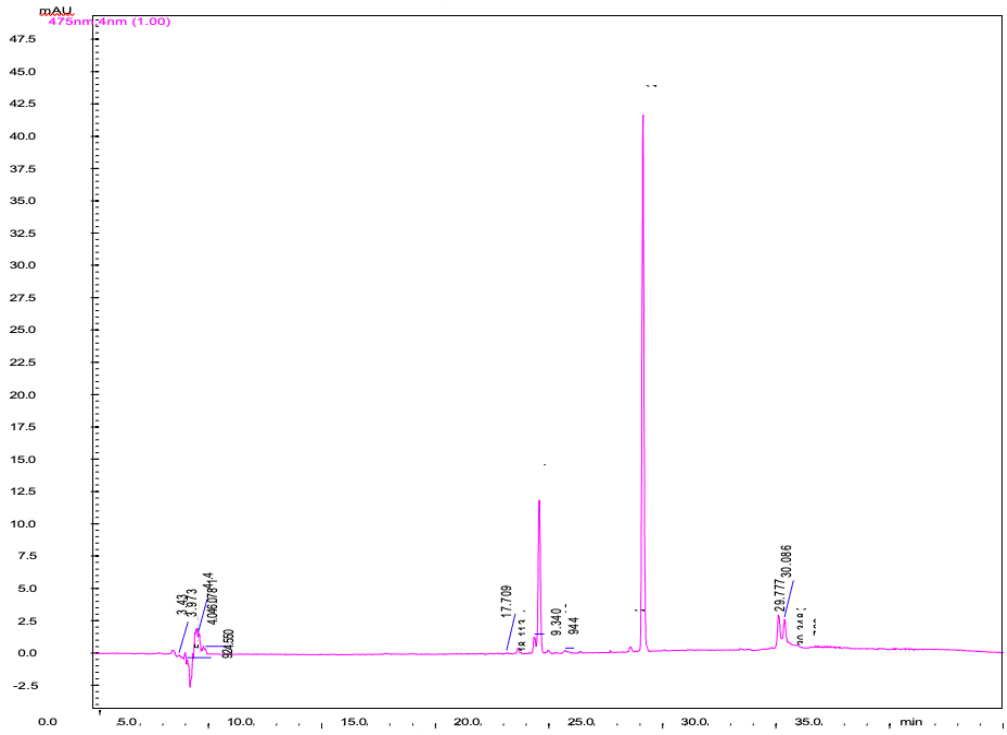

Figure 6. Chromatogram of carotenoid extracted from *Plasmodium falciparum* schizont stage. Carotenoids were extracted from synchronized cultures using a ternary solvent system (methanol/hexane/water) and the organic phase fraction was collected and run on a C- 30 column with a mobile phase of acetone/water for 40 minutes. Detection of the eluents was at 475nm.

On the unrooted tree, there are two major clades with multiple subclades branching out of each major clade (Figure 7). *Plasmodium, Cryptosporidium, Theileria, Babesia*, and *Toxoplasma* were found on one of the major clades, whereas Eimeria and the other apicomplexans were found on the other clades. As a result, the *PSY* gene in apicomplexans (yellow circle) split earlier in their evolution. The *Plasmodium PSY* gene forms a single subclade with 99 of bootstrap value, indicating a greater level of gene relatedness within this group and the likelihood that these species shared a common ancestor at some stage in their evolution. Surprisingly, *P falciparum* established a subclade with *P. reichenowi*, a chimpanzee parasite, with 99 of bootstrap value, indicating that the *P. falciparum PSY* gene is most closely related to *P. reichenowi* among all the sequences utilized in this study.

The Neighbor-Joining approach was used to infer the evolutionary history. The ideal tree is presented, with a branch length sum of 15.24929587. Next to the branches are the percentage of duplicate trees in which the related taxa clustered together in the bootstrap test (100 repetitions). A total of 30 nucleotide sequences were examined. For each sequence pair, all unclear locations were deleted. The total number of places in the final dataset was 5432. MEGA 6 was used to conduct evolutionary analysis.

Discussion

In vitro inhibition assay

Over the last decade, efforts have been made in numerous areas, including vector control, vaccine development, and medicine research projects, to eradicate malaria from the world's impacted regions (malERA Consultative Group on Vaccines 2011; Raghavendra et al. 2011; Rieckmann 2006; Schwartz et al. 2012). The genetic plasticity of *P. falciparum* allows it to elude the host immune system (Jeffares et al. 2007; Wright and Rayner 2014) as well as develop resistance to some of the existing medications used to treat and control malaria (Djimdé et al. 2001; Dondorp et al. 2010; Schellenberg et al. 2006). More effort and resources must be directed toward vector management, vaccine development, and therapeutic research to win the battle against the illness. Currently, the hunt for a viable vaccine candidate to aid in the eradication of the illness is well underway (Casares et al. 2010; Crompton et al. 2010; Malik et al. 2012). Novel chemicals and their effects on new or established targets in *P. falciparum* metabolic pathways are also being studied (Crowther et al. 2011; Qidwai and Khan 2012). In apicomplexans, the apicoplast organelle is an attractive new target (Kalanon and McFadden 2010; Maréchal and Cesbron-Delauw 2001). In apicomplexans, the apicoplast organelle is an attractive new target (Kalanon and McFadden 2010; Maréchal and Cesbron-Delauw 2001). Metabolic processes such as fatty acid synthesis and carotenoid production are housed inside it (Seeber and Soldati-Favre 2010).

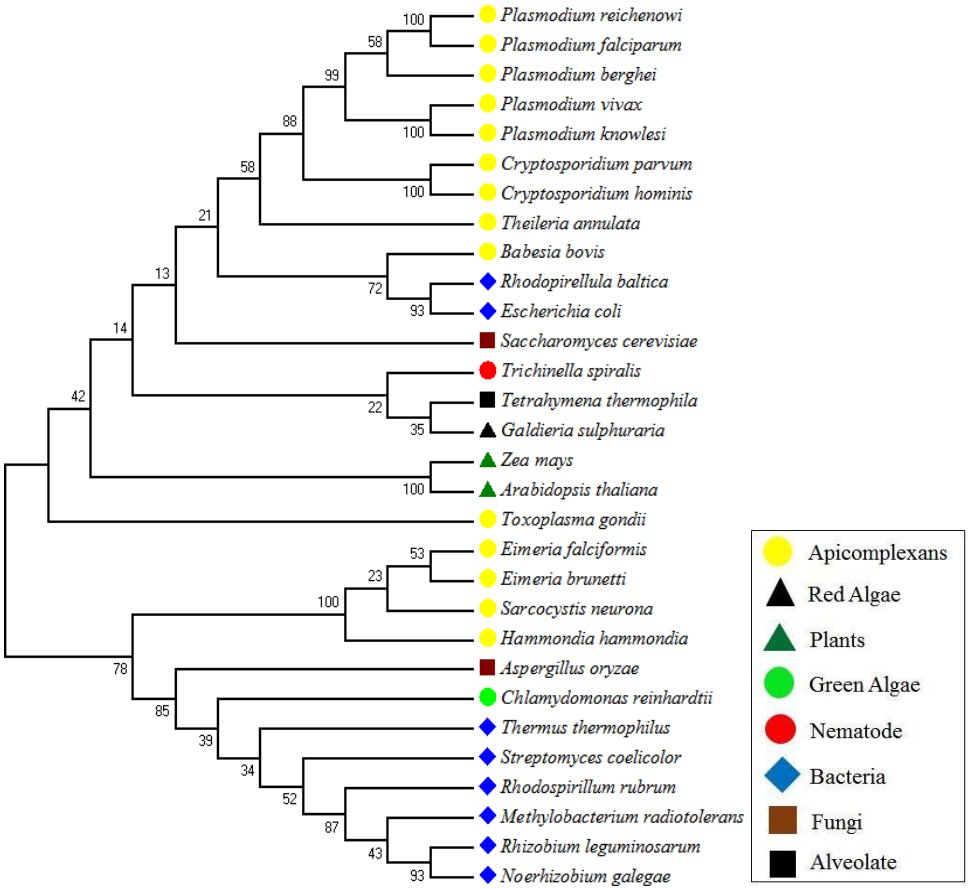

Figure 7. Phylogenetic relationship of *PSY*/OPPS gene in *Plasmodium falciparum* and other species.

Research has recently focused on the apicoplast, partially because this organelle is unique to the parasite and because it provides a fresh window into the parasite's metabolism (Goodman and McFadden 2013; Ralph et al. 2001). The carotenoid biosynthesis route is a fascinating metabolic route that occurs in the apicoplast and has gotten a lot of attention from scientists. The parasite has this route, but this route is absent in human (Tonhosolo et al. 2009). Fluridone, which inhibits phytoene desaturase in plants, is a well-known inhibitor of this process (McCowen et al. 1979). Other inhibitors of carotenoid biosynthesis, such as norflurazon and fosmidomycin, have been studied in the past and proven to be efficient at suppressing parasite growth in a dose-dependent manner in *Plasmodium* and *Toxoplasma* (Tonhosolo et al. 2009; Umeda et al. 2011; Yeh and DeRisi 2011). Fluridone's effect on *Toxoplasma* has also been examined, with results indicating that suppression caused a delay in egress and stimulated growth of the parasite's slow-growing, dormant cyst stage (Nagamune et al. 2008). However, the effect of fluridone on *Plasmodium* has not been explored. The goal of this research was to see how fluridone affected the carotenoid production pathway in *P. falciparum*.

Artemisinin was utilized as a control medicine in this research because its inhibitory capability against *P. falciparum* is known (Klonis et al. 2011). Fluridone was utilized as a comparison drug since its inhibitory capability against *P. falciparum* is unknown. The results of the inhibition assays (Figures 4.1 to 4.3) against the asexual stages revealed that fluridone was less effective than artemisinin at reducing parasite population, when comparing the concentrations at which each compound achieved its half-maximum inhibitory concentration against each stage. This could be owing to the incapability of fluridone to successfully traverse the membrane barriers surrounding the intraerythrocytic parasite, such as the RBC and parasite's lipid bilayers, as well as the parasitophorous vacuole encircling the parasite, preventing the molecule from reaching its intended target. The ring stage of the parasite life cycle was the most responsive to fluridone treatment of the three asexual stages because it had the lowest IC50 value (17.00 mM) of the three asexual stages (Figure 1).

For an inhibitor to reach its target, it must be able to cross any barrier that stands between it and the target, such as enzymes and ligands, in sufficient numbers to disrupt or inhibit the target's activity (Clay and Sharom 2013). The plasma membrane is selectively permeable, allowing only certain chemicals to flow through while preventing others from doing so (Vaara, 1992). The inhibitor's physical and chemical features can help or hinder its passage across the phospholipid bilayer. Simple diffusion or osmosis allows small, non-polar (hydrophobic) substances like water, oxygen, and carbon dioxide to pass through the gaps in the

membrane (Haines, 1994). Larger, charged molecules like glucose and amino acids, on the other hand, are transported across the membrane through active or passive diffusion through channels or pores (Stillwell 2013). Fluridone (Figure 2.4) is a fluorine-containing heterocyclic molecule that belongs to the nitrogen-containing heterocyclic class. Because this is a big molecule, it may require active or passive transport across the membrane via pores or channels. This could explain the high IC50 values obtained for fluridone treatment of the three intraerythrocytic stages of *P. falciparum* due to the restriction of fluridone mobility across membranes (parasitophorous vacuole and RBC and parasite membranes). The difference in the targets or modes of action of artemisinin and fluridone could also account for the high IC50 values seen for fluridone therapies. Artemisinin has been shown to inhibit hemoglobin uptake in *P. falciparum* intraerythrocytic stages (Klonis et al. 2011), whereas fluridone inhibits the activity of phytoene desaturase, the enzyme that catalyzes the conversion of phytoene to lycopene in the carotenoid biosynthesis pathway (Klonis et al. 2011 & Tonhosolo et al. 2009). When phytoene desaturase is inhibited by fluridone, parasites may be able to salvage lycopene existing in the host blood circulation (which comes from ones diet), but proteins derived from hemoglobin digestion may not be salvaged.

Carotenoid profiling and HPLC analyses

Since the discovery of the apicoplast in 1996 (Mcfadden et al. 1996) and the association of certain pathways in apicomplexans, including the isoprenoid biosynthesis pathway (Tonkin et al. 2008), scientists have been interested in determining whether this organelle serves a function in this parasite group and could be targeted for chemotherapeutic management. In apicomplexans, the carotenoid biosynthesis pathway has been connected to the manufacture of isoprenoid precursors (Eisenreich et al. 2004). The condensation of two molecules of GGPP to generate phytoene, the first committed step of the carotenoid biosynthesis pathway, is catalyzed by phytoene synthase). Nagamune et al. (2008) were the first to show that carotenoids are synthesized and that inhibiting this pathway leads to development and growth inhibitions in apicomplexans (*Toxoplasma*). Tonhosolo and colleagues have also shown carotenoid production in *P. falciparum* intraerythrocytic stages (2009). However, only a few carotenoids have been found to be synthesized by *P. falciparum*, including β-carotene, phytoene, and lutein, leaving an incomplete picture of the carotenoid synthesis landscape in *P. falciparum.*

The types and quantities of carotenoids generated in three asexual stages of *P. falciparum* were studied in this study. The carotenoids were extracted using a ternary solvent solution that contained methanol, hexane, and water from synchronized *P. falciparum* cells at the ring, trophozoite, and schizont phases. Because carotenoids are soluble in organic solvents, they partition into the organic phase of the extraction solvent (methanol and hexane), which was then employed for reverse-phase HPLC analysis. The non-linear gradient was utilized to progressively decrease the polarity of the mobile phase by progressively increasing the volume of acetone to water in the mobile phase. This was done to allow non-polar chemicals (carotenoids, for example, and any other compounds removed) to elute later in the run. Because carotenoids have similar structures and could all elute together, the C-30 column is a favored column for successful separation. The C-30 column provides a greater number of interaction sites for the carotenoids to engage with the column than a C-18 column, ensuring complete partitioning of positional isomers, as occurs in carotenoids. The C-30 column increases the contact period of the eluents with the packing elements of the column, extending the retention period and considerably improving the selectivity of the carotenoid isomers (Breitenbach et al. 2001; Emenhiser et al. 1995).

Only one identifiable peak with retention time corresponding to lutein, and with one of the standards employed, was visible on the chromatogram for the ring stage extract (Figure 4). This could be because the carotenoids generated at this stage are so low that they are below detection limits. This shows that carotenoids' functions in the early stages of the parasite life cycle may be noncompulsory. Carotenoids protect organisms from oxidative damage by quenching photosensitizers, interacting with singlet oxygen molecules, and scavenging peroxy radicals. This then reduces the accumulation of hazardous oxygen species created during active metabolism, which is one of the major roles played by carotenoids in the organisms (Shimidzu et al. 1996; Stahl and Sies 2003). There are probably not enough free radicals present currently in the parasite's life cycle to cause activation and robust synthesis of these carotenoids in significant quantities, resulting in low levels of carotenoids at the ring stage.

Three peaks were found in the chromatogram for the trophozoite stage extract (Figure 5), compared to a single peak for the ring stage extract (Figure 4). Two of the peaks exhibited retention periods that matched the standards that were employed. α -carotene (19.573 minutes) and β-carotene (30.303 minutes) were found as the peaks. The retention time of the third peak, which was 17.763 minutes, is unknown because it did not relate to any of the standards utilized in this study. However, because its retention duration falls within the range for carotenoids in our study, it is suspected to be a carotenoid. In comparison to the ring (Figure 4) and trophozoite (Figure 5), the schizont stage (Figure 6) generated several additional carotenoids. When comparing the schizont, ring, and trophozoite stages, it was discovered that the schizont stage had the highest quantities of carotenoids. This supports the findings of Tonhosolo et al. (2009), who found that carotenoid synthesis begins in the ring stages and builds up in the schizont stage. In their study, Tonhosolo et al. (2009) found carotenoids such as lutein and -carotene, which were also found in this study. Other carotenoids such as -carotene, apo-carotenal, lycopene, and abscisic acid were also profiled in *P. falciparum* for the first time in this study.

The presence and quantity of abscisic acid (with a retention period of 24.114 minutes) generated in the

schizont stage was also discovered to be quite fascinating and interesting. Abscisic acid (ABA) is a phytohormone that controls a variety of critical plant processes, including stress responses, embryo development, and seed dormancy (Nakashima and Yamaguchi-Shinozaki 2013; Nambara et al. 2010). A surge in abscisic acid (ABA) levels signaled a calcium-dependent egress of the parasites from the host cells in *T. gondii* (Nagamune et al. 2008), a similar apicomplexan. But the inhibiting abscisic acid synthesis resulted in the formation of cysts, a dormant form of the parasite (Nagamune et al. 2008). Exogenous abscisic acid was shown to induce the formation of cyclic adenosine diphosphate ribose (cADPR, a second-messenger) in *Toxoplasma gondii*, stimulate calcium-dependent protein secretion, and induce parasite egress from the infected host cell in a density-dependent manner. This confirms the role of ABA in *Toxoplasma*. In addition, specific disruption of ABA production by the inhibitor fluridone delayed egress and induced formation of the *Toxoplasma* parasite's slow-growing, latent cyst stage. In *Toxoplasma*, a closely related apicomplexan to *Plasmodium*, ABA-mediated calcium signaling governed the decision between lytic and chronic stage growth, a developmental switch that is critical in pathogenesis and transmission (Nagamune et al. 2008).

The absence of ABA in the ring and trophozoite stages was most likely due to the lack of or extremely low quantities of this phytohormone produced at these stages, which were below detection limits. However, there was an unexpected surge in ABA levels that was only found in the schizont stage. This could be the result of synthesis from the many individual merozoites still imprisoned in the parasitophorous vacuole. The discovery of an increase in abscisic acid levels in only the schizont stage is fascinating because it is the first time the phytohormone has been linked to *P. falciparum*. This means it could be serving the same crucial role in mediating parasite egress in this parasite as it is in *T. gondii*. To date, there has been no evidence of a signal for parasite egress from infected RBCs during the schizont stage, when merozoites are discharged to infect fresh RBCs. Whether or not ABA regulates or relates to merozoite egress in *P. falciparum* is unknown. Given that *P. falciparum* and *T. gondii* belong to the same Phylum Apicomplexa and share similar features such as the presence of the parasitophorous vacuole and the use of similar machinery for invading, it is possible to hypothesize that ABA may play a similar role in *P. falciparum* as it does in *T. gondii*, where it mediates parasite egress from its host cell (Kemp et al. 2013).

Bioinformatics and phylogenetic analysis of the phytoene synthase gene

Plasmodium falciparum, the most common *Plasmodium* species that infects people; it produces the most morbidity and mortality, with millions of clinical cases and over one million deaths reported each year (Greenwood et al. 2005; Hay et al. 2004). Although significant progress has been made in the management and control of *P. falciparum* (Kappe et al. 2010), the evolutionary origins and relatedness of this parasite and other *Plasmodium* diseases remain a source of debate and interest in recent years. Malaria phylogenetic research can aid in the development of new treatments and vaccines, as well as the understanding of host-pathogen interactions and the evolution of treatment resistance in the pathogen (Datta and Chauhan 2010). The chimpanzee parasite, *P. reichenowi*, has recently been shown to be the closest known relative of *P. falciparum*. This was thought to have diverged from its human counterpart, around the same time as the progenitors of chimps and humans, more than 5 million years ago (Escalante and Ayala, 1994; Jeffares et al. 2007; Rich et al. 1998). Different studies have found other *Plasmodium* strains in chimps, western gorillas, and bonobos in recent years. This suggests the probability that *P. falciparum* in humans emerged because of cross-species transmission from one or more of these apes (Rich et al. 2009; Krief et al. 2010; Prugnolle et al. 2010). *Plasmodium* species and other apicomplexan parasites have plastids, which suggests their fondness for cyanobacteria and green algae. *Plasmodium* species are assumed to be of prokaryotic origin since the apicoplast is produced through secondary endosymbiosis of an algal progenitor (McFadden 2011). Because the apicoplast lost its photosynthetic function in its new host, it kept certain prokaryotic remnants, the apicomplexan group of organisms is assumed to be connected to algae and plants (Foth and McFadden 2003; Arisue and Hashimoto 2014).

Plants, algae, and their endosymbiont apicomplexans have all been studied for isoprenoid and carotenoid production (Botella-Pava et al. 2004; Cunningham et al. 2007; Janoukovec et al. 2015). Isoprenoids and carotenoids are synthesized in apicomplexans via a separate mechanism (Goodman and McFadden 2013). The enzyme phytoene synthase (PSY), which catalyzes the first committed step of the isoprenoid to carotenoid biosynthesis pathway, is also found in apicomplexans parasites such as *P. falciparum* (Tonhosolo et al. 2009). Except for the *PSY gene* coding for the PSY enzyme, which has been identified through functional tests (Rodrguez-Villalón et al. 2009), no genetic evidence has been obtained for the enzymes assumed to be involved in the carotenoid biosynthesis pathway. Studies have looked at the structure and evolutionary relationship of the *PSY gene* in plants and other creatures (Giorio et al. 2008; Li et al. 2009; López-Emparán et al. 2014). This has recently been investigated in *P. falciparum* (Agarwal et al. 2015). The evolutionary relationship of the PSY gene in apicomplexans and other creatures is, however, poorly understood.

This study examined the evolutionary history and relationships of the phytoene synthase (*PSY*) gene in *P. falciparum* and other organisms. PSY orthologues were found in all *Plasmodium* species whose genome sequences were available, according to a BLAST search. Toxoplasma, Eimeria, Cryptosporidium, Babesia, and other apicomplexans employed in this phylogenetic analysis all had orthologues of this gene. However, because the apicomplexan species (shown by the yellow circles) bifurcate into two separate clades on the tree, all these orthologues in the apicomplexans were not closely related (Figure 7). *Plasmodium, Cryptosporidium, Theileria, Toxoplasma,* and *Bebasia* species formed a big

monophyletic group with other species such as plants (green triangle) and algae (black triangle), and the other apicomplexans (*Sarcocystis*, *Eimeria*, and *Hammondia* species) formed another big clade. This shows a huge and substantial evolutionary event that generated a divergence in this gene; but most significantly, the *PSY* was still retained by the apicomplexans, implying that the *PSY* and carotenoid synthesis are crucial to the apicomplexan parasites.

Figure 10 shows that apicomplexan species (yellow circle) are members of a vast monophyletic group that also includes plants (green triangle) and algae (black triangle), supporting the theory that the apicoplast evolved from photosynthetic ancestry (McFadden 2011). All the *Plasmodium* species included in this study formed a subclade on a branch of the tree with a bootstrap value of 99, showing a high level of relatedness in the *PSY* sequences in this species. When taxa or species constitute a clade, it means they have a high level of relatedness when compared to members of other clades. Species that share a clade on a branch of the tree with a bootstrap value of 70 or higher indicate that there is a higher level of support for the existence or formation of that node, and the organisms that make up the node are likely to have shared a common ancestor at some point in their evolution (Soltis and Soltis 2003). With a bootstrap value of 100, *P. falciparum* and *P. reichenowi* (the chimpanzee strain of *Plasmodium*) occupied the same clade as the other human strains employed in this investigation. This evidence backs with the theory that *P. reichenowi* is closest known relative of *P. falciparum* (Escalante and Ayala 1994; Jeffares et al. 2007).

In conclusion, the inhibition assays demonstrated that fluridone inhibited all three asexual stages of *P. falciparum* in a dose-dependent manner, with the ring stages being the most responsive to fluridone treatment. When compared to artemisinin, fluridone, a known plant carotenoid biosynthesis inhibitor, was not as effective at reducing parasite growth. This research also discovered that carotenoid production in the asexual stages is cumulative, beginning with the ring stage and ending with the schizont stage, with large quantities of abscisic acid created at this time. *PSY* orthologues were found in all the apicomplexan species analyzed using bioinformatics and phylogenetic analysis. It also revealed a significant amount of relatedness between the *PSY gene* in all the *Plasmodium* species examined. The *PSY* of *P. falciparum* is most like that of *P. reichenowi*, the chimpanzee malaria parasite, confirming the theory that *P. falciparum* is chimpanzee-derived. Because the apicomplexans formed a monophyletic group with the plants and algae included in this study, the tree also supports the notion that the apicoplast has photosynthetic ancestry. The above-presented data is significant because it sheds more light on the carotenoid biosynthesis pathway in *P. falciparum* and apicomplexans. This included the types and quantities of carotenoids synthesized and the compounds that affected the pathway. This study also strongly supports the notion that the pathway can be targeted for the control and possibly eradication of diseases caused by the parasite.

REFERENCES

Agarwal S, Sharma V, Phulera S, Abdin MZ, Ayana R, Singh S. 2015. Structural insights into a key carotenogenesis related enzyme phytoene synthase of *P. falciparum*: A novel drug target for malaria. Syst Synth Biol 9 (1): 27-37. DOI: 10.1007/s11693-015-9168-8.

Arisue N, Hashimoto T. 2014. Phylogeny and evolution of apicoplasts and apicomplexan parasites. Parasitol Int 64 (3): 254-259. DOI: 10.1016/j.parint.2014.10.005.

Bousema T, Drakeley C. 2011. Epidemiology and infectivity of *Plasmodium falciparum* and *Plasmodium vivax* gametocytes in relation to malaria control and elimination. Clin Microbiol Rev 24: 377-410. DOI: 10.1128/CMR.00051-10.

Breitenbach J, Braun G, Steiger S, Sandmann G. 2001. Chromatographic performance on a C30-bonded stationary phase of monohydroxycarotenoids with variable chain length or degree of desaturation and of lycopene isomers synthesized by various carotene desaturases. J Chromatograph A 936 (1-2): 59-69. DOI: 10.1016/S0021-9673(01)00945-1.

Casares S, Brumeanu TD, Richie TL. 2010. The RTS,S malaria vaccine. Vaccine 28 (31): 4880-4894. DOI: 10.1016/j.vaccine.2010.05.033.

Choi S-R, Mukherjee P, Avery MA. 2008. The fight against drug-resistant malaria: Novel plasmodial targets and antimalarial drugs. Curr Med Chem 15 (2): 161-171. DOI: 10.2174/092986708783330575.

Clay AT, Sharom FJ. 2013. Lipid bilayer properties control membrane partitioning, binding, and transport of P-glycoprotein substrates. Biochem 52 (2): 343-354. DOI: 10.1021/bi301532c.

Crompton PD, Pierce SK, Miller LH. 2010. Advances and challenges in malaria vaccine development. J Clin Investig 120 (12): 4168-4178. DOI: 10.1172/JCI44423.

Crowther GJ, Napuli AJ, Gilligan JH, Gagaring K, Borboa R, Francek C, Chen Z, Dagostino EF, et al. 2011. Identification of inhibitors for putative malaria drug targets among novel antimalarial compounds. Mol Biochem Parasitol 175 (1): 21-29. DOI: 10.1016/j.molbiopara.2010.08.005.

Cunningham FX, Lee H, Gantt E. 2007. Carotenoid biosynthesis in the primitive red alga Cyanidioschyzon merolae. Eukaryotic Cell 6 (3): 533-545. DOI: 10.1128/EC.00265-06.

Datta N, Chauhan VS. 2010. Origin and evolution of human malaria parasite, *P. falciparum* and *P. vivax*. In: Sharma VP. (Editor). Nature at Work: The Ongoing Saga of Evolution. Springer, India.

Djimdé A, Doumba OK, Cortese JF, Kayentao K, Doumbo S, Diourte Y, Dicko A, Xin-Zhuan S, Takashi N, Fidock DA, Wellems TE, Plowe CV. 2001. A molecular marker for chloroquine-resistant falciparum malaria. New England J Med 344 (4): 257-263. DOI: 10.1056/NEJM200101253440403.

Dondorp AM, Yeung S, White L, Nguon C, Day NPJ, Socheat D, von Seidlein L. 2010. Artemisinin resistance: Current status and scenarios for containment. Nat Rev Microbiol 8 (4): 272-280. DOI: 10.1038/nrmicro2331.

Emenhiser C, Sander LC, Schwartz SJ. 1995. Capability of a polymeric C30 stationary phase to resolve cis-trans carotenoid isomers in reversed-phase liquid chromatography. J Chromatograph A 707 (2): 205-216. DOI: 10.1016/0021-9673(95)00336-L.

Escalante AA, Ayala FJ. 1994. Phylogeny of the malarial genus *Plasmodium*, derived from rRNA gene sequences. Proc National Acad Sci USA 91 (24): 11373-11377. DOI: 10.1073/pnas.91.24.11373.

Foth BJ, McFadden GI. 2003. The apicoplast: A plastid in *Plasmodium falciparum* and other apicomplexan parasites. Int Rev Cytol 224: 57-110. DOI: 10.1016/S0074-7696(05)24003-2.

Giorio G, Stigliani AL, D'Ambrosio C. 2008. Phytoene synthase genes in tomato (*Solanum lycopersicum L.*) - new data on the structures, the deduced amino acid sequences, and the expression patterns. FEBS J 275 (3): 527-35. DOI: 10.1111/j.1742-4658.2007.06219.x.

Goodman CD, McFadden GI. 2013. Targeting apicoplasts in malaria parasites. Expert Opinion on Therapeutic Targets 17 (2): 167-77. DOI: 10.1517/14728222.2013.739158.

Gornicki P. 2003. Apicoplast fatty acid biosynthesis as a target for medical intervention in apicomplexan parasites. Int J Parasitol 33 (9): 885-896.DOI: 10.1016/s0020-7519(03)00133-4.

Greenwood BM, Bojang K, Whitty CJ, Targett GA. 2005. Malaria. Lancet 365 (9469): 1487-1498. DOI: 10.1016/S0140-6736(05)66420-3.

Haines TH. 1994. Water transport across biological membranes. FEBS Lett 346 (1): 115-122. DOI: 10.1016/0014-5793(94)00470-6.

Hay SI, Guerra CA, Gething PW, Patil AP, Tatem AJ, Noor AM, Kabaria CW, Manh BH, Elyazar IRF, Brooker S, Smith DL, Moyeed RA, Snow RW. 2009. A world malaria map: *Plasmodium falciparum* endemicity in 2007. PLoS Med 6 (3): e1000048. DOI: 10.1371/journal.pmed.1000048.

Hay SI, Guerra CA, Tatem AJ, Noor AM, Snow RW. 2004. The global distribution and population at risk of malaria: Past, present, and future. Lancet Infect Dis 4 (6): 327-336. DOI: 10.1016/S1473-3099(04)01043-6.

Jeffares DC, Pain A, Berry A, Cox AV, Stalker J, Ingle CE, Thomas A, Quail MA, Siebenthal K, Uhlemann AC, Kyes S, Krishna S, Newbold C, Dermitzakis ET, Berriman M. 2007. Genome variation and evolution of the malaria parasite *Plasmodium falciparum*. Nat Genet 39 (1): 120-125. DOI: 10.1038/ng1931.

Jiang N, Chang Q, Sun X, Lu H, Yin J, Zhang Z, Wahlgren M, Chen Q. 2010. Co-infections with *Plasmodium knowlesi* and other malaria parasites, Myanmar. Emerg Infect Dis 16: 1476-1478. DOI: 10.3201/eid1609.100339.

Jordão FM, Kimura EA, Katzin AM. 2011. Isoprenoid biosynthesis in the erythrocytic stages of *Plasmodium falciparum*. Memórias Do Instituto Oswaldo Cruz 106 (1): 134-141. DOI: 10.1590/S0074-02762011000900018.

Kalanon M, McFadden GI. 2010. Malaria, *Plasmodium falciparum* and its apicoplast. Biochem Soc Transactions 38 (3): 775-782. DOI: 10.1042/BST0380775.

Kappe SHI, Vaughan AM, Boddey JA, Cowman AF. 2010. That was then but this is now: malaria research in the time of an eradication agenda. Science 328 (5980): 862-866. DOI: 10.1126/science.1184785.

Kemp LE, Yamamoto M, Soldati-Favre D. 2013. Subversion of host cellular functions by the apicomplexan parasites. FEMS Microbiol Rev 37 (4): 607-631. DOI: 10.1111/1574-6976.12013.

Klonis N, Crespo-Ortiz MP, Bottova I, Abu-Bakar N, Kenny S, Rosenthal PJ, Tilley L. 2011. Artemisinin activity against *Plasmodium falciparum* requires hemoglobin uptake and digestion. Proc National Acad Sci USA 108 (28): 11405-11410. 10.1073/pnas.1104063108.

Krief S, Escalante AA, Pacheco MA, Mugisha L, André C, Halbwax M, Fischer A, Krief JM, Kasenene JM, Cranfield M, Cornejo OE, Chavatte JM, Lin C, Letourneur F, Grüner AC, McCutchan TF, Rénia L, Snounou G. 2010. On the diversity of malaria parasites in African apes and the origin of *Plasmodium falciparum* from Bonobos. PLoS Pathogens 6 (2): e1000765. DOI: 10.1371/journal.ppat.1000765.

Lambros C, Vanderberg JP. 1979. Synchronization of *Plasmodium falciparum* erythrocytic stages in culture. J Parasitol 65 (3): 418-420. DOI: 10.2307/3280287.

Li F, Tsfadia O, Wurtzel ET. 2009. The phytoene synthase gene family in the Grasses. Plant Signal Behav 4 (3): 208-211. DOI: 10.4161/psb.4.3.7798.

López-Emparán A, Quezada-Martinez D, Zúñiga-Bustos M, Cifuentes V, Iñiguez-Luy F, Federico ML. 2014. Functional Analysis of the *Brassica napus L.* Phytoene Synthase (PSY) Gene Family. PloS One 9 (12): e114878. DOI: 10.1371/journal.pone.0114878.

Maier AG, Rug M. 2013. In vitro culturing *Plasmodium falciparum* erythrocytic stages. Method Mol Biol 923: 3-15. DOI: 10.1007/978-1-62703-026-7_1.

malERA Consultative Group on Vaccines. 2011. A research agenda for malaria eradication: Vaccines. PLoS Med 8 (1): e1000398. DOI: 10.1371/journal.pmed.1000398.

Malik S, Gupta M, Braich J. 2012. Current scenario of malaria vaccine. Int J Basic Clin Pharmacol 1 (2): 60-66. DOI: 10.5455/2319-2003.ijbcp002112.

Maréchal E, Cesbron-Delauw MF. 2001. The apicoplast: A new member of the plastid family. Trends Plant Sci 6 (5): 200-205. DOI: 10.1016/S1360-1385(01)01921-5.

McCowen MC, Young CL, West SD, Parka SJ, Arnold WR. 1979. Fluridone, a new herbicide for aquatic plant management. J Aquat Plant Manage 17: 27-30.

McFadden GI. 2011. The apicoplast. Protoplasma 248 (4): 641-650. DOI: 10.1007/s00709-010-0250-5.

Nagamune K, Hicks LM, Fux B, Brossier F, Chini EN, Sibley LD. 2008. Abscisic acid controls calcium-dependent egress and development in *Toxoplasma gondii*. Nature 451: 207-210. DOI: 10.1038/nature06478.

Nakashima K, Yamaguchi-Shinozaki K. 2013. ABA signaling in stress-response and seed development. Plant Cell Rep 32 (7): 959-970. DOI: 10.1007/s00299-013-1418-1.

Nambara E, Okamoto M, Tatematsu K, Yano R, Seo M, Kamiya Y. 2010. Abscisic acid and the control of seed dormancy and germination. Seed Sci Res 20 (2): 55-67. DOI: 10.1017/S0960258510000012.

Paniagua-Michel J, Olmos-Soto J, Ruiz MA. 2012. Pathways of carotenoid biosynthesis in bacteria and microalgae. Methods Mol Biol 892: 1-12. DOI: 10.1007/978-1-61779-879-5_1.

Perlmann P, Troye-Blomberg M. 2000. Malaria blood-stage infection and its control by the immune system. Folia Biologica 46: 210-218.

Prugnolle F, Durand P, Neel C, Ollomo B, Ayala FJ, Arnathau C, Etienne L, Mpoudi-Ngole E, Nkoghe D, Leroy E, Delaporte E, Peeters M, Renaud F. 2010. African great apes are natural hosts of multiple related malaria species, including *Plasmodium falciparum*. Proc National Acad Sci USA 107 (4): 1458-1463. DOI: 10.1073/pnas.0914440107.

Qidwai T, Khan F. 2012. Antimalarial drugs and drug targets specific to fatty acid metabolic pathway of *Plasmodium falciparum*. Chemical Biol Drug Design 80 (2): 155-172. DOI: 10.1111/j.1747-0285.2012.01389.x.

Raghavendra K, Barik TK, Reddy BPN, Sharma P, Dash AP. 2011. Malaria vector control: from past to future. Parasitol Res 108 (4): 757-779. DOI: 10.1007/s00436-010-2232-0.

Ralph SA, D'Ombrain MC, McFadden GI. 2001. The apicoplast as an antimalarial drug target. Drug Resist Updat 4 (3): 145-511. DOI: 10.1054/drup.2001.0205.

Rich SM, Leendertz FH, Xu G, LeBreton M, Djoko CF, Aminake MN, Takang EE, Diffo JLD, Pike BL, Rosenthal BM, Formenty P, Boesch C, Ayala FJ, Wolfe ND. 2009. The origin of malignant malaria. Proc National Acad Sci USA 106 (35): 14902-14907. DOI: 10.1073/pnas.0907740106.

Rich SM, Licht MC, Hudson RR, Ayala FJ. 1998. Malaria's Eve: Evidence of a recent population bottleneck throughout the world populations of *Plasmodium falciparum*. Proc National Acad Sci USA 95 (8): 4425-4430. DOI: 10.1073/pnas.95.8.4425.

Rieckmann KH. 2006. The chequered history of malaria control: are new and better tools the ultimate answer? Annals Trop Med Parasitol 100 (8): 647-662. 10.1179/136485906X112185.

Rodríguez-Concepción M, Boronat A. 2013. Isoprenoid Synthesis in Plants and Microorganisms. In: Bach TJ, Rohmer M. (Editors), Isoprenoid Synthesis in Plants and Microorganisms: New Concepts and Experimental Approaches. Springer, New York.

Sato S. 2011. The apicomplexan plastid and its evolution. Cell Mol Life Sci 68 (8): 1285-1296. DOI: 10.1007/s00018-011-0646-1.

Schellenberg D, Abdulla S, Roper C. 2006. Current issues for anti-malarial drugs to control *P. falciparum* malaria. Curr Mol Med 6 (2): 253- 260. DOI: 10.2174/156652406776055168.

Schwartz L, Brown GV, Genton B, Moorthy VS. 2012. A review of malaria vaccine clinical projects based on the WHO rainbow table. Malar J 11: 11. DOI: 10.1186/1475-2875-11-11.

Seeber F. 2003. Biosynthetic pathways of plastid-derived organelles as potential drug targets against parasitic apicomplexa. Curr Drug Targets Immune Endocr Metabol Disord 3 (2): 99-109. DOI: 10.2174/1568008033340261.

Seeber F, Soldati-Favre D. 2010. Metabolic pathways in the apicoplast of apicomplexa. Int Rev Cell Mol Biol 281: 161-228. DOI: 10.1016/S1937-6448(10)81005-6.

Sermwittayawong N, Singh B, Nishibuchi M, Sawangjaroen N, Vuddhakul V. 2012. Human *Plasmodium knowlesi* infection in Ranong province, southwestern border of Thailand. Malaria J 11: 36. DOI: 10.1186/1475-2875-11-36.

Sharma R, Dutta AK. 2011. Malaria and national vector-borne disease control programme. Indian J Pediatrics 78: 1527-1535. DOI: 10.1007/s12098-011-0554-2.

Shiff C. 2002. Integrated Approach to Malaria Control. Clin Microbiol Rev 15: 278-293. DOI: 10.1128/CMR.15.2.278-293.2002.

Shimidzu N, Goto M, Miki W. 1996. Carotenoids as singlet oxygen quenchers in marine organisms. Fisheries Sci 62 (1): 134-137. DOI: 10.2331/fishsci.62.134.

Soltis DE, Soltis PS. 2003. Applying the bootstrap in phylogeny reconstruction. Statistical Sci 18 (2): 256-267. DOI: 10.1214/ss/1063994980.

Stahl W, Sies H. 2003. Antioxidant activity of carotenoids. Mol Aspects Med 24 (6): 345-351. DOI: 10.1016/S0098-2997(03)00030-X

Stillwell W. 2013. Membrane Transport. An Introduction to Biological Membranes. Elsevier B. V., Amsterdam.

Toledo-Ortiz G, Huq E, Rodríguez-Concepción M. 2010. Direct regulation of phytoene synthase gene expression and carotenoid

biosynthesis by phytochrome- interacting factors. Proc National Acad Sci USA 107 (25): 11626-11631. DOI: 10.1073/pnas.0914428107.

Tonhosolo R, D'Alexandri FL, de Rosso VV, Gazarin ML, Matsumura MY, Peres VJ, Merino EF, Carlton JM, Wunderlich G, Mercadante AZ, Kimura EA, Katzin AM. 2009. Carotenoid biosynthesis in intraerythrocytic stages of *Plasmodium falciparum*. J Biol Chem 284 (15): 9974-9985. DOI: 10.1074/jbc.M807464200.

Tonhosolo R, D'Alexandri FL, Genta FA, Wunderlich G, Gozzo FC, Eberlin MN, Peres VJ, Kimura EA, Katzin AM. 2005. Identification, molecular cloning, and functional characterization of an octaprenyl pyrophosphate synthase in intra-erythrocytic stages of *Plasmodium falciparum*. Biochem J 392 (1): 117-126. DOI: 10.1042/BJ20050441.

Tonkin CJ, Kalanon M, McFadden GI. 2008. Protein targeting to the malaria parasite plastid. Traffic 9: 166-175.

Trager W, Jensen JB. 1976. Human malaria parasites in continuous culture. Science 193 (4254): 673-675. DOI: 10.1126/science.781840

Umeda T, Tanaka N, Kusakabe Y, Nakanishi M, Kitade Y, Nakamura KT. 2011. Molecular basis of fosmidomycin's action on the human malaria parasite *Plasmodium falciparum*. Sci Rep 1: 9. DOI: 10.1038/srep00009.

Vaara M. 1992. Agents that increase the permeability of the outer membrane. Microbiol Rev 56 (3): 395-411. DOI: 10.1128/MMBR.56.3.395-411.1992.

van der Meer JY, Hirsch AKH. 2012. The isoprenoid-precursor dependence of *Plasmodium spp*. Nat Prod Rep 29: 721. DOI: 10.1039/c2np20013a.

Welsch R, Beyer P, Hugueney P, Kleinig H, von Lintig J. 2000. Regulation and activation of phytoene synthase, a key enzyme in carotenoid biosynthesis, during photomorphogenesis. Planta 211 (6): 846-854. 10.1007/s004250000352.

Wiesner J, Borrmann S, Jomaa H. 2003. Fosmidomycin for the treatment of malaria. Parasitol Res 90 (2): 71-76. DOI: 10.1007/s00436-002-0770-9.

World Health Organisation. 2014. World Malaria Report 2014. World Health Organisation, Geneva.

Wright GJ, Rayner JC. 2014. *Plasmodium falciparum* Erythrocyte Invasion: Combining Function with Immune Evasion. PLoS Pathogens 10 (3): e1003943. DOI: 10.1371/journal.ppat.1003943.

Yeh E, DeRisi JL. 2011. Chemical rescue of malaria parasites lacking an apicoplast defines organelle function in blood-stage *Plasmodium falciparum*. PLoS Biol 9 (8): e1001138. DOI: 10.1371/journal.pbio.1001138.

Table S1. Table showing the gene ID of PSY/OPPS in the various organisms used for the phylogenetic relationship study

Organism	Gene ID	Database
Plasmodium falciparum 3D7	PF3D7_0202700, PFB0130w	PlasmoDB, NCBI
Plasmodium vivax	PVX_003575	PlasmoDB
Plasmodium berghei ANKA	PBANKA_0300800	PlasmoDB
Plasmodium reichenowi	gi|832044551	PlasmoDB
Plasmodium knowlesi strain H	PKNH_0418400	PlasmoDB
Cryptosporidium hominis TU502	cgd5_4532	ToxoDB
Cryptosporidium parvum Iowa II	cgd7_3730	ToxoDB
Eimeria brunette	EBH_0010260	ToxoDB
Eimeria falciformis	EfaB_MINUS_800.g99_1	ToxoDB
Hammondia strain H.H.34	HHA_224490	ToxoDB
Theileria annulata	TA03505	ToxoDB
Toxoplasma gondii	TGME49_269430	ToxoDB
Sarcocystis neurona	SN3_00400385	ToxoDB
Arabidopsis thaliana	gi|240256493	NCBI
Aspergillus oryzae	gi|169781061	NCBI
Babesia bovis T2Bo	gi|156087461	NCBI
Chlamydomonas reinhardtii	gi|159486413	NCBI
Escherichia coli	gi|387615344	NCBI
Galdieria sulphuria	gi|545700663	NCBI
Methylobacterium radiotolerans	gi|170746450	NCBI
Neorhizobium galegae	gi|752716557	NCBI
Rhizobium leguminosarum	gi|752843554	NCBI
Rhodopirellula baltica	gi|32470666	NCBI
Rhodospirillum rubrum	gi|83591340	NCBI
Saccharomyces cerevisiae	gi|330443520	NCBI
Streptomyces coelicolor	gi|32141095	NCBI
Tetrahymena thermophila	gi|229594551	NCBI
Thermus thermophilus	gi|593268528	NCBI
Trichinella spiralis	gi|331705224	NCBI

ASIAN J TROP BIOTECHNOL
Volume 18, Number 1, June 2021
Pages: 28-31

ISSN: 0216-6887
E-ISSN: 2301-8658
DOI: 10.13057/biotek/c180103

Short Communication: Analysis of purity and concentration of DNA extracted from intron patho gene-spin extraction on processed crab food product samples

ALFI SOPHIAN♥, RATNA PURWANINGSIH, MUINDAR, EKA PUTRI JUNIARTI IGIRISA, MUHAMMAD LUTHFI AMIRULLAH

Laboratory of Microbiology, National Agency of Drug and Food Control in Gorontalo. Jl. Tengah Toto Selatan, Bone Bolango 96123, Gorontalo, Indonesia. Tel./fax.: +62-435-822052, ♥email: alfi.sophian@pom.go.id

Manuscript received: 25 August 2020. Revision accepted: 9 June 2021.

Abstract. *Sophian A, Purwaningsih R, Muindar, Igirisa EPJ, Amirullah ML. 2021. Short Communication: Analysis of purity and concentration of DNA extracted from intron patho gene-spin extraction on processed crab food product samples. Asian J Trop Biotechnol 18: 28-31.* The purpose of this study was to optimize the Intron patho gene-spin DNA/RNA extraction kit on processed crab food products so that it can be used for testing samples, other than viral and bacterial samples. The method used in purity and concentration analysis to analyze total DNA (yield) is the absorbance method using a nanophotometer. The method used to isolate the sample DNA is the centrifuge column or spin column method. The research data showed that the extracted sample concentration was in the range of 15.15-15.75, with an average of 15.46. While the purity values measured at the A260/A280 wavelengths were obtained with a purity range between 2,124-2,346. The total DNA analysis (yield) results obtained an average of 755.04, with the lowest yield value of 575.50 and the highest yield value of 787.50. As a suggestion for further research, it is hoped that modification can be made to perfect the isolated DNA so that it has better purity and concentration values.

Keywords: DNA, gene, intron, PCR, RNA

INTRODUCTION

Processed crab food products are very popular with Indonesians. The process of processing it into other food ingredients such as chips, crackers and frozen food is a way to increase the economic value of processed crab products. The future challenge of this product is the authentication of products whose raw materials have high economic value. The potential for fraud by changing the main raw material is an act of violation of the law.

Currently, POM ensures the quality of goods in circulation is of guaranteed quality and safety. The strategic function of the POM in ensuring high quality is becoming more difficult; especially if improvements in the technical capacity of personnel and the personnel who support their main duties and functions. For this reason, this study was conducted to provide a new reference in the form of test results on processed crab products. With this research, it is hoped that it can become a reference in developing technical testing to support surveillance activities.

In DNA testing, extraction is an early stage that has a very important role in the success of testing using PCR. This is in line with the opinion expressed by Jhosi et al. (2016) and Fulton et al. (1995) which states that DNA extraction is the key to the success of PCR analysis. According to Ibrahim (2010) in PCR analysis, DNA extraction results with good quality and quantity are needed to proceed to the amplification stage. The presence of contaminant compounds in the extracted DNA, such as polysaccharides and polyphenols, makes the enzyme work slow in the PCR amplification process (Hoarau et al. 2007). The Intron patho gene-spin (viral DNA/RNA) extraction kit is an extraction kit made for the extraction of DNA and RNA virus types. However, this kit can also be used for plasma, blood, serum cell-free body fluids, cells, and tissue samples. Because one of the specifications of this kit is that it can be used to extract cell and tissue samples, it is possible that this kit can be used to extract processed crab food products.

The novelty aspect of this research is to optimize the Intron patho gene-spin DNA/RNA extraction kit against processed crab food products so that it can be used for testing samples, other than virus samples, so it can be used as one of the references in extracting samples from processed crab food products. Additionally it may be a reference source in modifying the types of extraction kits in situations that allow modifications to be made.

MATERIALS AND METHODS

Materials

The materials used in this study were processed crab food products, which were sampled from several restaurants selling processed crab menus. Also Intron Patho Gene-Spin (viral DNA/RNA) Extraction (cat. 17154.100) extraction kits were used.

Sample preparation

Purchased samples from several restaurants were washed clean, so that the crab meat that was to be extracted

had no other matrix besides crab meat. Furthermore, the crabmeat was then separated between the meat and the shell, after which it is crushed and homogenized. The homogenized sample was then be extracted.

DNA isolation

The sample was weighed to be 1 g and put it in a 2 mL microcentrifuge tube. 500 µL of VL buffer solvent was added. It was incubated for 10 minutes at room temperature, while occasionally vortexing for 1 minute every 2 minutes of incubation. Next 700 µL of BL buffer was added and then incubated again for 2 minutes then vortex 1 minute. 750 µL of the solution was transferred into the spin column, then centrifuged at a speed of 14.000 rpm for 1 minute. The liquid was discarded before adding 750 RW 1 buffer. This was then put in the centrifuge at a speed of 14.000 rpm for 1 minute. The liquid was discarded, before 750 RW 2 buffer was added. This was then centrifuged at 14.000 rpm for 1 minute. The spin column was transferred into the 1.5 mL microcentrifuge tube, before adding 50 µL of EB buffer. Incubation was for 2 minutes, then centrifuged at 14.000 rpm for 2 minutes. The spin column was discared and the extracted DNA was then calculated for its concentration and purity using a nano photometer.

DNA yield

After knowing the concentration and purity values, the next step was to calculate the yield. DNA yield is the final DNA product calculated using the formula:

DNA yield (µg) = DNA concentration × total sample volume (mL)

Purity and concentration analysis

Analysis of purity and concentration were performed using a nano photometer NP80 (IMPLEN), method setting; Nucleic acid, dsDNA type, nano volume mode, 2 µL sample volume, nucleic acid factor 50.00, background correction 320 nm, air bubble recognition off, manual dilution factor 1.000.

Data analysis

Data analysis was performed by comparing the purity and concentration values against the standard DNA extract sample where the purity was in the range (1.8-2.0) while the concentration was greater than 20 ng/mL.

RESULTS AND DISCUSSION

Data from concentration and purity analysis

The analysis of concentration and purity was carried out using a nano photometer and the results were obtained (Table 1). From the table, the concentration value of the extracted sample was in the range of 15.15-15.75, with an average of 15.46. The purity values measured at the A260/A280 wavelengths were obtained with a purity range between 2.24-2.346. According to Sambrook et al. (1989), the purity value of DNA extract above 2 indicates that the DNA extraction results still contain protein contamination. Whereas if the purity results show a value of less than 1.8, this would indicate that the DNA extract still contains phenol residues and other solvent contaminants.

DNA extraction results are good if the purity value is in the range 1.8-2.0, the concentration is greater than 20 (ng/µL) (Kirby 1990; Artama 1991). However, to conclude that an extracted sample can be tested using real-time PCR, the purity and concentration values that are the benchmark for isolation are said to be good because real-time PCR technology is possible if the amplification process can occur with low concentrations even though it depends. on the sensitivity of a PCR device.

DNA yield

After analyzing the slides and concentrations, the total or yield DNA was them analyzed. From the research conducted, an average of 755.04 was obtained. With the lowest yield value of 575.50 and the highest yield value of 787.50. Further results are presented in Table 2.

One of the methods to perform yield analysis is by using the absorbance method. This method is done by using a spectrophotometric instrument. The absorbance readings were carried out at a wavelength of 260 nm or (A260). This is because DNA at this wavelength absorbs light so that the resulting turbidity can be used to estimate the amount of DNA detected. To ensure this, the reading is carried out at the linear range of the instrument (0.1-1.0).

Table 1. Extracted nano photometer data.

Sample	Concentration ng/µL	Purity (A260/A280)
Sample 1	15.65	2.268
Sample 2	15.40	2.124
Sample 3	15.60	2.346
Sample 4	15.55	2.221
Sample 5	15.15	2.349
Sample 6	15.35	2.225
Sample 7	15.45	2.225
Sample 8	15.35	2.255
Sample 9	15.75	2.188
Sample 10	15.40	2.200
Average	15.46	2.240

Table 2. DNA yield.

Sample	Concentration ng/µL	Total dilution volume (µL)	Yield
Sample 1	15.65	50	782.50
Sample 2	15.40	50	770.00
Sample 3	15.60	50	780.00
Sample 4	15.55	50	777.50
Sample 5	15.15	50	575.50
Sample 6	15.35	50	767.50
Sample 7	15.45	50	772.50
Sample 8	15.35	50	767.50
Sample 9	15.75	50	787,50
Sample 10	15.40	50	770.00
Average	15.46	50	755.05

Discussion

The method used was slightly modified at the extraction stage, namely by adding the length of time and incubation temperature. The manual kit suggests the incubation be carried out at room temperature for 10 minutes. In this study, the incubation was carried out at 70°C for 30 minutes while occasionally in the vortex. Modifications at this stage were carried out to produce perfect lysis of the sample to be extracted. The observations made on the characteristics of the extracted sample show that the turbidity frame is getting higher with the length of time and homogenization is carried out using the vortex.

Based on the extraction data read using a nano photometer, it is known that the extracted DNA does not have good purity and concentration values. This could be because this kit is made only for the extraction of DNA or RNA viruses, so optimization of the processed crab sample does not guarantee the success of the extraction.

The principle of the extraction kit used in this study was to use the silicon dioxide method, which is made in a spin column that can absorb DNA. This method generally has no difference from the phenol-chloroform method in DNA extraction. This method, DNA extraction, will go through three stages: cell lysis, DNA separation, and DNA purification (Corkill and Rapley 2008). DNA extraction begins with lysis where at this stage the sample is lysed for 30 minutes with occasional vortices every 3 minutes to get a better lysis process.

The observations made on the samples in the vortex showed that the samples were getting cloudier when compared to before vortex. This gives an idea that the cells have undergone lysis which is marked by turbidity occurring in the lysis solution. The lysis process is an important step in DNA extraction because at this stage the trapped DNA in the cell will be removed. The cell lysis process occurs in the early stages of extraction, which works by two mechanisms: enzymatic and chemical. The enzymatic mechanism occurs by adding proteinase-K. According to Surzycki (2000), the proteinase K enzyme functions to break the amino acid carboxyl group in the peptide bonds that make up the peptidoglycan layer of the cell wall. While the chemical mechanism occurs by adding sodium dodecyl sulfate (SDS) detergent. The addition of SDS serves to dissolve lipids in the cell membrane so that cell membrane destabilization occurs and binds to proteins and polysaccharides on the cell membrane to open (Surzycki 2000; Demeke et al. 2009). In the process of cell lysis, the cell wall covering has been destroyed so that the DNA will mix with other cell macromolecules.

According to Held (2001), the analysis of concentration and purity was carried out using a nano photometer, which reads DNA absorption at wavelength A260/A280. However, the absorption reading method at the A260/A280 wavelength is the method most used. Another opinion was expressed by Matlock (2015) which states that the results of the analysis of purity and good concentration on the sample do not guarantee that the sample is successfully amplified. Another equally important factor is the sample itself. However, the purity and concentration analysis method to see the quality and quality of isolated nucleic acids using a nano photometer is an effective method to determine the quality of the extracted results in a short time.

The results of the purity analysis of the samples showed values and concentrations outside the good DNA extraction category were between (1.7-2) for purity and above 20 ng/µL for concentration. However, Kapa Biosystems (2014) revealed a different matter: to carry out PCR analysis, isolated DNA concentrations with a value between 10-100 ng/µL are needed. However, these results are not necessarily usable, but a confirmation test using PCR is needed. The results of the DNA yield showed that the amount of DNA was quite large, namely around 755.04. This value is very good when compared to the DNA yield value required for DNA amplification using real-time PCR.

It is suggested that this should be continued until the confirmation test stage to prove the results of DNA extraction, even though it does not mean that the category of good DNA extraction results can still be used. This is important because every real-time PCR tool has a different detection limit level so that the accuracy and detection ability will be different. The smallest value that can be detected ranges from 0.01-2 p/µL, (Perandin et al. 2004; Cnops et al. 2011; Kamau et al. 2013; Xu et al. 2015; Srisutham et al. 2017).

Based on the research conducted, it was discovered that the results of the analysis of purity and concentration outside of the DNA standard extracted were good. Therefore in future research, modifications are needed so that the kit used can have good DNA extracted results for use in samples of processed crab food products.

ACKNOWLEDGEMENTS

The authors would like to thank the Head of the National Agency of Drug and Food Control (NADFC) in Gorontalo, Indonesia for laboratory support.

REFERENCES

Artama WT. 1991. Genetical manipulation. Center for Inter-University-Biotechnology. Gadjah Mada University, Yogyakarta. [Indonesian]

Cnops L, Jacobs J, Van Esbroeck M. 2011. Validation of a four-primer real-time PCR as a diagnostic tool for single and mixed Plasmodium infections. Clin Microbiol Infect 17 (7): 1101-1107. DOI: 10.1111/j.1469-0691.2010.03344.x

Corkill G, Rapley R. 2008. The Manipulation of Nucleic Acid: Basic Tools & Techniques in Molecular Biomethods Handbook. 2nd ed. Humana Press, New York.

Demeke T, Ratnayaka I, Phan A. 2009. Effects of DNA extraction and purification methods on real-time quantitative PCR analysis of roundup ready soybean. J Assoc Off Anal Chem Int 92 (4): 1136-1144. DOI: 10.1093/jaoac/92.4.1136

Fulton TM, Chunwongse J, Tanksley SD. 1995. Microprep protocol of extraction DNA from tomato and other herbaceous plants. Plant Mol Biol Rep 13 (3): 207-209. DOI: 10.1007/BF02670897

Held PG. 2001. Nucleic Acid Purity Assessment using A260/A280 Ratios. Application note. Senior Scientist & Applications Lab Manager. Biotek.

Hoarau G, Coyer JA, Stam WT, Olsen JL. 2007. A fast and inexpensive DNA extraction/purification protocol for brown macroalgae. Mol Ecol Notes 7: 191-193. DOI: 10.1111/j.1471-8286.2006.01587.x

Ibrahim RIH. 2010. A modified CTAB protocol for DNA extraction from young flower petals of some medicinal plant species. Geneconserve 10 (4): 165-182.

Joshi RS, Garg P, Zaitlen N, Lappalainen T, Watson CT, Azam N, Ho D, Li X, Antonarakis SE, Brunner HG, Buiting K. 2016. DNA methylation profiling of uniparental disomy subjects provides a map of parental epigenetic bias in the human genome. Am J Hum Genet 99 (3): 555-566. DOI: 10.1016/j.ajhg.2016.06.032

Kamau E, Alemayehu S, Feghali KC, Saunders D, Ockenhouse CF. 2013. Multiplex qPCR for detection and absolute quantification of Malaria. PLoS One 8 (8): e71539. DOI: 10.1371/journal.pone.0071539

Kapa Biosystems. 2014. KAPA2G Fast HotStart PCR Kit Technical Data Sheet. Kapa Biosystems Inc., Wilmington, MA.

Kirby LT. 1990. DNA Fingerprinting: An Introduction. M. Stockton Press, New York. DOI: 10.1007/978-1-349-12040-6

Matlock B. 2015. Assessment of Nucleic Acid Purity. Technical Note 52646. Thermo Fisher Scientific, Wilmington, MA, USA

Perandin F, Manca N, Calderaro A, Piccolo G, Galati L, Ricci L, Medici MC, Arcangeletti MC, Snounou G, Dettori G, Chezzi C. 2004. Development of a real-time PCR assay for detection of *Plasmodium falciparum*, *Plasmodium vivax* and *Plasmodium ovale* for routine clinical diagnosis. J Clin Microbiol 42 (3): 1214. DOI: 10.1128/JCM.42.3.1214-1219.2004

Sambrook J, Fritsch F, Miniatis T. 1989. Molecular Cloning Laboratory Manual. 3rd edition. Cold Spring Harbor Laboratory Pr, New York (US).

Srisutham S, Saralamba N, Malleret B, Re L. 2017. Four human Plasmodium species quantification using droplet digital PCR. PLoS One 12 (4): e0175771. DOI: 10.1371/journal.pone.0175771

Surzycki S. 2000. General aspects of DNA isolation and purification. Basic Tech Mol Biol 1-32. DOI: 10.1007/978-3-642-56968-5_1

Xu W, Morris U, Aydin SB, Msellem MI, Shakely D, Petzold M. 2015. SYBR greeb real-time PCR-RFLP assay targeting the Plasmodium cytochrome B gene-A highly sensitive molecular tool for malaria parasite detection and species determination. PLoS One 10 (3): e0120210. DOI: 10.1371/journal.pone.0120210

ASIAN J TROP BIOTECHNOL
Volume 18, Number 1, June 2021
Pages: 32-36

ISSN: 0216-6887
E-ISSN: 2301-8658
DOI: 10.13057/biotek/c180104

Density of coliform bacteria in well water filtered using a filter coated with silver nanoparticles

LILIS NURVIANTI MUFIDAH[1], PRABANG SETYONO[2,♥], ARI SUSILOWATI[1]

[1]Department of Biology, Faculty of Mathematics and Natural Sciences, Universitas Sebelas Maret. Jl. Ir. Sutami 36A, Surakarta 57126, Central Java, Indonesia

[2]Department of Environmental Science, Faculty of Mathematics and Natural Sciences, Universitas Sebelas Maret. Jl. Letjend. Urip Sumoharjo, Surakarta 57128, Central Java, Indonesia. Tel./fax. +62-271-663375, ♥email: prabangsetyono@gmail.com

Manuscript received: 4 March 2021. Revision accepted: 11 June 2021.

Abstract. *Mufidah LN, Setyono P, susilowati A. 2021. Density of coliform bacteria in well water filtered using a filter coated with silver nanoparticles. Asian J Trop Biotechnol 18: 32-36.* The poor filtration process causes low water quality due to coliform bacteria. Today's nanoparticle technology is growing, one of which is silver nanoparticles known to have antimicrobial properties. Silver nanoparticles can be an alternative for making water filters while also killing bacteria. Therefore, this study was conducted to see the density of coliform bacteria in well water filtered using a filter coated with silver nanoparticles. It is an experimental study with five significant steps: synthesis of silver nanoparticles via reduction, coating filter paper with silver nanoparticles via the shake flask method, water filtration, bacterial density determination via the Most Probable Number (MPN) method, and coliform bacteria viability determination. The main parameter observed in this study was the density of coliform bacteria in well water through a filtering process, namely the MPN value. The synthesis of silver nanoparticles in the form of a gray-green-brown colloidal solution was formed at a wavelength of 437 nm. Silver nanoparticles can stick to the filter paper, which will be used for filtering, indicated by the change in the color of the paper to grayish brown. The MPN value of the control group in all wells was >1,100/100 mL, while the treatment group's wells were 1,2,3, 9.05; 553.65; and 1.5/100 mL. The t-test analysis of the MPN value showed a significant difference between the control and treatment groups with a significance value of <0.05, i.e., 0.04. The coating of silver nanoparticles on the water filter also killed coliform bacteria, which was indicated by the absence of bacteria growth from the filter paper used. The density of coliform bacteria in well water filtered using a filter coated with silver nanoparticles was lower than the control (without silver nanoparticle coating).

Keywords: Coliform, filtering, Most Probable Number, silver nanoparticles, water quality

INTRODUCTION

Water is a source of life because water is vital for all organisms, including humans, animals, and plants. According to Istipsaroh et al. (2016), water is the primary resource with many benefits in life, especially for humans. Humans cannot survive without water because most of the human body consists of water.

Human needs for water always increase from time to time, not only because of the increasing number of people who need water but because of the increasing intensity and variety of water needs. Humans use water to meet their needs, such as washing, bathing, and daily consumption. The rising number of people, the increasing human demand for clean water, and the increasing pollution level (Boretti and Rosa 2019; Hertika et al. 2021). Human activities can lead to water pollution, such as throwing garbage out of place and a lack of awareness of the cleanliness of the surrounding environment (Ferronato and Torretta 2019).

Well water or groundwater comes from the ground or infiltration of rainwater. Well water is widely used by the community, especially in rural areas. However, not all communities have water sources that meet health requirements. Population growth causes the need for clean water or water suitable for consumption. The well water used by the community has reasonable physical, chemical, and biological qualities, which still need to be tested to determine its suitability of the water for daily use (WHO 2006).

People tend to pay less attention to the water quality they consume in the current era, both water content and processing. According to Pradana and Marsono (2013), this is due to the advancement of technology and the increasing busyness of society. Hence, people choose a more practical way to meet their consumption water needs at a lower cost, one of which is filtering techniques.

The poor filtering process can cause water quality not to meet the regulations on drinking water quality. One of the causes is that the coliform bacteria content will be greater due to the filtering system or equipment used. According to Khaq (2016), coliforms are a group of bacteria as an indicator to determine the contamination of pathogenic bacteria in a water source. Examples of a group of bacteria called coliforms are *Escherichia coli, Enterobacter aerogenes, Citrobacter freundii,* and *Shigella* sp., which causes diarrhea.

Nanoparticle technology, called nanotechnology today, is growing. According to Wahyudi et al. (2011), one of the nanotechnology applications in the engineering of metal particles and metal oxides such as silver (Ag), copper (Cu), TiO_2, ZnO, and nanometer-sized MgO, which are applied to various antimicrobial products such as textiles, pulp, and

paper, ceramics, and so on. Nanotechnology can be used as an alternative to water filters by manufacturing and applying structures/materials with nanometer dimensions.

The antimicrobial properties of colloidal silver can kill all pathogenic microorganisms, and there have been no reports of microbes that are resistant to silver (Ariyanta et al., 2014). The antimicrobial properties of silver can be used as an alternative for making water filters while also killing bacteria by coating the filter.

So far, many studies have been carried out on the application of silver nanoparticles. Some examples of silver nanoparticle applications that have been carried out include silver nanoparticles as a catalyst, a real-time optical sensor, and an antimicrobial agent (Haryono et al. 2008). As an antimicrobial agent, silver nanoparticles are used for lining wound dressings (Ariyanta et al., 2014). In addition, silver nanoparticles can be inoperable on other materials such as water and air filters and textile fibers. Therefore, this study was conducted to test a water filter coated with silver nanoparticles against the density of coliform bacteria.

This study aimed to determine the density of coliform bacteria in well water filtered using a filter coated with silver nanoparticles.

MATERIALS AND METHODS

Research time and place

This research was carried out from October 2018 to April 2019 at the Biology Laboratory and Integrated Mathematics and Natural Sciences Laboratory of Faculty Mathematics and Natural Sciences, then the Central Laboratory of Universitas Sebelas Maret, Surakarta, Central Java, Indonesia.

Ingredient

The materials used in this research include silver nanoparticles synthesis materials, silver nanoparticle activity test materials, silver nanoparticle coating materials on filter paper, water filtering materials, coliform bacteria test materials, and bacterial viability test materials. The materials used to synthesize silver nanoparticles include $AgNO_3$ 1.0 mm, sodium citrate 1%, and aquadest. The test materials for silver nanoparticle activity include sample water, silver nanoparticles, and NA medium. The silver nanoparticle coating material includes filter paper no. 1, aquadest, and silver nanoparticles on filter paper. Water filtering materials include sample water and filter paper infused with nanoparticles. Distilled water, lactose broth single media, lactose broth double media, BGLB media, aluminum foil, plastic wrap, and label paper are used in the coliform bacteria test. The materials used to determine bacterial viability are NA medium and filter paper used to filter water.

Procedures

Silver nanoparticle synthesis

Synthesis of silver nanoparticles was made by heating 150 mL of $AgNO_3$ with a concentration of 1.0 mm to boiling in an Erlenmeyer flask. 1% sodium citrate was added to this solution in 15 mL of distilled water dropwise. The mixture was stirred using a magnetic stirrer until it turned pale yellow during the heating process. Pale yellow indicates that silver nanoparticles have been formed (Mailu et al., 2010).

Silver nanoparticle characterization

According to Ariyanta et al. (2014) research, the silver nanoparticles formed were then characterized. Characterization was carried out using UV-vis Spectro, which determines whether or not silver nanoparticles are formed. The appearance of the absorbance peak at a wavelength of ± 410 nm to determine that silver nanoparticles have been formed.

Silver nanoparticle activity test

The silver nanoparticles that have been created are then combined with sample water in a ratio of 1:2, 1:3, or 1:5, depending on the amounts of silver nanoparticles present in the sample water. When silver nanoparticles are mixed with sample water, the results are diluted by a factor of 10^{-2} and 10^{-3}, and each dilution is planted on NA media for two repetitions.

Silver nanoparticle coating on filter paper

The coating of silver nanoparticles on filter paper was carried out by Duran et al. (2007). The filter paper used is filter paper no. 1. Filter paper soaked in silver nanoparticles, then incubated using a shaker incubator for 36 hours and allowed to stand for 5 minutes. The filter paper coated with silver nanoparticles was dried again in an oven at a temperature of 70°C for 5 minutes.

Water sampling (well water)

The wells used were three sampling locations around the river flow, Banjarsari District, Surakarta. The sample container used was washed and sterilized by covering the mouth of the bottle using aluminum foil and coated with plastic wrap, and then sterilized using a sterilization autoclave. The sampling device is lowered into the well. Then the sampling device is removed after filling the sample. The water is transferred from the sampling device into the sample container preheated with a Bunsen burner. After being filled, it is heated again with a Bunsen burner and closed again (SNI 6989.58:2008).

Water filter

Filter paper that has been coated with silver nanoparticles is then applied to filter water samples. The filter paper is placed or affixed to the funnel. Then the funnel is inserted into the culture bottle as a container. The water sample was then poured into a funnel that had been pasted with nanoparticle filter paper at a speed of 10 mL/min. The filtered water was then tested for bacteria using the Most Probable Number (MPN) method.

Coliform bacteria density and viability test

Coliform bacteria test was carried out on filtered water samples and filter paper used for filtering water samples. Coliform bacteria in filtered water samples were counted

using the MPN method. In contrast, on filter paper used for filtering water, samples were grown on NA media and seen whether coliform bacteria were alive or not.

Most Probable Number (MPN) test. The test for the MPN consists of two stages: the presumptive stage and the confirmed stage. 10 mL, 1 mL, and 0.1 mL samples were inoculated on Lactose Broth media in three series of tubes for each volume, then incubated at 37°C for 24 hours. Positive tubes were identified by the presence of gas and a change in the purity of the Durham tube. The verified test is next performed on the positive tube from the presumptive test. A sample of 1 ose needle inoculated with Lactose Broth media was transferred to BGLB media and incubated at 37°C for 24 hours. The number of positive tubes (cloudy and gaseous) was counted, and the number of coliform bacteria per 100 mL of sample was calculated using the MPN table.

Bacterial viability test. The viability test was carried out by planting the filter paper directly on NA media and incubating it for 24 hours at 37°C. Planting results were observed to see the viability of bacteria.

Data analysis

The data obtained is the number of coliform densities in water filtered using silver nanoparticles and controls (without silver nanoparticles). The data were then compared and analyzed using the T-test method.

RESULTS AND DISCUSSION

Silver nanoparticle synthesis

The principle of synthesizing silver nanoparticles uses a reduction reaction with silver nitrate ($AgNO_3$) precursor and sodium citrate as a reducing agent. The reduction reaction occurs when the dropwise addition of a reducing agent and a stabilizer, namely sodium citrate solution, is added to a boiling silver nitrate solution. The colloidal solution synthesized by silver nanoparticles is shown in Figure 1.

The colloidal solution formed from the synthesis of silver nanoparticles is gray-green brown. The color indicates that silver nanoparticles have been formed, as stated by Zielinska et al. (2009), that the color of the colloidal silver nanoparticle solution is red to grayish-green depending on the ratio of the reducing agent. Apart from looking at the appearance of the color, it is necessary to carry out characterization to ensure further that silver nanoparticles have been formed.

Silver nanoparticle characterization

The purpose of characterizing colloidal silver nanoparticle solution is to ensure that silver nanoparticles form successfully in the solution. Characterization utilizing a UV-Vis spectrophotometer in which UV light with a wavelength of 300 to 600 nm is fired onto a colloidal solution of silver nanoparticles. Silver nanoparticles formed successfully will exhibit wavelengths between 400 and 500 nm, as these are the wavelengths of silver nanoparticles (Bagyalakshmi and Haritha 2017). The findings of the UV-Vis spectrophotometer's characterization are displayed in Figure 2.

The UV-Vis spectrophotometer determined the colloidal silver nanoparticle solution had a wavelength of 437 nm and an absorbance of 1.49403. These findings are consistent with previous research, which indicates that the produced silver nanoparticles have a wavelength of 418-419 nm (Ariyanta et al. 2014), a wavelength of 420 nm (Jain and Pradeep 2004), and a wavelength of 411.4-432.7 nm (Wahyudi et al., 2011). Characterization with a UV-Vis spectrophotometer revealed that silver nanoparticles were generated throughout the manufacturing procedure.

Silver nanoparticle activity

The silver nanoparticles that have been formed are tested for their antibacterial activity by mixing a colloidal solution of silver nanoparticles and sample water with various comparisons to then calculate the number of bacteria that grow with the total plate count. The results of the antibacterial activity test with a total plate count are presented in Table 1.

In the control group, seeding a solution of colloidal silver nanoparticles and sample water at a dilution of 10-2 revealed that bacteria grew in wells 1 and 2 but were too few to count (TFTC), but well 3 had 25 x 102 cfu/mL. Bacterial growth on the growing media was not seen in the treatment group; it means that when silver nanoparticles come into direct contact with a material, they behave as an effective antibacterial.

Figure 1. Solution of colloidal silver nanoparticles

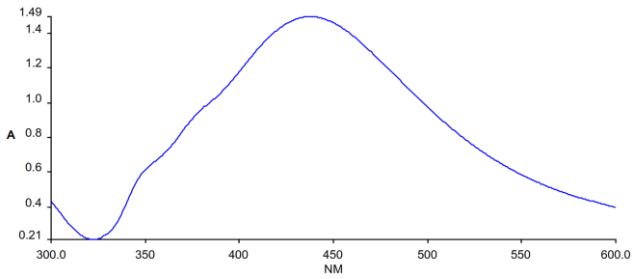

Figure 2. Graph of wavelength and absorbance of colloidal silver nanoparticle solution

Silver nanoparticle coating on filter paper

The filter paper gets coated by immersing the filter paper in a colloidal solution containing silver nanoparticles. The results of putting silver nanoparticles on filter paper are shown in Figure 3. After 36 hours of soaking in a colloidal silver nanoparticle solution, the filter paper produced a color change. Initially white, the filter paper gradually took on a grey-brown hue. This color change indicates the presence of silver nanoparticles on the filter paper. These findings corroborate Jain and Pradeep's research (2004) on silver nanoparticle coatings on polyurethane.

Most Probable Number (MPN) filtrate

The MPN method determines the density of coliform bacteria in the filtrate. The MPN test consists of two stages: estimation and affirmation. The presumptive test is used to predict the presence of coliform bacteria. In contrast, the confirmation test is used to confirm the presence of coliform bacteria based on the outcome of the presumptive test. The comparison of MPN test reactions during the estimation and confirmation stages is shown in Figure 4. A color change in the media and the formation of bubbles in the Durham tube (Figure 4 A1, A2, B1) indicate the presence of coliform bacteria in the sample water; on the other hand, if no color change occurs in the media and no bubbles form in the Durham tube (Figure 4 A3, A4, B2), there are no coliform bacteria in the sample water. The MPN value of filtered water from three wells with two replications is reported in Table 2.

According to the MPN value, there is a decrease in the density of coliform bacteria in the sample water filtered with a filter coated with silver nanoparticles compared to water filtered with a filter not coated with silver nanoparticles. MPN levels for water samples in all control groups exceeded 1100/100 mL, but MPN values in the silver nanoparticle coating treatment were 9.05; 553.65; and 1.5/100 mL, respectively. The t-test analysis revealed a significant difference between the control and treatment groups, with a significance value of 0.05 or 0.04. This demonstrates that adding silver nanoparticles to the filter reduces the density of coliform bacteria in the filtering process.

Table 1. Bacterial growth in well water after added colloidal silver nanoparticles

Well	Control (without nanoparticles silver)	Treatment (addition of silver nanoparticles)		
		1:2	1:3	1:5
1	TFTC ($5x10^2$ cfu/mL)	Not growing	Not growing	Not growing
2	TFTC ($8x10^2$ cfu/mL)	Not growing	Not growing	Not growing
3	$25x10^2$ cfu/mL	Not growing	Not growing	Not growing

Note: 1:2; 1:3; 1:5 = ratio of colloidal silver nanoparticle solution and sample water

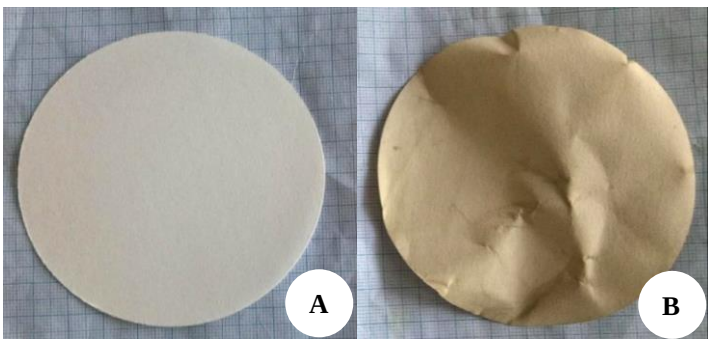

Figure 3. Filter paper: A. No silver nanoparticle coating, B. After silver nanoparticle coating

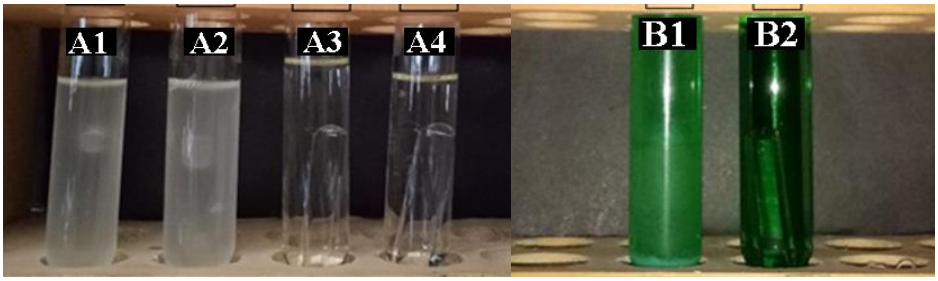

Figure 4. Reaction to MPN Test: A. Prediction test; B. Affirmation test

Table 2. MPN value of well water after filtration

Category	Well	Coliform Test (MPN/100 ml)
Control	1	>1100
	2	>1100
	3	>1100
Treatment	1	9.05
	2	553.65
	3	1.5

Table 3. Observation of bacterial viability on filter paper

Category	Well	Bacterial viability	
		Growing	Not growing
Control	1	√	
	2	√	
	3	√	
Treatment	1		√
	2		√
	3		√

Bacterial viability on filter paper

Bacterial viability testing on filter paper is used to establish whether silver nanoparticles can actively kill bacteria or work mechanically to decrease the pores in the filter paper. Table 3 summarizes the results of observations of bacterial viability on filter paper.

The results of the bacterial viability test on the filter paper used for filtering are shown in Table 3. When uncoated filter paper was planted on NA medium after filtering, bacteria grew (control group). In contrast, when coated filter paper was planted on NA media, bacteria did not grow (treatment group). These findings suggest that covering filter paper with silver nanoparticles acts as a filter and kills bacteria throughout the water filtering process.

Ariyanta et al. (2014) also reported on the capacity of silver nanoparticles to kill germs. According to his research, the wound dressing cloth coated with silver nanoparticles eliminated the bacteria *E. coli*, *Bacillus subtilis*, and *Staphylococcus aureus* in vitro using the shake flask method followed by a total plate count to determine the bacteria's quantity.

According to Franci et al. (2015), silver nanoparticles can physically interact with the surface of bacterial cells. It damages the cell membrane, causing structural changes that make the bacterium more permeable. It is well established that when silver nanoparticles accumulate on the cell membrane of *E. coli* bacteria, they generate a gap that penetrates the bilayer, increasing permeability and ultimately cell death.

In conclusion, the density of coliform bacteria was significantly lower in well water filtered through a filter coated with silver nanoparticles than in control water (without silver nanoparticle coating).

REFERENCES

Ariyanta HA, Wahyuni S, Priatmoko S. 2014. Preparasi nanopartikel perak dengan metode reduksi dan aplikasinya sebagai antibakteri penyebab infeksi. Indones J Chem Sci 3 (1): 1-6. [Indonesian]

Bagyalakshmi J, Haritha H. 2017. Green synthesis and characterization of silver nanoparticles using *Pterocarpus marsupium* assessment of its in vitro antidiabetic activity. Am J Adv Drug Deliv 5 (3): 118-130. DOI: 10.21767/2321-547X.1000019.

Boretti A, Rosa L. 2019. Reassessing the projections of the world water development report. NPJ Clean Water 2: 15. DOI: 10.1038/s41545-019-0039-9.

Duran N, Marcato PD, de souza GIH. 2007. Antibacterial effect of silver nanoparticles produced by fungal process on textile fabrics and their effluent treatment. J Biomed Nanotechnol 3 (2): 203-208 DOI: 10.1166/jbn.2007.022.

Ferronato N, Torretta V. 2019. Waste mismanagement in developing countries: A review of global issues. Intl J Environ Res Public Health 16 (6): 1060. DOI: 10.3390/ijerph16061060.

Franci G, Falanga A, Galdiero S, Palomba L, Rai M, Morelli G, Galdiero M. 2015. Silver nanoparticles as potential antibacterial agents. Molecules 20: 8856-8874. DOI: 10.1002/1097-4636(20001215)52:4<662::aid-jbm10>3.0.co;2-3.

Haryono A, Sondari D, Harmami SB, Randy M. 2008. Sintesa Nanopartikel Perak dan Potensi Aplikasinya. Jurnal Riset Industri 2 (3): 156- 163. [Indonesian]

Hertika AMS, Supriatna, Darmawan A, Nugroho BA, Handoko AD, Qurniawatri AY, Prasetyawati RA.2021. The hematological profile of Badher fish (*Barbonymus altus*) to evaluate water quality in the Badher Bank Conservation Area, Tawangrejo Village, Blitar District, East Java, Indonesia. Biodiversitas 22: 2532-2541. DOI: DOI: 10.13057/biodiv/d220510.

Istipsaroh, Laili S, Zayadi H. 2016. Uji kualitas air sumur Kelurahan Merjosari Kecamatan Lowokwaru Kota Malang. J Ilmiah Biosaintropis 2 (1) : 19-24. [Indonesian]

Jain P, Pradeep T. 2004. Potential of silver nanoparticle-coated polyurethane foam as an antibacterial water filter. Biotechnol Bioeng 90 (1): 59-63. DOI: 10.1002/bit.20368.

Khaq KN. 2016. Deteksi cemaran bakteri *Coliform* dan *Salmonella* sp. pada tempe yang dikemas daun pisang di Daerah Salatiga. Agric 28 (1&2): 79-86. DOI: 10.24246/agric.2016.v28.i1.p79-86. [Indonesian]

Mailu SN, Waryo TT, Ndangili PM, Ngece FR, Baleg AA, Baker PG, Iwuoha EI. 2010. Determination of anthracene on ag-au alloy nanoparticles/overxidized-polypyrrole composite modifies glassy carbon electrodes. Sensor 10: 9449-9465. DOI: 10.3390/s101009449.

Pradana YA, Marsono BJ. 2013. Uji kualitas air minum si ulang di Kecamatan Sukodono, Sidoarjo ditinjau dari perilaku dan pemeliharaan alat. J Teknik Pomits 2 (2): 83-86. [Indonesian]

Wahyudi T, Sugiyana D, Helmy Q. 2011. Sintesis nanopartikel perak dan uji aktivitasnya terhadap bakteri *E. coli* dan *S. aureus*. Arena Tekstil 26 (2): 1-60. DOI: 10.31266/at.v26i1.1442. [Indonesian]

World Health Organization (WHO). 2006. Guidelines for Drinking-Water Quality: Incorporating First Addendum. Vol. 1, Recommendations. 3rd ed. WHO, Geneva.

Zielinska A, Skwarek E, Zaleska A, Gazda M, Hupka J. 2009. Preparation of silver nanoparticles with controlled particle size. Proc Chem 1: 1560-1566. DOI: 10.1016/j.proche.2009.11.004.

ASIAN J TROP BIOTECHNOL
Volume 18, Number 1, June 2021
Pages: 37-45

ISSN: 0216-6887
E-ISSN: 2301-8658
DOI: 10.13057/biotek/c180105

Screening of phosphate solubilizing bacteria from sugarcane plant rhizosphere as biofertilizer agent for sorghum growth (*Sorghum bicolor*)

RISKI MARETA AYU PRISILLIA, ARI SUSILOWATI♥, SOLICHATUN
Department of Biology, Faculty of Mathematics and Natural Sciences, Universitas Sebelas Maret. Jl. Ir. Sutami 36A Surakarta 57126, Central Java, Indonesia. Tel./fax. +62-271-663375, ♥email: arisusilowati@staff.uns.ac.id

Manuscript received: 4 February 2022. Revision accepted: 5 March 2022.

Abstract. *Prisillia RMA, Susilowati A, Solichatun. 2021. Screening of phosphate solubilizing bacteria from sugarcane plant rhizosphere as biofertilizer agent for sorghum growth (*Sorghum bicolor*). Asian J Trop Biotechnol 18: 37-45.* Sorghum plants (*Sorghum bicolor* L.) development in Indonesia is still behind due to limited application in a few locations. Sorghum is a crop that can be grown on marginal terrain. The scarcity of nutrients in marginal land necessitates the addition of nutrients. Biofertilizer is a biological fertilizer that comprises microorganisms that act as nutrient suppliers and promote plant growth in the soil. This research included soil sampling, prospective testing, and screening to identify a biofertilizer solubilizing bacterium candidate. Bacterial screening entails bacterial identification, bacterial growth measurement, and a media pH test. The biofertilizer application experiment used a completely randomized design (CRD) with two factors: the first component was the addition of phosphate solubilizing bacteria, which was divided into two levels, without bacteria, and with bacteria. The second factor was variations in the NPK (Nitrogen, Phosphorus, Potassium) fertilizer concentrations of 0, 25, 50, and 100%, which correspond to 0; 0.625; 1.25, and 2.5 g NPK / plant, respectively. The vegetative phase of sorghum growth was observed for 50 days, and height, the number of leaves, leaves color, root length, fresh weight, and dry weight of sorghum plants were determined using ANOVA and DMRT test levels of 5%. Seven isolates of phosphate solubilizing bacteria were obtained from this research. Two possibly superior isolates were produced as biofertilizers: BPF 5 and 12 I. Compared to control treatments, adding BPF 5 and 12 I isolate in combination with varied NPK fertilizer concentrations significantly altered sorghum growth parameters, such as plant height, root length, fresh weight, and dry weight. The addition of BPF 12 I isolates at 0% and 25% fertilizer concentrations results in sorghum growth.

Keywords: Biofertilizer, phosphate solubilizing bacteria, sorghum plant growth

INTRODUCTION

Sorghum (*Sorghum bicolor* L.) production and development in Indonesia fall behind rice, corn, and other cereals due to sorghum's limited use as a food crop. Sorghum has excellent commercial development potential in Indonesia, owing to favorable agro-ecological conditions and the availability of sufficient acreage (Tuwu et al. 2012). Sorghum has many cultivated varieties, such as grain genotypes, fodder, fiber, sugar, and dual-purpose genotypes (Arbab and Dagash 2017). Sorghum can also be fermented to produce beer. Additionally, sorghum stalks and seeds can be utilized in the sugar business, and sorghum seeds can be converted to bioethanol. Biomass from sorghum harvesting can be utilized as a source material for biogas production (Sumarno et al., 2013). Sorghum growth and cultivation remain limited in some areas of Indonesia, most notably in Java, South Sulawesi, Southeast Sulawesi, West Nusa Tenggara (NTB), and East Nusa Tenggara (NTT), both as a source of indigenous food items and animal feed. Sorghum's tolerance for drought and waterlogging is one of its properties. Sorghum can be planted on a marginal, marsh, or acidic land (Anas 2007).

Because marginal lands have a limited supply of nutrients, they require additional nutrients such as fertilization to boost crop output. Excessive use of chemical fertilizers can harm the ecology of agricultural land, resulting in the loss of indigenous microbes and disrupting the soil's nutrient balance (Yuliar 2006). The use of an excessive dose of chemical fertilizer can be mitigated by using a biofertilizer that reduces the quantity and eliminates the need for chemical fertilizers (Sudiarti 2017). Biofertilizer is a biological fertilizer made up of microorganisms that encourage development by increasing the nutritional requirements of plants that act as a source of nutrients in the soil. They are readily absorbed by plants and have been shown to improve plant productivity (Nugraha et al., 2014). Numerous soil microbes in the rhizosphere, including non-symbiotic nitrogen-fixing bacteria, symbiotic nitrogen-fixing bacteria, and phosphate-solubilizing bacteria, can be employed as biofertilizers (Setyorini et al. 2006).

The rhizosphere is the zone between the root surface and the soil influenced by plant roots' exudation and microorganisms' interaction. The exudate produced by plant roots results in a greater bacterial population in the rhizosphere than in other soil regions (Akbari et al., 2007). Bacteria that solubilize phosphate can convert it to dissolved phosphate, which plants can take via the release of organic acids. Phosphate solubilizing bacteria can dissolve P ions attached to soil cations such as Al, Fe, Ca, and Mg and convert them to a form suitable for natural plant absorption (Subowo et al. 2010). Biofertilizer research to accelerate the growth of sorghum plants is still

in its infancy, and its use requires development. The goal of this research is to produce phosphate-solubilizing bacteria from the rhizosphere for use as a biofertilizer and a suitable concentration of chemical fertilizer for use in conjunction with the biofertilizer to accelerate the growth of sorghum plants in a controlled environment.

MATERIALS AND METHODS

Research site

This research was carried out from June to December 2019 at the Environmental Microbiology Laboratory, Center for Biological Research of the Indonesian Institute of Sciences (LIPI), located at Jl. Raya Jakarta-Bogor km. 46, Cibinong Science Center, Cibinong (16911), Bogor, West Java, Indonesia.

Materials

The soil samples were taken from the root zone of sugarcane plants from sugarcane estates in Tasik Madu, Karanganyar. Sorghum seeds were employed in this investigation (*Sorghum bicolor* l.) Seeds were obtained from the south Sulawesi cereal crops research institute. The nutrient agar (NA) media employed in this investigation contained 5 g peptone, 3 g beef extract, 20 g agar, and 1,000 mL sterile distilled water. The lysogeny broth (LB) media had 10 g polypeptone, 5 g yeast extract, 5 g sodium chloride, 10 g agar, and 1,000 mL of sterile distilled water. Selective media for phosphate solubilizing bacteria, namely Pikovskaya media (PK), consisted of dextrose 10 g, $Ca_3(PO_4)$ 2.5 g, yeast extract 0.5 g, $MnSO_4$ 0.0001 g, MgSO4 0.1 g, $FeSO_4$ 0.0001 g, $(NH_4)_2SO_4$ 0.25 g, KCL 0.2 g, agar 18 g, and sterile distilled water 1000 mL.

Experimental design

The biofertilizer application to sorghum plants was designed experimentally using a completely randomized design (CRD). The treatment entailed two components; the first was the administration of phosphate solubilizing bacteria, which came in two forms: without bacteria and with bacteria. The second factor is the change in NPK fertilizer concentration, which is divided into four levels: 0%, 25%, 50%, and 100%, which correspond to 0; 0.625; 1.25, and 2.5 g NPK/plant, respectively (Sudiarti 2013). The NPK fertilizer utilized in this study is Phonska NPK fertilizer, which PT Petrokimia Gresik manufactures. It contains 15% nitrogen (N), 15% phosphate (P_2O_5), and 15% potassium (K_2O). Three replications of each treatment were obtained, and the following treatment combinations were obtained: (i) The first treatment consisted of no bacteria (control) and a 0% NPK fertilizer concentration. (ii) The second treatment consisted of no bacteria (control) and a concentration of NPK fertilizer equal to 100%. (iii) The third treatment involved the administration of phosphate solubilizing bacteria and NPK fertilizer at doses of 0%, 25%, and 50%.

Soil sampling and isolation of rhizosphere bacteria

The rhizosphere was sampled by extracting soil from around the plant roots at a depth of 20 cm below the soil surface. Three random soil samples were gathered and composited. Bacteria were isolated from sugarcane plantation soil using a dilution procedure, which involved weighing 1 g of soil into a test tube containing 9 mL of sterile distilled water and vortexing for 15 minutes. The obtained suspension was diluted to a concentration of 10^{-5} dilution sessions (Amaria et al., 2013). The dilution results were multiplied by 100 and then grown in NA medium using the pour plate method and incubated at room temperature for 2 x 24 hours. Each bacterial colony growing on the NA medium was isolated using the streak plate method and purified until a single colony was produced. Each purified isolate was cultured in a slanted NA and LB medium.

Phosphate solubilizing bacteria potential test

The isolated bacteria were then cultured in PK using the spot method with sterile toothpicks. The edge of the petri dish was wrapped in plastic wrap and incubated at room temperature for 7 x 24 hours to avoid contamination. On pk media, the activity of phosphate solubilizing bacteria was assessed by the presence of a clear zone (Rao 1994). Observations determined the presence or absence of a clear zone. If the isolate produced a clear zone, it was chosen for further investigation, and the phosphate dissolution index was calculated using the following formula (Sharon et al., 2016):

$$\text{Phosphate Solubility Index (SI):} \frac{\text{Clear Zone Diameter} - \text{Colony Diameter}}{\text{Colony Diameter}}$$

Bacteria identification

Identification of bacteria was performed macroscopically and microscopically. Macroscopic observations were made by examining the morphology of the single colonies that formed following the application of the streak plate method. Single colony observations included colony shape, color, borders, and the height of bacterial colonies (Cappuccino and Sherman 1998). Microscopic observations were made by examining the Gram staining data. Microscopic investigations of the form of bacterial cells were also made. Purple staining indicates that the bacteria are Gram-positive, whereas red staining indicates Gram-negative bacteria (Fitri and Yasmin 2011).

Preparation of liquid Pikovskaya media containing phosphate solubilizing bacteria

Phosphate solubilizing bacteria isolates were rejuvenated on NA media for 1 x 24 hours, then grown on LB media with the same Optical density (OD) value as measured using a spectrophotometer with a wavelength of 600 nm. Then it was cultured into 50 mL of liquid PK. Each Erlenmeyer containing phosphate solubilizing bacteria was shaken using a shaker incubator at 120 rpm for seven days (Rahayu et al. 2014).

Measurement of growth of phosphate solubilizing bacteria

OD measurement of phosphate solubilizing bacteria taken from liquid P.K. media. Then the bacterial culture in the medium was taken at 0.5 mL diluted with 7 mL of sterile distilled water and then put into a cuvette and measured using a spectrophotometer with a wavelength of 600 nm (Purnomo et al. 2017). With three replications, OD analysis was carried out every 1 x 24 hours from day 0 to day 7.

Media pH test

Measurement of changes in pH was carried out by taking 2 mL of the bacterial culture from liquid PK media in a test tube and measuring it using a pH meter. Analysis of changes in the pH of the media for each bacterial isolate was carried out every 1 x 24 hours starting from day 0 to day 7 with two replications.

Bacterial growth standard curves

The standard curve for bacterial growth was constructed by determining the population of live bacteria using the pour plate method and measuring the optical density of the bacteria using a spectrophotometer (Hadioetomo 1993). The optical density was determined directly on bacterial cultures grown in an LB medium using a spectrophotometer set to a wavelength of 600 nm. Inoculum is extracted from the rejuvenated stock culture and placed one time utilizing the ose into 50 mL of LB medium, then shaken. Bacterial culture from shaken LB media is added in a volume of up to 1 mL to 9 mL of physiological salt. Several dilution sessions and NA media growth using the pour plate method were performed (Nurhayati et al., 2007). Measurements were taken every two hours for 24 hours, from the 0th to the 24th hour. The number of bacteria growing on NA media was determined as follows using the TPC formula (Sukmawati and Hardianti 2018):

$$\frac{cfu}{ml} = \frac{(Number\ of\ Colonies)\left(\frac{1}{Sample Volume}\right)}{Dilution\ Factor}$$

Making biofertilizer

A 2% molasses solution was prepared by heating 14 mL molasses in 686 mL water to a boil and allowing it to cool before adding each bacterial culture. The molasses included 10% cultures (70 mL of bacterial culture from LB media in 630 2% molasses) (Sudiarti 2013). Bacterial cultures were added to molasses at a concentration of 2% with the same OD value. OD absorbance is determined using a spectrophotometer with a wavelength of 600 nm. Total Plate Count (TPC) was determined in bacterial cultures using a series of dilutions up to 10^{-5} and incubation at 37°C for 24 hours. TPC was determined using the cfu/mL unit (Sudiarti 2017) with three replications.

Preparation of sorghum seeds

Sorghum seeds are chosen for their uniform shape and lack of physical damage. Seeds were sterilized by washing with distilled water and 1% sodium hypochlorite to remove fungus infection and then immersed in hot water at 60°C for 24 hours to aid in germination. Seeds that swell and settle due to water absorption are used as research items.

Planting of sorghum seeds

Sorghum seeds are planted in ultisol soil. The soil was sterilized first in an autoclave at 121°C and 1 atm pressure for 20 minutes and then in an oven (Karti and Setiadi 2011). After baking, the soil was placed in polybags of the same size and weight as 300 g, and the pH of the soil was determined using a soil tester. Each polybag contained three sorghum seeds and was watered with 50 mL of sterile distilled water. Sorghum is grown for 13 days after planting and then treated with NPK fertilizer at various concentrations, namely 0%, 25%, 50%, and 100%, followed by biofertilizer in the form of molasses solution containing inoculated phosphate solubilizing bacteria and without inoculation bacteria (control) at a biofertilizer concentration of 15 mL/plant (Sudiarti 2013).

Observation of sorghum growth

For 50 days, observations of sorghum growth in the vegetative phase were made (Aqil and Bunyamin 2013). They were determined every three days by measuring the sorghum plant's height with a ruler and counting the leaves produced. Then, during the harvesting process, leaf color was determined using the Munsell color chart book's standards, root length was determined using a ruler, and the wet and dry weight of the complete sorghum plant was determined using a scale.

Analyses of data

This research gathered both qualitative and quantitative data. The Analysis of Variance (ANOVA) test was used to assess quantitative data on sorghum development to identify the effect of phosphate solubilizing bacteria and fluctuations in the content of NPK fertilizer at various concentrations. If a substantial difference exists, it will be further tested using Duncan's Multiple Range Test (DMRT) with a 5% test level. Simultaneously, descriptive analysis is used to analyze the qualitative data.

RESULTS AND DISCUSSION

Isolation and characterization of phosphate solubilizing bacteria

Bacterial isolates and purification from soil samples collected from sugarcane farms in Tasikmadu, Karanganyar resulted in the isolation and purification of 19 bacterial isolates, 15 of which were bacteria and four of which were actinomycetes. The isolated bacteria were then examined for their capacity to dissolve phosphate using Pikovskaya selective media containing $Ca_3(PO_4)_2$ (tricalcium phosphate). Five bacteria and two actinomycetes isolated exhibited a distinct zone, suggesting their ability to dissolve phosphate. The transparent zone generated by organic acids is composed of dissolved p. Organic acids can bind to the calcium ions in $Ca_3(PO_4)_2$ and liberate H_2PO_4, resulting in a clear colored zone (Widawati and Suliasih 2005).

Macroscopical and microscopical examinations were used to identify phosphate solubilizing bacteria. Macroscopic identification was accomplished by observing colony structure, edge, elevation, and color (Cappucino 1998), whereas microscopic observations were accomplished through Gram staining. Table 1 summarizes the observations of morphological characteristics and phosphate solubilizing bacterial cells.

Observation of phosphate solubilizing bacteria obtained bacteria with a variety of morphological characteristics. The acquired bacterial isolates were almost entirely circular colonies with flat (entire) colonies, with only one undulating. Three isolates were milky white, one was yellowish-white, one was brownish-white, and one was orange-yellow. Six isolates were Gram-positive in *Bacillus* and *Coccus* cells, while one isolate was Gram-negative in *Coccus* cells. Suryanto and Munir (2006) discovered that spherical colonies contained more bacteria than white colonies. Dewi (2008) found several Gram-positive bacteria in the form of *Coccus* and *Bacillus* cells. Gram staining is used to characterize bacterial cells and distinguish between Gram-positive and Gram-negative bacteria. It is purple in Gram-positive bacteria because of crystal violet iodine, which is retained even when treated with an alcohol bleach solution. In Gram-negative, on the other hand, it is red because crystal violet dissolves in an alcohol bleach solution, imparting a red hue to the safranin solution (Lay 1994).

Two isolates of actinomycetes, BPF 5 and BPF 15, were macroscopically examined for colony morphological characteristics, including substrate hyphae color, aerial hyphae color, and reverse pigment (Listiana et al., 2018). Microscopic investigations of hyphae structure using lactophenol staining. Septate (septate) hyphae were detected, and nonseptate hyphae (Nuryadi et al. 2016). The colonies of BPF 5 isolates were strongly connected to the media, with white substrate hyphae, gray aerial hyphae, brownish-yellow reverse pigment, and a non-insulated hyphae structure. By contrast, BPF 15 isolates were adherent to the media via white substrate hyphae. The aerial hyphae are gray, the reverse pigment is greenish-yellow, and the hyphae are septate (septate). Figure 1 shows the morphological characteristics of actinomycetes isolates.

Actinomycetes are prokaryotic organisms that include Gram-positive bacteria and are frequently found in various soil types (Akbari et al., 2017). Actinomycetes can be identified from other bacteria when examined in colonies in solid media. Actinomycetes colonies are distinct in that they are hard due to their growth on agar media, whereas other bacterial colonies are soft. Actinomycetes are characterized by their circular shape, flat edges, and uneven, starchy surfaces. The floury surface comprises many hyphae (Sulistyani and Akbar 2014). Actinomycetes are a kind of bacteria that generate hyphae (mycelium) composed of a substrate and aerial hyphae. Aerial hyphae develop from the mycelium substrate and quickly blanket the colony, like cotton or flour (Kumalasari et al., 2012). Hyphae that sprout straight from the substrate are called substrate hyphae. The reverse pigment is a color that develops at the bottom or base of an actinomycetes culture (Listiana et al., 2018). Additionally, actinomycetes can degrade phosphate, promoting plant growth and productivity (Chang et al. 1986).

Phosphate dissolution in Pikovskaya media

When cultivated on Pikovskaya agar media, bacteria can dissolve phosphate, as evidenced by forming a clear zone around the colony. The phosphate solubilization index (SI) is calculated as the ratio of the clear zone diameter formed by phosphate solubilizing bacteria to the diameter of their colonies. The dissolving index quantifies a bacterium's ability to qualitatively release phosphate, and the higher the dissolution index value, the greater the bacterium's ability to release phosphate (Elfiati et al., 2016). Table 2 contains the phosphate solubility index.

Table 1. Morphological characters and phosphate solubilizing bacterial cells

Isolate	Characterization					
	Colony morphology				Gram	Cell shape
	Shape	Edge	Elevation	Color		
BPF 5	Circular	Entire	Convex	Gray milky white with gray spots in the middle	+	Bacilli
BPF 6	Circular	Entire	Flate	Yellow-orange	+	Cocci
BPF 7	Circular	Entire	Raised	Brownish white	+	Cocci
BPF 12 I	Circular	Entire	Raised	Yellowish white (transparent)	-	Cocci
BPF 12 II	Irregular	Undulate	Flate	Milky white	+	Cocci
BPF 13	Circular	Entire	Raised	Orange white	+	Cocci
BPF 15	Circular	Entire	Flate	Milky white	+	Cocci

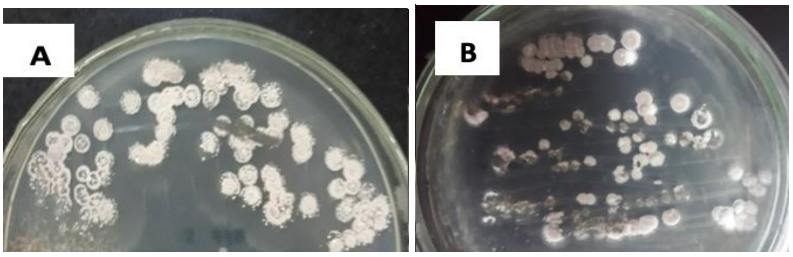

Figure 1. Observation of morphological characters at 100 x magnification (A) isolate BPF 5 and (B) isolate BPF 15

Table 2. Phosphate solubilization index for seven days of incubation

Isolate	Phosphate solubility index							SI Means
	Day -							
	1	2	3	4	5	6	7	
BPF 5	-1.00	-1.00	1.00	0.67	1.00	1.00	1.25	0.42
BPF 6	-1.00	2.00	2.00	1.00	1.00	0.67	0.67	0.90
BPF 7	0.50	0.67	1.00	1.33	1.00	0.60	0.50	0.80
BPF 12 I	2.00	2.50	3.00	2.00	2.67	2.25	2.50	2.42
BPF 12 II	1.50	2.00	2.50	1.67	2.00	2.33	2.67	2.10
BPF 13	0.50	0.67	0.50	0.75	0.60	0.80	0.67	0.64
BPF 15	-1.00	-1.00	0.50	0.50	1.00	1.50	1.00	0.36

The phosphate solubilization ability of 7 isolates capable of dissolving $Ca_3(PO_4)_2$ was indicated by forming a clear zone around the bacterial colonies. Observations were made for seven days, and various clear zones were created. The BPF isolate, which had the highest phosphate SI, was characterized by forming the largest clear zone, namely BPF 12 I of 2.42 with a clear zone of 1.4 cm. In contrast, the actinomycetes isolates were BPF 5 of 0.42 with a clear 0, 9 cm zone. It indicated that BPF 12 I and BPF 5 isolates had higher phosphate solubilization activity in releasing P bound to $Ca_3(PO_4)_2$ media, and organic acids produced by BPF isolates reacted with $Ca_3(PO_4)_2$ to form a chelate of Ca release higher P so that the application of BPF isolates as biofertilizer is based on the speed of BPF isolates in dissolving phosphate and the diameter of the clear zone which is expected to improve plants experiencing P deficiency. Superior phosphate solubilizing bacteria can produce the largest clear zone diameter compared to other bacterial colonies (Rahayu et al., 2014). Each isolate will create a phosphate SI that varies from one another. It is due to producing organic acids such as acetic acid, lactic acid, oxalic acid, malic acid, and citric acid produced by bacteria (Richardson 2001).

Growth of phosphate solubilizing bacteria on Pikovskaya media media

Bacterial growth can be measured by cell concentration or cell density. The bacterial growth curve can be divided into four phases: the lag phase (adaptation phase), log phase (exponential phase), stationary phase, and death phase. The results of measuring bacterial growth by looking at the absorbance value of OD can be seen in Figure 2. Based on Figure 2, the growth chart of phosphate solubilizing bacteria increased from day 0 to day 7. On day 0, BPF isolates experienced a lag phase (adaptation phase), where the time needed by BPF isolates to adapt to their new environment. From day 1 to day 3, BPF isolates experienced a log phase (exponential phase). BPF isolates experienced a cell division phase that would divide until the maximum number of cells was reached. From the 4th day to the 6th day, there was a stationary phase, in which the number of dead cells was the same as the number of living cells (constant growth), while on the 7th day, there was an increase in the growth of all BPF isolates and had not yet experienced the death phase. The growth medium used is rich in P, so bacteria take a long time in the metabolic process to dissolve P.

One way to determine the quality of a biofertilizer is the number of bacteria. The calculation results of the number of bacterial colonies showed that the number of phosphate solubilizing bacterial colonies was 1010 CFU/mL. It is in accordance with the quality standard of the biofertilizer, which must at least reach a concentration of 107 CFU/mL (Simanungkalit et al. 2006). BPF isolates that had the highest average number of bacterial colonies during the incubation period were BPF 6 of 86.66 x 1010 CFU/mL and 12 I of 81.69 x 1010 CFU/mL, while actinomycetes isolates were BPF 15 of 103.83 x 1010 CFU/mL and BPF 5 of 98.09 x 1010 CFU/mL so that they can be used as biofertilizer candidates. The application of biofertilizers with a high number of bacterial cell densities can compete with microorganisms found in the soil so that they can dominate around plant roots (Santoso 2000).

Changes in pH in Pikovskaya media media

The decrease in pH is one of the causes of the dissolution of Ca-phosphate into orthophosphate ions. The mechanism of phosphate dissolution results in changes in pH due to the synthesis of organic compounds released into the media (Widawati et al. 2008). Changes in the pH of the media during the seven-day incubation period can be seen in Figure 3.

According to Figure 3, the pH in the media decreased starting on day 0, which was caused by heating during sterilization, which disrupted the Ca-phosphate bond, resulting in the formation of dissolved phosphate (Rahayu et al. 2014), where the initial pH before sterilization was Neutral pH is 7. After seven days of incubation, the pH of the media was changed from neutral (pH 7) to acid (pH 5 - 4). According to Figure 3, the BPF 12 I isolation had the most significant drop in medium pH (4.14). In contrast, the actinomycetes isolate BPF 5 had the most significant decrease in media pH (4.45). It indicates that BPF 12 I and BPF 5 isolates exhibited the highest phosphate solubilization activity by producing high levels of organic acids, which resulted in a significant decrease in the pH of the media, implying that the use of phosphate solubilizing bacterial biofertilizers can increase the availability of P nutrients by liberating bound phosphate ions into available forms that plants can absorb, thereby improving soil fertility in areas with phosphate deficiency.

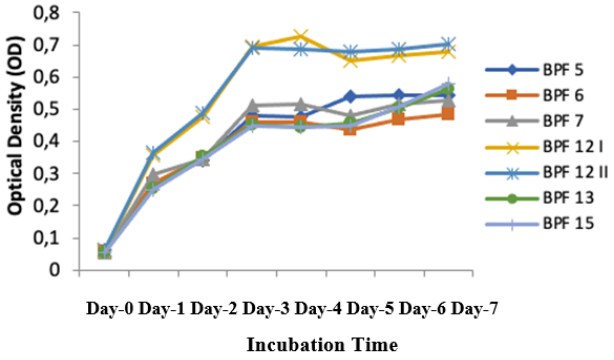

Figure 2. Phosphate solubilizing bacteria growth

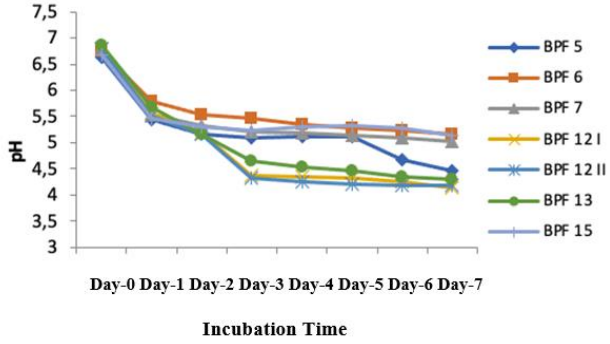

Figure 3. Changes in pH of P.K. media on BPF isolates

The pH of the media decreased during the incubation period due to the activity of BPF isolates that created organic acids as a mechanism for dissolving phosphate. Organic acids react with phosphate-binding elements such as Al_3^+, Fe_3^+, and Ca_2^+ to generate stable organic chelates in plant-utilizable forms (Firdausi et al., 2016). Bacterial organic acids result from oxidative respiration or fermentation of organic carbon sources to liberate phosphate ions bound to media containing Ca_3PO_4 and convert them to H_2PO_4- ions via the exchange of acid anions with phosphate anions or the formation of stable organic chelates (Elfiati 2005).

Sorghum plant measurement

Measurement of plant height and number of leaves was carried out when the plant was 13 days old with a height of 10 cm and the number of leaves in four pieces (Figure 4). The application of various concentrations of NPK fertilizer combined with biofertilizer in the form of BPF 12 I and BPF 5 isolates with an absorbance value of 0.557 OD and a colony number of 4.7 x 108 cfu/mL. Measurement of plant height and number of leaves was carried out periodically when the plants were 13, 17, 20, 23, 26, 29, 32, 35, 38, 41, 44, 47, and 50 days after planting. Measurements of root length, wet weight, dry weight, and leaf color were measured during the harvesting process for plants aged 50 days after planting. Figure 4 demonstrates that the BPF 12 I treatment with 0% and 25% NPK fertilizer concentrations produced significantly higher plant height, number of leaves, root length, wet weight, and dry weight than other treatments. The results from the BPF treatment with a 50% NPK fertilizer content were less than optimum. 0% and 100% resulted in the most diminutive average plant height, several leaves, root length, wet weight, and dry weight of plants, indicating that a low concentration of NPK fertilizer mixed with BPF 12 I could improve plant growth.

Because the significance value for the ANOVA test was 0.00 (0.05), it was determined that the application of various concentrations of NPK fertilizer and biofertilizer had a significant effect on the height, root length, wet weight, and dry weight of sorghum plants. Thus, the DMRT test was continued. Because the significance value of 0.77 (0.05) indicated that the administration of various NPK fertilizers and biofertilizers quantities had no significant influence on the number of leaves, the DMRT test was discontinued, and the Tukey test was used. (BNJ) level 5% to determine the effect of the treatments, which are shown in Table 3.

According to Table 3, the BPF 12 I treatment and NPK fertilizer concentrations of 0% and 25% had significantly distinct impacts on plant height, root length, wet weight, and dry weight, but not on the BPF 5 fertilizer concentration of 0% NPK. The number of leaves produced by treatments with varied concentrations of NPK fertilizer mixed with BPF 5 and 12 I was not substantially different from the control treatment.

Table 3. Growth of sorghum after treatment with 0%, 25%, 50%, and 100% concentration of NPK fertilizer and biofertilizer in the form of BPF 5 and BPF 12 I isolates.

Treatment	Plant height (cm)	Number of leaves (strands)	Root length (cm)	Wet weight (g)	Dry weight (g)
Control 0%	$24.56^{a} \pm 0.10$	$4.98^{a} \pm 0.42$	$17.67^{a} \pm 2.10$	$36.66^{a} \pm 1.42$	$16.48^{a} \pm 1.13$
Control 100%	$25.71^{ab} \pm 0.64$	$5.21^{a} \pm 0.46$	$20.60^{b} \pm 2.02$	$40.78^{b} \pm 0.57$	$20.49^{b} \pm 1.73$
BPF 5 0%	$28.48^{e} \pm 0.51$	$5.37^{a} \pm 0.58$	$23.88^{cd} \pm 0.96$	$51.86^{de} \pm 1.89$	$27.65^{de} \pm 0.72$
BPF 5 25%	$27.97^{de} \pm 0.43$	$5.45^{a} \pm 0.39$	$23.40^{c} \pm 0.70$	$49.08^{cd} \pm 1.99$	$25.77^{cd} \pm 0.67$
BPF 5 50%	$26.66^{bc} \pm 0.46$	$5.30^{a} \pm 0.46$	$22.34^{bc} \pm 0.83$	$46.59^{c} \pm 2.09$	$24.08^{c} \pm 0.54$
BPF 12 I 0%	$30.00^{e} \pm 0.88$	$5.60^{a} \pm 0.49$	$25.88^{e} \pm 0.60$	$55.35^{f} \pm 1.48$	$30.72^{f} \pm 1.62$
BPF 12 I 25%	$28.95^{e} \pm 0.27$	$5.54^{a} \pm 0.51$	$24.59^{cd} \pm 0.87$	$52.97^{ef} \pm 2.34$	$28.00^{e} \pm 1.29$
BPF 12 I 50%	$27.11^{cd} \pm 0.46$	$5.30^{a} \pm 0.48$	$23.09^{c} \pm 0.59$	$49.01^{cd} \pm 2.79$	$25.40^{c} \pm 0.70$

Note: The same letter in the same column shows no significant difference based on the DMRT test and BNJ test at = 5%

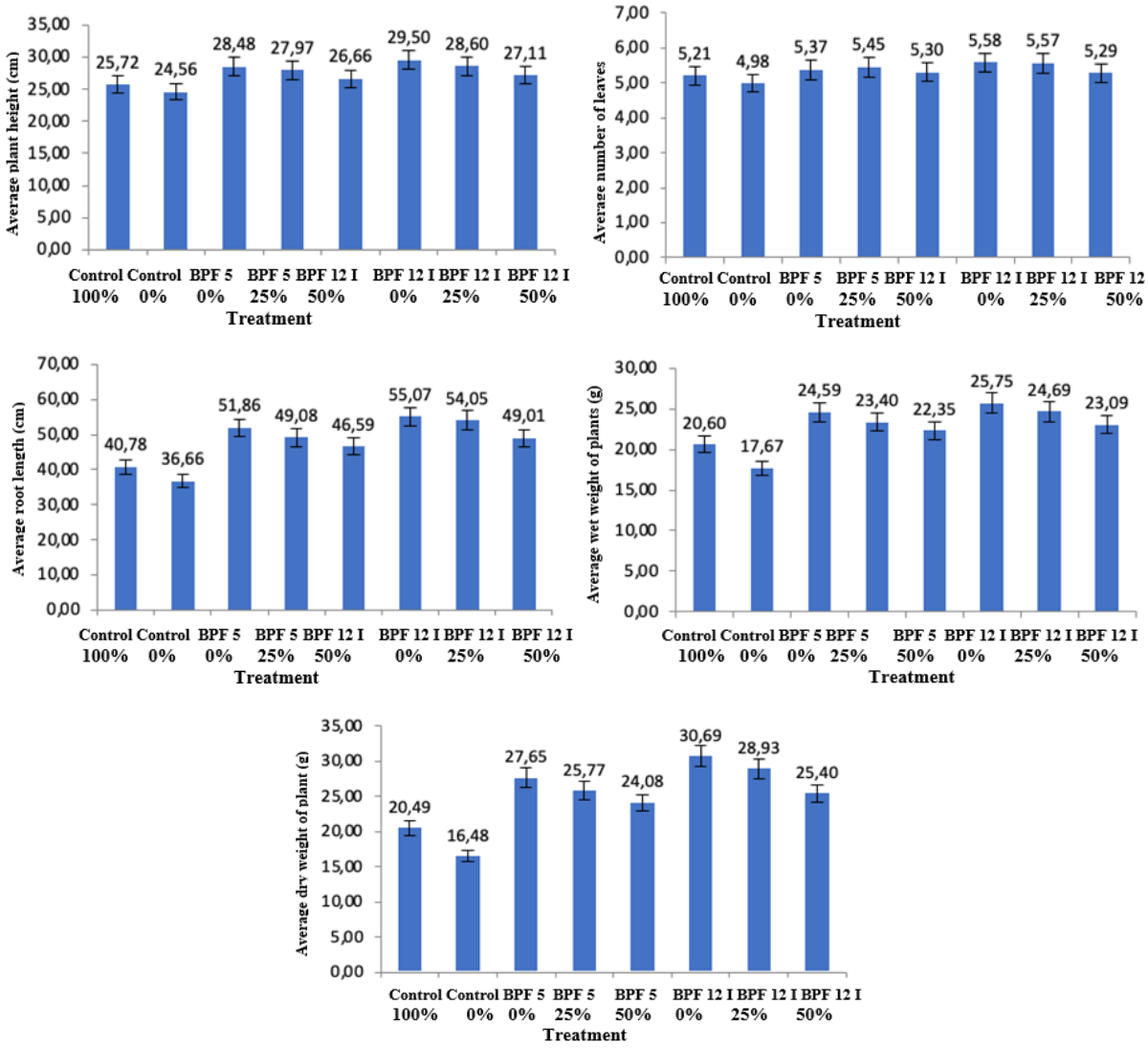

Figure 4. Sorghum plant growth 50 days after planting (DAP)

Because measurements are taken every three days until the plant reaches 50 days following planting, the data acquired are not statistically significant between treatments. Nonetheless, NPK fertilizer and biofertilizer administration can provide the nutrients necessary for plant growth. According to these findings, BPF 12 I treatment with 0% and 25% NPK fertilizer boosted plant growth compared to 50% NPK fertilizer and control treatment. Biofertilizers can help reduce the amount of NPK fertilizer used because both fertilizers can provide and complement the nutrients required by plants. As a result, crop yields are more optimal, and soil fertility is improved, providing long-term benefits and promoting sustainable agriculture (Pangaribuan et al. 2017).

Using 50% and 100%, NPK fertilizers resulted in less optimal sorghum growth. High concentrations of NPK fertilizers cause poisoning in plants, inhibiting chemical reactions such as metabolism, photosynthesis, and respiration, thereby impairing plant growth and productivity (Rahmatika and Sasmito 2017). When large doses of NPK fertilizer are applied to young seedlings, the plants will not thrive because they cannot synthesize the fertilizer (Pasaribu et al., 2018).

Leaf color was observed when the plant reached its maximal vegetative phase, approximately 50-60 days following planting. Leaf color was observed using the Munsell color chart to assess the chlorophyll content of plants. Table 4 summarizes the results of the leaf color analysis.

The findings of the leaf color observation using the Munsell color chart indicated that the level of greenish hue in the leaves varied according to the concentration of NPK fertilizer mixed with biofertilizer. According to Table 4, the BPF combination treatment with NPK fertilizer concentrations of 0%, 25%, 50%, and 100% showed darker green leaf color, namely 5 GY 6/6 and 5 6/8, compared to the 0% control treatment with 2.5 GY 6/10 and 5 GY 7/8. It is possible because the availability of nutrients such as N, P, and K affects the leaf's green hue. The darker the green color of the plant, the more nutrients it absorbs, which increases the plant's dry weight and yield (Nugroho 2015).

Table 4. Observation of sorghum leaf color based on Munsell Color Chart

Treatment	Fertilizer concentration	Leaf color	Color on Munsell
Control	100%	5 GY 6/6	
Control	100%		
Control	100%		
Control	0%	2.5 GY 6/10	
Control	0%	5 GY 7/8	
Control	0%		
BPF 5	0%	5 GY 7/8	
BPF 5	0%		
BPF 5	0%	5 GY 6/6	
BPF 5	25%	5 GY 6/8	
BPF 5	25%		
BPF 5	25%	5 GY 6/6	
BPF 5	50%	5 GY 6/8	
BPF 5	50%		
BPF 5	50%		
BPF 12 I	0%	5 GY 6/8	
BPF 12 I	0%		
BPF 12 I	0%	5 GY 6/6	
BPF 12 I	25%	5 GY 6/6	
BPF 12 I	25%		
BPF 12 I	25%		
BPF 12 I	50%	5 GY 6/6	
BPF 12 I	50%	5 GY 6/8	
BPF 12 I	50%		

The aging process is accelerated in the control treatment. Simultaneously, the addition of NPK and biological fertilizers results in a lighter and darker coloration of the leaves since the microbes included in biological fertilizers can offer nutrients during the vegetative period (Suryadi et al., 2019). The usage of NPK fertilizers containing nitrogen affects the color of the leaves as well. If these nutrients are in short supply, the leaves will become yellow or yellowish-green, impairing the photosynthetic process.

To conclude, seven isolates of bacteria with potential as phosphate solubilizing bacteria were recovered from the rhizosphere area of sugarcane. Five isolates of bacteria and two isolates of actinomycetes were obtained, with two isolates having outstanding potential, namely isolates BPF 12 I and BPF 5. The addition of phosphate-solubilizing bacteria from the Sugarcane rhizosphere to an NPK fertilizer substantially affected the growth of sorghum (*S. bicolor*) growth, particularly on parameters such as plant height and root length leaf color, wet plant weight, and dry plant weight. The combination of BPF 12 I isolate with fertilizer concentrations of 0% and 25% significantly affected and resulted in improved sorghum growth.

REFERENCES

Akbari GA, Arab S.M, Alikhani HA, Allahdadi I, Arzanesh MH. 2007. Isolation and selection of indigenous *Azospirillum* spp. and the IAA of superior strains effects on wheat roots. World J Agric Res 3 (4): 523-529.

Amaria W, Taufiq E, Harni R. 2013. Seleksi dan identifikasi jamur antagonis sebagai agens hayati jamur akar putih (*Rigidoporus microporus*) pada tanaman karet. Buletin Ristri 4 (1): 55-64. DOI: 10.21082/jtidp.v1n2.2014.p79-86. [Indonesian]

Anas. 2007. Pengembangan tanaman sorgum sebagai basis diversifikasi pangan. Seminar Nasional Apresiasi Pengembangan Sorgum. Kupang Nusa Tenggara Timur: Departemen Pertanian Direktorat Jenderal Tanaman Pangan, Direktorat Budidaya Serealia. [Indonesian]

Aqil M, Bunyamin Z. 2013. Optimalisasi pengelolaan agroklimat pertanaman sorgum. Seminar Nasional Serealia 2017: 371-379.

Arbab MBM, Dagash YMI. 2017. Microdosing technology of fertilizer for sorghum production at Shambat, Sudan. Cell Biol Dev 1: 18-22. DOI: 10.13057/cellbioldev/t010104.

Cappuccino JG, Sherman N. 1998. Microbiology A Laboratory Manual. 10th Edition. Person, USA.

Chang YC, Baker R, Kleifeld O, Chet I. 1986. Increased growth of plants in the presence of the biological control agent *Trichoderma harzianum*. Plant Dis 70 (2):145-148. DOI: 10.1094/PD-70-145.

Dewi IM. 2008. Isolasi Bakteri dan Uji Aktifitas Kitinase Termofilik Kasar dari Sumber Air Panas Tinggi Raja, Simalungun, Sumatera Utara. [Tesis]. Sekolah Pascasarjana Universitas Sumatera Utara, Medan. [Indonesian]

Elfiati D. 2005. Peranan Mikroba Pelarut Fosfat terhadap Pertumbuhan Tanaman. [Skripsi]. Fakultas Pertanian, Universitas Sumatra Utara, Medan. [Indonesian]

Elfiati D, Delvian, Hanum H. 2016. Indeks Pelarutan Fungi Pelarut Fosfat dengan Menggunakan Empat Sumber Fosfat. Prosiding Seminar Nasional Lahan Suboptimal, Palembang 20-21 Oktober 2016. [Indonesian]

Firdausi N, Wirdhatul M, Tutik N. 2016. Pengaruh kombinasi media pembawa pupuk hayati bakteri pelarut fosfat terhadap pH dan unsur hara fosfor dalam tanah. J Sains dan Seni ITS. 5 (2): 53-56. [Indonesain]

Fitri L, Yasmin Y. 2011. Isolasi dan pengamatan morfologi koloni bakteri kitinolitik. J Ilmiah Pendidikan Biologi, Biologi Edukasi. 3 (2): 20-25. [Indonesian]

Hadioetomo RS. 1993. Mikrobiologi Dasar dalam Praktek: Teknik dan Prosedur Dasar Laboratorium. Gramedian, Jakarta. [Indonesian]

Karti PDMH, Setiadi Y. 2011. Respon pertumbuhan, produksi dan kualitas rumput terhadap penambahan fungi mikoriza arbuskula dan asam humat pada tanah masam dengan aluminium tinggi. JITV 16 (2): 104-111. [Indonesian]

Kumalasari AM, Fathurahman RN, Nur RM. 2012. Potensi Actinomycetes sebagai sumber senyawa bioaktif antibiotik dari Kawasan Karst Bantimurung, Sulawesi Selatan. J Pelita 7 (1): 59 - 72. [Indonesian]

Lay WB. 1994. Analisis Mikroba di Laboratorium. PT Raja Grafindo Persada, Jakarta. [Indonesian]

Listiana E, Anugrahwati DR, Muthahanas I. 2018. Isolasi dan identiikasi bakteri endofitik Actinomycetes dari tanaman lokal Lombok. Crop Argo 1 (1): 138 - 144. [Indonesian]

Nugraha R, Ardyati T, Suharjono. 2014. Eksplorasi bakteri selulolitik yang berpotensi sebagai agen biofertilizer dari tanah perkebunan apel Kota Batu, Jawa Timur. J Biotropika 2 (3): 159-163. [Indonesian]

Nugroho WS. 2015. Penetapan standar warna daun sebagai upaya identifikasi status hara (N) tanaman jagung (*Zea mays* L.) pada tanah regosol. Planta Trop J Agro Sci 3 (1): 8-15. DOI: 10.18196/pt.2015.034.8-15. [Indonesian]

Nuryadi WH, Rakmawati A, Prihatini I. 2016. Isolasi dan identifikasi kapang endofit dari pohon sengon provenan Kepulauan Solomon berdasarkan morfologi dan Molekuler (Analisis Rdna Its (*Internal Transcribed Spacer*). J Biologi 5 (6): 15- 27. [Indonesian]

Pangaribuan DH, Hendarto K, Prihartini K. 2017. Pengaruh pemberian kombinasi pupuk anorganik tunggal dan pupuk hayati terhadap pertumbuhan dan produksi tanaman jagung manis (*Zea mays saccharata* Sturt) serta populasi mikroba tanah. J Flora Teknologi 12 (1): 1-9. DOI: 10.32520/jai.v1i1.582. [Indonesian]

Pasaribu PL, Hasibuan S, Batubara LR. 2018. Pengaruh pemberian feses kelinci dan pupuk NPK majemuk intan super terhadap pertumbuhan dan produksi tanaman buncis tegak (*Phaseolus vulgaris* L.). BERNAS Agric Res J 14 (3): 79-90. [Indonesian]

Purnomo AJ, Anggraeni A, Astuti RK, Lestari AB, Antasari GA. 2017. Potensi bakteri penambat nitrogen dan penghasil hormon IAA dari sampel *Rhizosfer* paku epifit di mulut Gua Anjani, Kawasan Karst Menoreh. Biotropic 1 (2): 9-15. DOI: 10.29080/biotropic.2017.1.2.9-15. [Indonesian]

Rahayu F, Mastur, Santoso B. 2014. Potensi beberapa isolat bakteri pelarut fosfat asal lahan tebu di Jawa Timur berdasarkan aktivitas enzim fosfatase. Buletin Tanaman Tembakau, Serat dan Minyak Industri 6 (1): 23-31. DOI: 10.21082/bultas.v6n1.2014.23-31. [Indonesian]

Rahmatika W, Sasmito IB. 2017. Efektivitas biofertilizer extragen dan pupuk NPK yaramila terhadap pertumbuhan dan produksi tanaman kubis bunga (*Brassica oleracea* var. botrytis L.). J Hijau Cendekia 2 (2): 67- 70. [Indonesian]

Rao S. 1994. Mikroorganisme Tanah dan Pertumbuhan Tanaman Edisi *2*. UI-Press, Jakarta. [Indonesian]

Richardson AE. 2001. Prospect for using soil microorganisms to improve the acquisition of phosphorus by plants. Aust J Plant Physiol 58: 797-906.

Setyorini D, Didi A, Rasti S, Diah S. 2006. Pupuk Organik dan Pupuk Hayati. Balai Besar Litbang Sumberdaya Lahan Pertanian Badan Penelitian dan Pengembangan Pertanian, Bogor. [Indonesian]

Sharon G, Sampson TR, Geschwind DH, Mazmanian SK. 2016. The central nervous system and the gut microbiome. Cell 167: 915-932. DOI: 10.1016/j.cell.2016.10.027.

Simanungkalit RDM, Husein E, Saraswati. 2006. Baku Mutu Pupuk Hayati dan Sistem Pengawasannya. Balai Besar Penelitian dan Pengembangan Sumberdaya Lahan Pertanian, Bogor. [Indonesian]

Subowo, YB, Sugiharto W, Suliasih, Widawati S. 2010. Pengujian pupuk hayati Kalbar untuk meningkatkan produktivitas tanaman kedelai (*Glycine max*) var. Baluran. Cakra Tani 25: 112-118. DOI: 10.20961/carakatani.v25i1.15756. [Indonesian]

Sudiarti D. 2013. Pengaruh biofertilizer dan pupuk NPK terhadap pertumbuhan tinggi tanaman tembakau (*Nicotiana tabacum*). Bioshell 2 (1): 68-76. [Indonesian]

Sudiarti D. 2017. Efektivitas biofertilizer pada pertumbuhan tanaman kedelai edamame (*Glycin max*). J Sain Health 1 (2): 97-106. DOI: 10.51804/jsh.v1i2.110.97-106. [Indonesian]

Sukmawati, Hardianti F. 2018. Analisis *Total Plate Count* (TPC) Mikroba pada ikan asin kakap di Kota Sorong Papua Barat. J Biodjati 3 (1): 72-78. DOI: 10.15575/biodjati.v3i1.2368. [Indonesian]

Sulistyani N, Akbar AN. 2014, Aktivitas isolat Actinomycetes dari rumput laut (*Eucheuma cottonii*) sebagai penghasil antibiotik terhadap *Staphylococcus aureus* dan *Escherichia coli*. J Ilmu Kefarmasian Indonesia 12 (1): 4-12. [Indonesian]

Sumarno, Damardjati DS, Syam M, Hermanto. 2013. Sorgum Inovasi Teknologi dan Pengembangan. Badan Penelitian dan Pengembangan Pertanian, Jakarta. [Indonesian]

Suryadi M, Mulyati, Jaya IKD. 2019. Efektivitas pupuk petrobio dan NPK terhadap pertumbuhan dan hasil tanaman kol bunga (*Brassica oleracea* var. botrytis L.). Crop Argo 12 (1): 46-58. DOI: 10.29303/caj.v12i01.260. [Indonesian]

Suryanto D, Munir E. 2006. Potensi pemanfaatan isolat kitinolitik lokal untuk pengendalian hayati jamur. Prosiding Seminar Hasil-hasil Penelitian, FMIPA USU 15-25. [Indonesian]

Tuwu ER, Sutariati GAK, Suaib. 2012. Pengaruh kadar air benih dan jenis kemasan terhadap vigor benih sorgum (*Sorgum bicolor* [L.] Moench) dalam enam bulan masa simpan. Berkala Penelitian Agronomi 1 (2): 184-193. [Indonesian]

Widawati S, Nurkanto A, Sudiana IM. 2008. Phosphate solubilizing activities of Actinomycetes isolated from Waigeo, Raja Ampat islands, West Papua. Biodiversitas 9 (2): 87-90. DOI: 10.13057/biodiv/d090202.

Widawati S, Sulasih. 2005. Augmentation of potential phosphate solubilizing bacteria (PSB) stimulate growth of green mustard (*Brasica caventis* Oed.) in marginal soil. Biodiversitas 7 (1): 10-14. DOI: 10.13057/biodiv/d070104.

Yuliar. 2006. Program Penelitian Nutrisi Hayati untuk keseimbangan Ekosistem. Pusat Penelitian Biologi-Lembaga Ilmu Pengetahuan Indonesia (LIPI), Bogor. [Indonesian]